Modeling optimal design parameters of constructed wetlands receiving agricultural runoff

By

Daniyal Ahmed Siddiqui

Submitted to the graduate degree program in Department of Civil, Environmental, and Architectural Engineering and the Graduate Faculty of the University of Kansas in partial fulfillment of the requirements for the degree of Doctor of Philosophy.

_____

Chair: Edward F. Peltier

_____

C. Bryan Young

_____

Joshua K. Roundy

_____

Amy Hansen

_____

Nathaniel Brunsell

Date Defended: Nov 16th, 2020

The dissertation committee for Daniyal Ahmed Siddiqui certifies that this is the approved version of the following dissertation:

Modeling optimal design parameters of constructed wetlands receiving agricultural runoff

Chair: Edward F. Peltier

Date Approved: Dec 14th, 2020

Abstract

Constructed wetlands intercepting surface runoff from agricultural fields have been shown to act as a nutrient buffer, providing water quality improvements in the runoff water to be deposited safely downstream. Three surface flow wetlands were constructed in the Deer Creek-Clinton Lake sub watershed of the Upper Wakarusa Watershed, in Douglas County, Kansas, as a part of a pilot project to retain and improve runoff water quality from terraced fields with tile outlet runoff. A monitoring study conducted from 2014-15 showed that the wetlands were acting as efficient solids-removal systems. Nitrogen removal results, however, were on the lower end of the performance spectrum with high variation. This study was carried out to model the hydraulic, hydrological and water treatment parameters of the wetlands and to better understand their performance capacity.

A custom curve number prediction model incorporating antecedent precipitation and vegetation patterns was developed to estimate the runoff produced from the terraced agricultural watersheds. The standard SCS unit hydrograph method was modified to match the fast-moving tile drained surface runoff. The model was adapted to account for changes in vegetation patterns onsite, which were observed to have a significant impact on the runoff volume. A dynamic wetland water budget model, also developed as part of this work, showed the variability in the performance of the wetlands between dry and wet weather conditions. During wet weather periods of high flows (early May to mid-June), the wetlands acted as flow-through systems with water levels at or above the weir outflow height. Contrarily, during dry weather periods, the water levels fall, and the outflow decreases significantly. These changes in water levels had a direct influence on the hydraulic retention times. A Monte Carlo simulation was developed to evaluate the likely distribution of retention times under different antecedent seasonal conditions.

Based on the Monte Carlo analysis, the median retention time was calculated to be less than 4hrs in both wetlands. The 90% retention time was determined to be around 10 hrs, demonstrating the dramatic effect of wet and dry weather conditions.

Nutrient removal calculations were performed using a relaxed tank in series model due to the tendency of constructed wetlands to behave as something in between plug flow and well mixed systems. This assessment was combined with Bayesian analysis to evaluate the likely ranges of the predicted nutrient and sediment removal from the wetlands. The calculated reaction rate values were found to be on the lower end of those observed in published literature for similar studies. Modeling results suggest that nitrogen concentrations are likely to decrease by 10-30%, compared to 30-50% for phosphorus and 65-85% for suspended solids, as runoff moves through the wetlands during and after a storm event.

Future implementation of the constructed wetlands would significantly benefit from improvements in the wetland design. The presence of tile outlet terraced watersheds with saturated soil conditions demands special considerations for optimal wetland performance. These considerations include smaller than usual watershed to wetland ratio to increase retention time of the runoff water, higher aspect ratio to facilitate the removal of low velocity zones and more aggressive planting practices. Scenarios modeled for the study sites showed that the increase in removal efficiency potential would be the most evident for phosphorus and solids and less for nitrogen concentrations. A tenfold increase in reaction rate parameter was able to achieve an upwards of 50% nitrogen removal but would require significant changes in wetland design and maintenance. Similar improvements can be achieved by decreasing the watershed to wetland ratio to 5:1. Increasing the aspect ratio of the wetlands was not enough to achieve high nitrogen removal efficiencies. This study demonstrates the potential for coupled watershed-wetland

models to aid in constructed wetland design. Future improvements in the modeling work could provide even deeper insights into improving wetland performance but would require extensive data collection.

Acknowledgements

I would first like to express my gratitude to Dr. Edward Peltier for his continuous support and guidance throughout my PhD journey. He took a chance on me back in 2016 by not only allowing me to work on this project but by also arranging for my financial requirements. I am grateful that he allowed me to serve as a graduate teaching assistant regularly in his courses. That particular experience has contributed significantly towards building up my confidence. One reason why I really enjoyed working with him is how he allowed me to explore different technical routes to accomplish a certain task and never restricted me to take a predefined approach.

I would also like to thank my committee members for sparing out the time to help me out whenever I got stuck. Dr. Bryan Young and Dr. Joshua Roundy has been particularly helpful in proofreading my writeups and helping me out in my modeling work. Dr. Amy Hansen ad Dr. Nathaniel Brunsell joined the committee much later and have been supportive since then. I would also like to thank Dr. Pamela Sullivan who served as a member of my committee till 2019 and have been nothing but helpful all the way through. Dr. Sullivan and her student Marvin Stops were also the co-authors of the Kansas Water Office report.

Additionally, the following people assisted me with the project: Dr. Carter, Matt Chomicky and undergraduate students Katie Wipfli, Guanyu Li and Allison Dobie.

Funding for this work was provided by the U.S. Environmental Protection Agency Region 7 through Wetland Program Development Grant CD97758901 and administered by the Kansas Water Office.

Data collected from 2014- 2015 during a previous project was used extensively in this work. That study was funded by USEPA Region 7 through Wetland Program Development Grant CD97743401, administered by the Kansas Water Office. Former KU MS students Hyunjung Lee and Llynnann Luellen conducted the primary work for field data collection and interpretation during that study.

I would like to thank my parents without whom I would not have been here. My father was the reason why I was able to buy the ticket to USA back in 2015 and pay my first-year tuition at KU. My mother has been a rock in supporting me emotionally all the way from Karachi, Pakistan around 8000 miles away.

I would also like to thank my friends that made sure that I don't feel homesick during my time here in USA. I would specifically like to thank my roommate Amirali Shalwani for sharing meals with me when we had little. I also want to thank my desi people, Hamza Bhai, Uzair, Maab and Shumail for all those Saturday nights they wasted at my apartment talking religion, philosophy, politics, cricket and other gibberish.

I would like to thank my wife, Amna to stand by me in these last couple of months. It has been tough, finding a job in current times and without her presence I am not sure if I would have been able to keep my sanity intact.

Finally, I would like to thank the year 2020 for making this graduation so rememberable. Difficult, but rememberable.

Table of Contents

List of Tables

List of Figures

Chapter 1

Introduction

Agricultural runoff can pose serious threats to receiving water quality [1]. This runoff can contain high loadings of both nitrogen and phosphorus, which can result in nutrient enrichment in receiving water bodies, a leading cause of surface water degradation in the United States [2]. High nutrient loadings are the major cause of algal blooms, which can release harmful toxins, decrease aquatic biodiversity and increase costs for drinking water treatment [3, 4]. In eastern Kansas, where surface reservoirs are a major source of drinking water and recreation, control of nutrient release from agricultural runoff is therefore a key component of efforts to protect water quality and supply [5].

Strategies used to control nutrient loadings into surface water bodies can involve both source control practices (changing farming practices, optimizing fertilizer application rates, etc.) [6] and on-site treatment by intercepting runoff before it discharges to local surface water bodies [7]. One option for on-site treatment is the use of constructed or restored wetlands to detain runoff and improve water quality before discharge [8, 9]. Wetlands are passive treatment systems that can adapt to high variations in runoff quantity and quality [10] and have been applied as an on-site treatment system for agricultural runoff both in the United States [11, 12] and worldwide [13, 14].

Wetlands are rated as one of the most biologically active ecosystems present [15]. Therefore, these systems carry the potential of converting large amount of pollutants present in common wastewater sources to harmless byproducts. The dominant resources used by wetlands to achieve these transformations include the natural energies of wind, soil, plants, sun and land area. This allows the treatment process to occur at minimal to zero chemical, mechanical and

fossil energy utilization. Therefore, treatment wetlands are generally considered to be one of the cheapest method available to treat urban and agricultural runoff [16].

Wetlands may be particularly suited to treatment of agricultural runoff because they are able to address removal of both dissolved and solid-associated nutrients, especially nitrogen [17]. Previous studies have shown that wetlands can achieve upwards of 50% removal of both influent nitrogen and phosphorus, but there is high variability, and many sites report much lower removals [18-21]. The large variation in wetland performance is a function both of the complexity of the systems and of differences in wetland design and operation from one system to another.

Nitrogen removal through wetlands is dependent upon various mechanisms including volatilization, adsorption, and plant and bacteria uptake and denitrification [22]. Moderate to low nitrogen removals have been generally reported in literature and the requirement of longer hydraulic retention times (HRTs) might be the reason behind the reduced performance [23]. Vymazal [24] compiled the total nitrogen removal efficiencies reported using different wetland types and the results varied in between (~40 – 55%) with wetlands having free-floating plants showing the highest removal.

Phosphorus interaction with wetland biota provides short-term and sustainable long-term removal rates given appropriate conditions and has been shown to be an economical alternative to chemical and biological treatment processes [25]. Phosphorus removal ranged from (40–60%) in all major types of wetland configuration including free-floating plants, free water surface, horizontal flow and vertical flow wetlands with the major removal mechanisms being sorption, precipitation, plant uptake and soil accretion [24]. Although early removal percentages are

generally high, performance has been found to decrease with time due to the leaching of previous loadings [25].

North-eastern Kansas topography requires the use of terracing in some areas to control sediment erosion from agricultural fields. Recently, the installation of tile outlet drainage systems in place of grassed waterways on terraced farmland has become more common due to reduced maintenance requirements and increased land availability for planting. Tile outlet terrace (TOT) systems move water quickly off-site by directly conveying surface runoff to a subsurface drain. This can result in increased nutrient and sediment loadings from the site compared to grassed waterways, a result of the faster flow rates in these systems and lack of filtration by vegetation [26, 27]. This increase in off-site transport could result in higher total loads transported to receiving waters. In turn, this could make it more difficult to achieve established total maximum daily limits (TMDLs) for eutrophication and sediments in the Upper Wakarusa Watershed and Clinton Lake [28].

Constructed wetlands represent a potential solution to the increased nutrient and sediment loadings from TOT systems. Constructed wetlands have a long-established history of use for water quality improvement and are well suited to treatment of runoff and other variable-flow sources. These wetlands can be placed between the TOT outlet and an off-site discharge point to provide additional storage volume and removal of both nutrients and suspended solids from site runoff prior to discharge. Previous studies on wetland treatment of tile drainage have shown removal rates of 35-55% for nitrogen [12, 18, 21] with a recent study on horizontal subsurface flow wetlands achieving up to 70% [29] and 0-50% for phosphorus [12, 21, 27]. However, predicting wetland performance generally requires data that accounts for local conditions, including climate, soil conditions, and farming techniques.

1.1 Study Sites

This research was conducted as part of a long-term monitoring project to assess the effectiveness of pilot wetlands (Lat:38.9835, Long:-95.4540) created to intercept tile runoff from terraced agricultural fields in the Deer Creek-Clinton Lake sub watershed of the Upper Wakarusa Watershed, in Douglas County, KS (Fig 1. 1). The average annual temperature for this area is 12.4°C, reaching a high of 30.3°C in the summer and low of -6.3°C in the winter. Average annual precipitation is 1013 mm with ~70% of the total precipitation falling in the spring and summer months (NOAA; 1981-2010 normal: https://www.ncdc.noaa.gov/) Approximately 75% of the total precipitation falls within the growing season, which spans ~196 days (Kansas Geological Survey (KGS); www.kgs.ku.edu).

All three sites are active agricultural sites that utilizes combination of terracing and tile outlet drainage systems to manage stormwater collection and transport from the farmed portions of the site during and after storm events. Two of the sites, Harvest Hills North (HHN) and Harvest Hills Middle (HHM), are separately draining portions of the same property, with a ridge serving as the topographic boundary between the two drainage areas. The third site, the Cain field site, is approximately 2 miles east of the Harvest Hills sites. All three sites drain to the upper reaches of Clinton Lake, a reservoir lake constructed and maintained by the U.S. Army Corps of Engineers. Clinton Lake is one of two drinking water supply sources for Lawrence, Kansas and surrounding communities, and has additional uses as a recreation area and for flood control. Total maximum daily loads (TMDLs) have been set for Clinton Lake for both phosphorus and total sediments to reduce loadings of these compounds. At present, there is no TMDL for nitrogen [30].

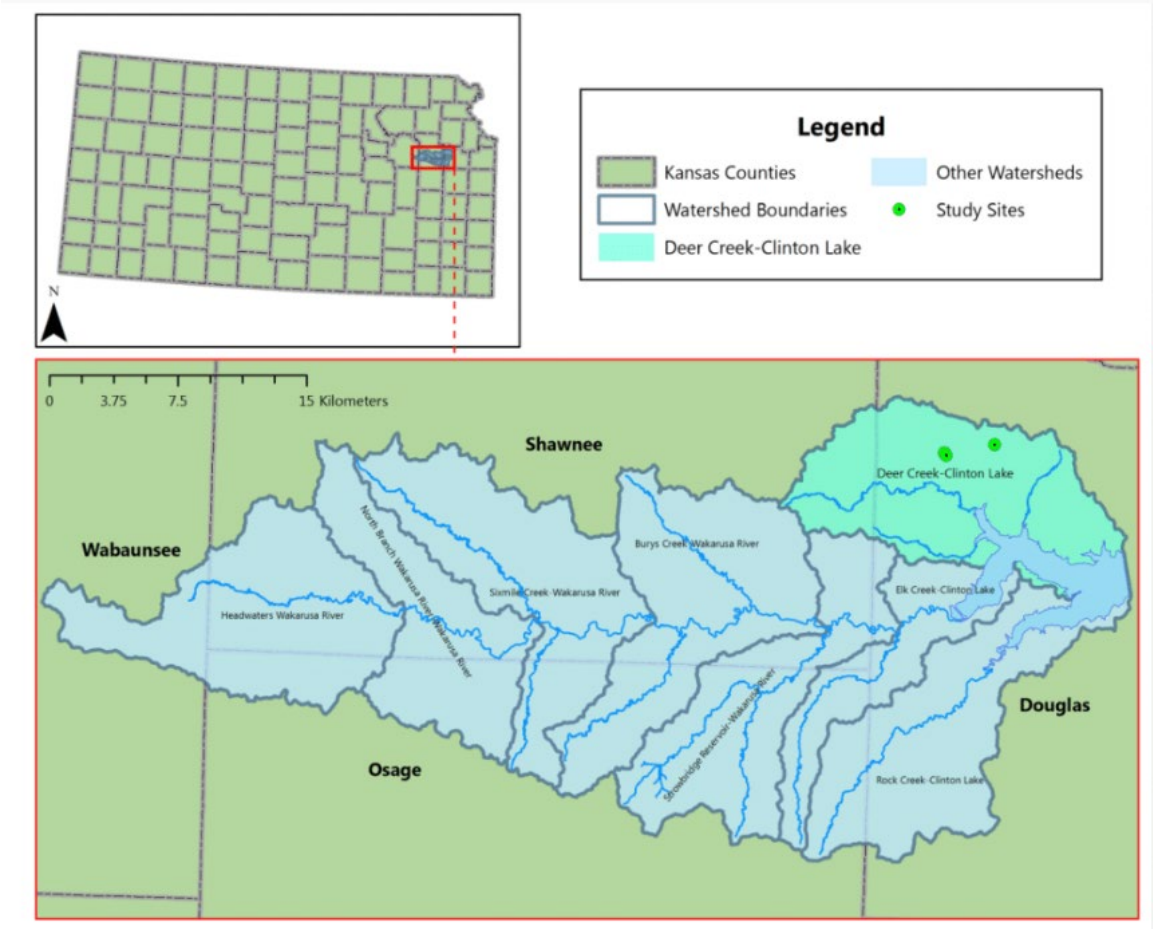

Fig 1. 1 Map showing the location of the Upper Wakarusa Watershed, the Deer Creek – Clinton Lake subwatershed and the study sites, from [30]

All three sites utilize a tile outlet terrace (TOT) drainage system to manage and remove stormwater runoff. These drainage systems replaced grassed waterways that previously channeled storm runoff from these fields to receiving waters. Prior to conversion to TOT drainage, deep gullies had formed in the fields and erosive head cuts at the edge of the waterways were progressing into the fields. These eroded waterways were filled in, regraded, and returned to arable land. The fields were trenched for installation of main tile-outlet drainage pipes. At each of the study sites, surface wetlands were installed between 2008 and 2011 to capture the effluent from the TOT system prior to discharge to surface receiving waters (Fig 1. 2). These wetlands were constructed following design guidelines from the Natural Resources

Conservation Service (NRCS) [31]. The wetlands have been operated with relatively little maintenance activities during their initial decade of operation.

1.1.1 Individual watershed description:

The HHN site consists of 18.9 acres, of which 14.8 acres are cropped. The cropped portion of the site consists of three terraces that funnel surface runoff to the TOT drainage system. On risers 1 and 3, drainage occurs through standpipe risers with perforations beginning at approximately 4 inches above the ground. Due to bedrock and available grading at this terrace, the effluent pipe at the second terrace does not have a perforated standpipe. Significant erosion occurs in and around this exposed area during heavy runoff events, creating a source of sediment into the wetland pond. Collected storm runoff drains through the TOT system to the wetland pond located in the northwest corner of the site. A small portion of uncropped land also drains to the pond through surface runoff.

The HHM site has a 21.9 acre watershed, of which 20.1 acres is cropped. The area drained by the TOT consists of three terraces, totaling 17.4 acres. Each terrace is drained by a standpipe of identical design to that at HHN. The remaining cropped acreage drains directly to the pond through overland flow and is not considered in our sampling. The TOT outlet pipe discharges into a wooded riparian area approximately 210 feet upstream (northwest) of the main wetland area in the southeast portion of the site. The wetland effluent is located on the south side of the pond.

The Cain site has a 41.3 acre watershed, of which 36.7 acres is cropped. The inflow pipe to the Cain wetland is below the normal pond level and has been partially blocked by beaver activity. As such, drainage into the pond from the TOT system is slow and the first two terraces are frequently ponded after a rain event. Due to this ponding, sampling equipment was placed in

the TOT drainage pipe on the third terrace, measuring and sampling flow from the upper four terraces. The total area upstream of the flow measuring device was 22.2 acres.

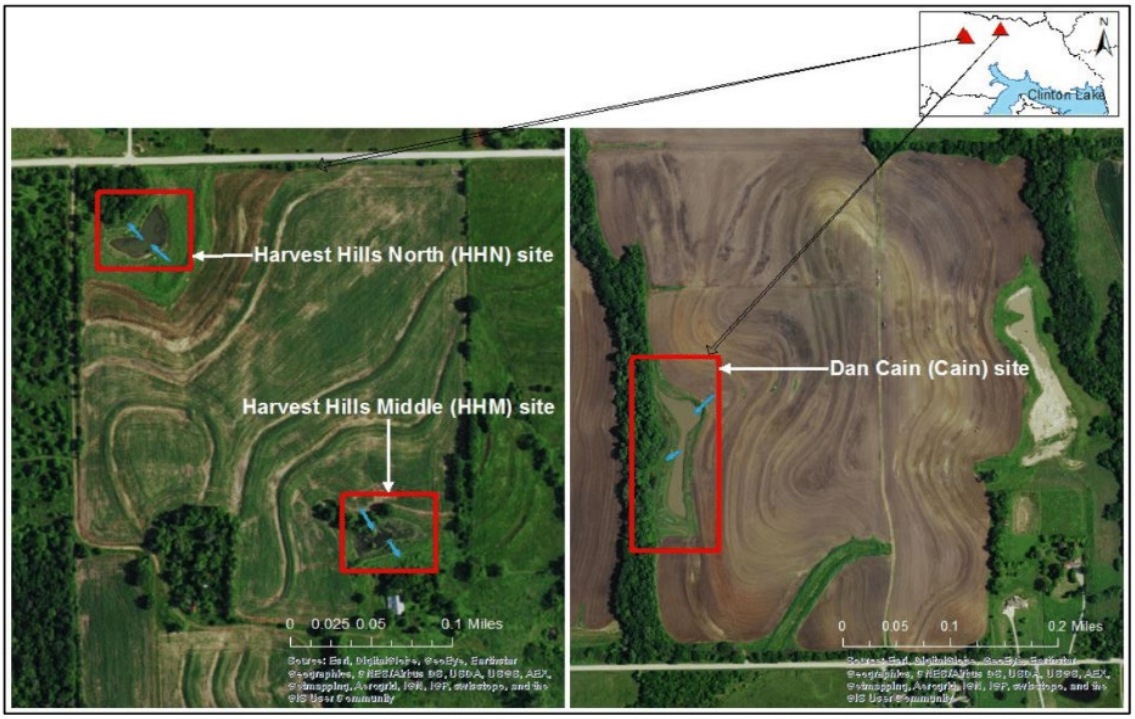

Fig 1. 2 Layout of the monitored wetlands on the study site, from [32]. Blue arrows show the inflow and outflow locations.

1.1.2 Individual wetland description:

The HHN wetland pond has a normal surface area of approximately 0.54 acres. As-built bathymetric data are not available for the site. As a result, the as-built storage for the site is unknown. Construction plans specified an estimated post-construction pond area of 0.47 acres with storage volume of 0.91 ac-ft. A site survey was conducted in 2016 to develop a stage-storage relationship for the wetland for elevations greater than 1003 ft (the water level at the time). Vegetation at the site has continued to develop around the pond fringe, but the center of the pond remains open, with little to no vegetation (Fig 1. 3).

The HHM wetland pond has a normal surface area of approximately 0.58 acres. As-built bathymetric data are not available for the site. As a result, storage volume for the site is unknown. Construction plans estimated a post-construction maximum permanent pool area of 0.50 acres with storage volume of 1.73 ac-ft. Similar to HHN, a site survey was conducted in 2016 to develop a stage-storage relationship for the wetland. Due to the water level at the time, the stage-storage relationship is for elevations greater than 1001 ft. There is significant vegetation establishment in the HHM wetland, particularly during the summer months (Fig 1. 4). Large stands of wetland grasses alternate with deeper, open-water sections of the wetland. Tall wetland grasses also dominate the fringe area of this wetland.

The Cain wetland pond has a normal surface area of approximately 1.71 acres. Construction plans estimate a post-construction maximum permanent pool area of 1.09 acres with storage volume of 3.78 ac-ft. A site survey was conducted in 2016 to develop a storage-elevation relationship for the wetland. Due to the water level at the time, the storage-elevation relationship is for elevations greater than 1030.5 ft. Fig 1. 5 shows a photograph of the Cain wetland taken from the southern end of the pond.

The outflow from the Cain wetland pond is a nominal 12-inch PVC pipe. As seen in Fig 1. 6, the outlet pipe protrudes out into the wetland basin. Beavers have gnawed on the pipe opening, creating a complicated outlet geometry. Samples were drawn from the 12-inch effluent pipe several feet downstream of the opening. When the water level in this pond is below the outfall pipe, as in Fig 1. 6, no surface outflow occurs from the wetland.

The effluent from the HHN and HHM wetland ponds passes through a 12-inch pipe and AgriDrain brand weir box. The weir box width is 12-5/16 inches. Fig 1. 7 shows a photograph of the AgriDrain weir box at HHM.

Fig 1. 3 Vegetation establishment at HHN wetland, picture taken in March 2019, from [33].

Fig 1. 4 Vegetation establishment at HHM wetland, picture taken in July 2019, from [33].

Fig 1. 5 Cain wetland pond photograph, from [34]

Fig 1. 6 Outflow pipe for Cain wetland, Picture taken in July, 2017, from [33]

Fig 1. 7 AgriDrain weir box outlet structure for HHM, from [34]

1.2 Purpose and Scope of the Study

Hydraulic and water quality data have been collected since 2014 from all three sites described above (Harvest Hills North – HHN, Harvest Hills Middle – HHM and Cain). An initial study, conducted from 2014-15 and published in 2016 [34], focused on monitoring water quality entering and exiting the treatment wetlands. Water quality results from 2014 and 2015 showed that, despite the similarities in drainage area and wetland design, notable differences existed in nitrogen removal between the two Harvest Hills wetlands [34]. The Cain site wetland, by contrast, had much lower inputs of dissolved nitrogen and phosphorus that the other two sites. Nitrogen and phosphorus removal at this site occur almost entirely through settling of suspended solids.

In 2016, a second study was launched to obtain further information on wetland performance, with a particular emphasis on nitrogen removal. To better interpret existing results and predict long-term wetland behavior, models were developed to simulate the full range of

events starting from runoff generation in the upland watersheds to quantification of the pollutant removal efficiencies of the wetlands. This thesis addresses the development, calibration, and implementation of these models, and their implications for wetland performance at this site and beyond. A step by step breakdown of the individual chapter descriptions are given next.

Firstly, the development of a modified Curve Number method to quantify the volume of runoff generated from the upland watersheds using the onsite recorded precipitation observations alongside different satellite environmental parameters were performed. This was coupled with the modified SCS unit hydrograph method to simulate the lag times associated with the runoff hydrographs of each recorded precipitation event (chapter 2). These hydrologic models were developed to determine the required input variables for the water budget model of each wetland which also includes the calculation of an evapotranspiration and seepage model to account for the water losses between storm events. A theoretical detention time distribution was also calculated to better understand the wetland hydraulics at the two Harvest Hills sites (chapter 3). The obtained retention time and water budget information were then used to model the nutrient removal efficiencies of the wetland using a relaxed tank in series model. Additionally, the uncertainty associated with the modeled parameters were explored using Bayesian analysis (chapter 4). (The Cain Site was not included in the wetland hydraulic and subsequent treatment modeling due to the inconsistent observed dataset and unusual outflow structure at the site.) Major findings from these models were then used to explore the potential improvements in wetland design to help identify the key parameters responsible for optimal wetland performance (chapter 5).

1.3 Project and Publication History

Earlier versions of chapters 2-4 of this thesis were included as chapters 5-7 in a final project report submitted to the Kansas Water Office and U.S. EPA Region 7 in June 2020 [33], with the exception of section 2.5. The author of this thesis served as the primary author for the corresponding chapters in that report. Field data and observations in that report were collected by project co-investigators Pamela Sullivan and Marvin Stops Jr. of the KU Department of Geography and Atmospheric Science and are cited accordingly when included in this thesis.

1.4 References

1. Ribaudo, M.O., et al., *Least-cost management of nonpoint source pollution: source reduction versus interception strategies for controlling nitrogen loss in the Mississippi Basin.* Ecological Economics, 2001. **37**(2): p. 183-197.
2. United States Environmental Protection Agency, *National Water Quality Inventory: Report to Congress*. 2017, Office of Water, USEPA: Washington, DC.
3. Anderson, D.M., P.M. Glibert, and J.M. Burkholder, *Harmful algal blooms and eutrophication: nutrient sources, composition, and consequences.* Estuaries, 2002. **25**(4): p. 704-726.
4. Correll, D.L., *The role of phosphorus in the eutrophication of receiving waters: A review.* Journal of environmental quality, 1998. **27**(2): p. 261-266.
5. State of Kansas, *A long term vision for the future of water supply in Kansas*. 2015, Kansas Water Office: Topeka, KS.
6. Randhir, T.O. and J.G. Lee, *Economic and water quality impacts of reducing nitrogen and pesticide use in agriculture.* Agricultural and Resource Economics Review, 1997. **26**(1): p. 39-51.
7. Qiu, Z., *A VSA-based strategy for placing conservation buffers in agricultural watersheds.* Environmental Management, 2003. **32**(3): p. 299-311.
8. Biddle, M.A., et al., *Effectiveness of Restored Wetlands for the Treatment of Agricultural Runoff*. 2008, National Risk Management Research Laboratory, Office of Research and Development, USEPA: Ada, OK.
9. Wang, M., et al., *Application of constructed wetlands for treating agricultural runoff and agro-industrial wastewater: a review.* Hydrobiologia, 2018. **805**(1): p. 1-31.
10. Mitsch, W.J. and J.G. Gosselink, *Wetlands*. 4th ed. 2007, Hoboken, NJ: John WIley & Sons.
11. Fink, D.F. and W.J. Mitsch, *Seasonal and storm event nutrient removal by a created wetland in an agricultural watershed.* Ecological Engineering, 2004. **23**(4-5): p. 313-325.
12. Hoagland, C.R., et al., *Plant nutrient uptake and biomass accumulation in a constructed wetland.* Journal of Freshwater Ecology, 2001. **16**(4): p. 527-540.

13. Arheimer, B. and H.B. Wittgren, *Modeling the effects of wetlands on regional nitrogen transport.* Ambio, 1994. **23**(6): p. 378-386.
14. Raisin, G., D. Mitchell, and R. Croome, *The effectiveness of a small constructed wetland in ameliorating diffuse nutrient loadings from an Australian rural catchment.* Ecological Engineering, 1997. **9**(1-2): p. 19-35.
15. Kadlec, R.H. and S. Wallace, *Treatment Wetlands*. 2008: CRC Press.
16. Kadlec, R.H. and S. Wallace, *Treatment wetlands*. 2009: CRC press.
17. Kadlec, R. and S. Wallace, *Treatment wetlands. CRC Press Taylor & Francis Group.* Boca Raton, London, New York, 2009: p. 267-347.
18. Groh, T.A., L.E. Gentry, and M.B. David, *Nitrogen removal and greenhouse gas emissions from constructed wetlands receiving tile drainage water.* Journal of environmental quality, 2015. **44**(3): p. 1001-1010.
19. Jordan, T.E., et al., *Nutrient and sediment removal by a restored wetland receiving agricultural runoff.* Journal of environmental quality, 2003. **32**(4): p. 1534-1547.
20. King, K.W., et al., *Phosphorus Transport in Agricultural Subsurface Drainage: A Review.* Journal of Environmental Quality, 2015. **44**(2): p. 467-485.
21. Kovacic, D.A., et al., *Effectiveness of constructed wetlands in reducing nitrogen and phosphorus export from agricultural tile drainage.* Journal of environmental quality, 2000. **29**(4): p. 1262-1274.
22. Al-Omari, A. and M. Fayyad, *Treatment of domestic wastewater by subsurface flow constructed wetlands in Jordan.* Desalination, 2003. **155**(1): p. 27-39.
23. Akratos, C.S. and V.A. Tsihrintzis, *Effect of temperature, HRT, vegetation and porous media on removal efficiency of pilot-scale horizontal subsurface flow constructed wetlands.* Ecological engineering, 2007. **29**(2): p. 173-191.
24. Vymazal, J., *Removal of nutrients in various types of constructed wetlands.* Science of the total environment, 2007. **380**(1-3): p. 48-65.
25. Kadlec, R., et al., *Constructed wetlands for pollution control: processes, performance, design and operation*. 2000: IWA publishing.
26. Royer, T.V., M.B. David, and L.E. Gentry, *Timing of riverine export of nitrate and phosphorus from agricultural watersheds in Illinois: Implications for reducing nutrient loading to the Mississippi River.* Environmental science & technology, 2006. **40**(13): p. 4126-4131.
27. King, K.W., et al., *Phosphorus transport in agricultural subsurface drainage: A review.* Journal of environmental quality, 2015. **44**(2): p. 467-485.
28. Strategy, K.W.R.a.P. *Upper Wakarusa River WRAPS 9 Element Watershed Plan*. 2011; Available from: http://www.kswraps.org/kdhe-approved-nine-element-watershed-plans.
29. Vymazal, J., et al., *Constructed wetlands with subsurface flow for nitrogen removal from tile drainage.* Ecological Engineering, 2020. **155**: p. 105943.
30. Chomicky, M., *Assessing the Potential of Constructed Wetlands to Reduce Nutrient and Sediment Loading from Agricultural Runoff in a Kansas Watershed.* University of Kansas, 2018.

31. NRCS, U., *Wetland Restoration, Enhancement, or Creation: National Engineering Handbook: Chapter 13, Part 650.* USDA Soil Conservation Service: Washington, DC, USA, 2008.
32. Lee, H., *Nutrient Removal in Constructed Wetlands Treating Agricultural Tile Drainage*. 2016, University of Kansas.
33. Peltier, E., et al., *Assessing the Water Quality Impacts of Constructed Wetlands on Tile Outlet Terrace Runoff (CD-97758901).* University of Kansas, 2020.
34. Peltier, E., et al., *Monitoring Effectiveness of Tile Outlet Terrace Fields with Constructed Wetlands for Sediment, Nutrient and Volume Reduction in Northeastern Kansas*. 2016, Kansas Water Office: Topeka, KS.

Chapter 2

Runoff Modeling

Hydraulic retention time is one of the dominant parameters determining nutrient removal efficiency in a treatment wetland [1]. Since flow rates and total water volume vary substantially at these sites throughout the year, a full water budget model must be constructed to determine water retention patterns. For the wetlands in this study, surface runoff is the primary source of influent water to the wetlands, and thus a key component in the water budget model. While field data on runoff volumes can provide an assessment of the water budget during the study period, estimating wetland hydraulic performance more generally requires the ability to predict runoff generation from storm events occurring under a wider range of conditions than we could collect data from. In addition, runoff modeling can provide insight on the unique factors affecting storm runoff generation on small, terraced agricultural watersheds that will help understand runoff behavior at similar sites. This section addresses the development, calibration, and implementation of a model to estimate surface runoff generation from the three field sites during storm events and transport to their respective treatment wetlands through the on-site tile drain systems.

From a runoff modeling perspective, these small terraced watersheds have several unusual features not commonly addressed in standard runoff models. All three sites have higher slopes than typical agricultural fields, a result of the terraced landscaping. The use of terraces also results in some surface water accumulation on site during runoff events, as water builds up around the standpipe drain located at the low spot of each terrace. Additionally, the sites are relatively small watersheds with one dominant source of vegetative cover that varies seasonally due to the crop planting, growth and harvesting cycle. For these reasons, it was necessary to

develop a site-specific model for runoff prediction that incorporated site topographic, cover and water management features. The approach developed here is one component of our overall modeling approach for these sites. However, it can also be used as a stand-alone model to more accurately estimate runoff from terraced, agricultural fields.

2.1 Approach

A land-surface runoff model integrating the topographic and environmental features of the field sampling sites was developed based on the Natural Resources Conservation Service Curve Number approach [2]. The CN approach for estimating runoff to rainfall ratios was developed for agricultural watersheds and has widespread familiarity within the expected user community. Data on runoff volumes and hydrographs for development and calibration of the model were taken from monitoring data collected from storm events of $\geq$ 1 inch that occurred between April and November 2015 at each site [3]. In total there were 11 storm events from the two Harvest Hills site and 9 from the Cain site fulfilling this threshold.

The runoff hydrographs were simulated to match the time taken by the runoff volume to enter the wetlands. The model (Fig 2. 1) was developed to account for the unusual nature of terraced fields with tile outlet drains, where runoff generated within each terrace accumulates at the bottom of that terrace during a storm event, and then drains away to the wetland. In this model, developed using The U.S. Army Corps of Engineers Hydrological Engineering Center – Hydrological Modeling System (HEC-HMS) software (https://www.hec.usace.army.mil/software/hec-hms/documentation.aspx), each terrace is represented both by a sub-basin and a reservoir. The sub-basin represents the full area of the terrace that generates runoff during a storm event. The reservoir increases in size as runoff builds up on the field surface during a storm event, and then begins to drain through the tile outlet

outflow structure once the estimated depth of water reaches the lowest orifices in the perforated standpipe riser. The riser outflow structures are connected sequentially to the site wetland such that flow from the uppermost (first) terrace combines with flow from subsequent risers as it passes through the tile outlet system.

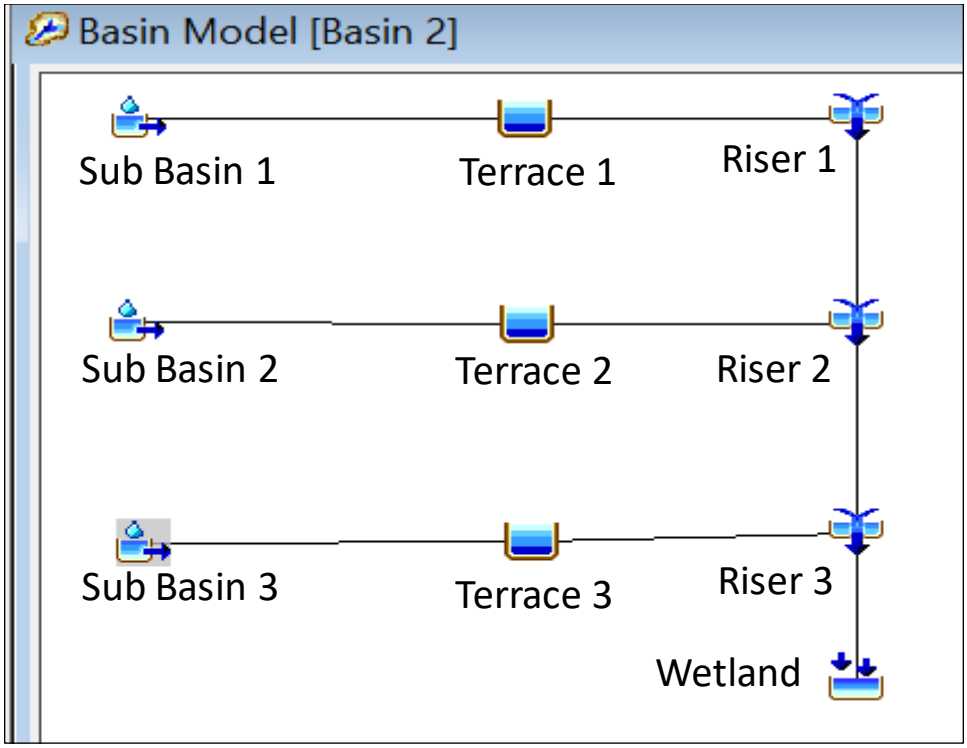

Fig 2. 1 Conceptual model of the runoff model for field TOT systems.

2.1.1 Field Data for Model Development

A 0.01-inch tipping bucket rain gauge (ISCO 674) was installed at the wetland influent sampling location at each site to measure precipitation (Fig 2. 2). Storm water inflows to the wetlands were measured using an area-velocity meter (ISCO 750) located at the outfall of the tile drain.

Fig 2. 2 Inflow monitoring equipment at HHN, picture taken August 2019.

To get a better estimate of water flow patterns, the Harvest Hills field sites were surveyed using a backpack GPS system in Fall 2017 to develop contour maps for each catchment area (Fig 2. 3). Elevation measurements were taken at 5 ft intervals which were then used to assign the relative dimensions of each terrace and the movement of water within the terraces. The developed contour map data were used to determine the stage-storage relationship for runoff buildup in each terrace during storm events using the ARCMAP software (https://desktop.arcgis.com/en/arcmap/). This relationship was used to determine the depth of water ponding during a given storm event (Fig 2. 4).

Field measurements of the standpipe risers at each site were used to determine riser diameter, orifice size, and orifice height relative to the soil surface. The bottom of the first orifice on the standpipe risers was located approximately 4 inches above the soil surface (Fig 2. 5). This distance was used with the stage-storage relationship to estimate the volume of runoff ponded on

each terrace prior to discharging into the tile outlet system. Terrace 2 at Harvest Hills North was modeled using a surface drain rather than a standpipe riser to reflect actual site conditions (see section 1.1). The transport time for water in the tile drains was calculated from the summation of the time taken by the rising and falling limb of the runoff hydrograph for each storm event.

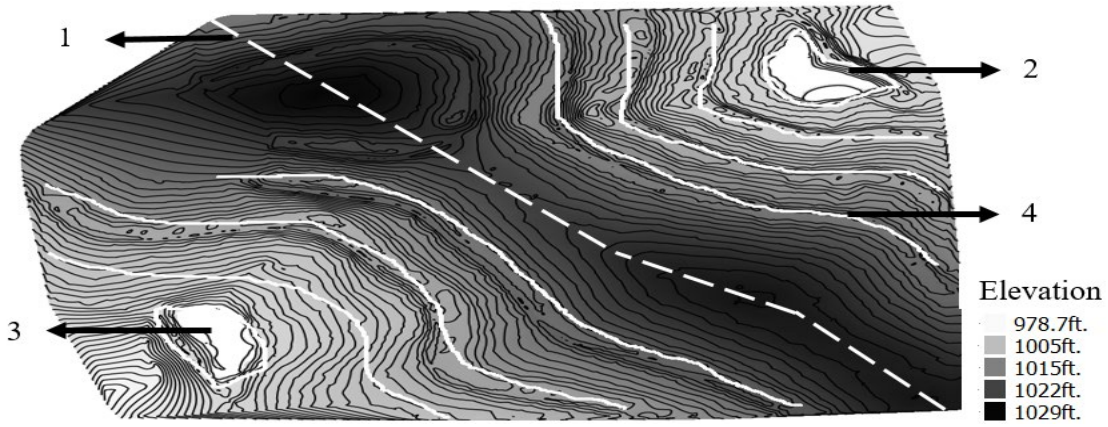

Fig 2. 3 Contour map of the HHN (lower left) and HHM (upper right) watersheds. The dashed line shows the division between the two watersheds, while white lines show the approximate locations of the terrace ridges. 1 = Watershed division line, 2 = HHM wetland, 3= HHN wetland, 4= Terrace borders.

Fig 2. 4 Ponded terrace at HHM, picture taken August 2019.

Fig 2. 5 Standpipe riser photograph

2.2 Calculating Curve Numbers

The curve number method for determining runoff from a given storm event uses Equation 2.1 below, to calculate the depth of runoff over a watershed from a given storm event [4]:

$$Q = \frac{(P - 0.2S)^2}{(P + 0.8S)} \tag{2.1}$$

where,

Q is the runoff depth

P is the rainfall depth

S is the maximum potential retention

All values have units of depth (typically inches). The maximum potential retention, S, is calculated using Eq. 2.2:

$$\mathrm{S} = \frac{1000}{CN} - 10 \tag{2.2}$$

where CN is the curve number for that watershed. The value of CN varies depending on soil type, land cover, and topographical conditions. A limitation of this model, as well as other

similar empirical models, is its tendency to use a single value for CN. This ignores the effect of short-term and seasonal variables, such as surface cover and soil moisture, on runoff retention. For example, higher CNs were noted during periods of less ground cover in a study of 177 small watersheds [5]. Over time, multiple attempts have been made, with varying degrees of success, to modify the CN method to account for soil wetness [6], vegetation cover [7] and topography [8].

Initial modelling using a standard curve number approach (Eq. 2.1 and Eq. 2.2 above) provided poor fits to the empirical runoff data. In particular, the use of a single curve number for a given watershed was not consistent with variations in runoff observed for similar rainfall events over the course of the 2015 sampling period. Based on these initial results, we conducted a regression assessment of multiple environmental factors that could affect the observed variation in curve number, including Atmospherically Resistant Vegetation Index (ARVI), Antecedent Precipitation Index (API), Modis Land Surface temperature (LST) – V6, MODIS Leaf Area Index (LAI) – V6 and MODIS Net Evapotranspiration (ET) – V6. LST, LAI and ET datasets were downloaded for the study sites from the USGS Earth Explorer online resource [9], unscaled and then extracted using the ARCMAP software. API and ARVI were extracted using the Landsat 8 bands and will be described in more detail in the following sections.

A regression trees technique was employed for this work to determine the significance hierarchy of the tested parameters and their contribution to the CN value (Fig 2. 6 - bottom). Regression trees are a part of the CART techniques, first presented by Leo Breiman, et al [10]. The regression trees use a splitting technique in which the data starts from a root node by determining the most significant predictor parameter contributing to the variability of the response variable and then keeps on splitting into child nodes with the available predictors to

improve the prediction accuracy of the response variable. An extension of the simple regression tree is the Random Forest technique which provides the importance of variables by doing an error analysis. This approach calculates how much the prediction error will increase for the model while shuffling the time series data of one variable at a time (Fig 2. 6_- top). The process determines the importance of that variable to the overall prediction of the response variable [11].

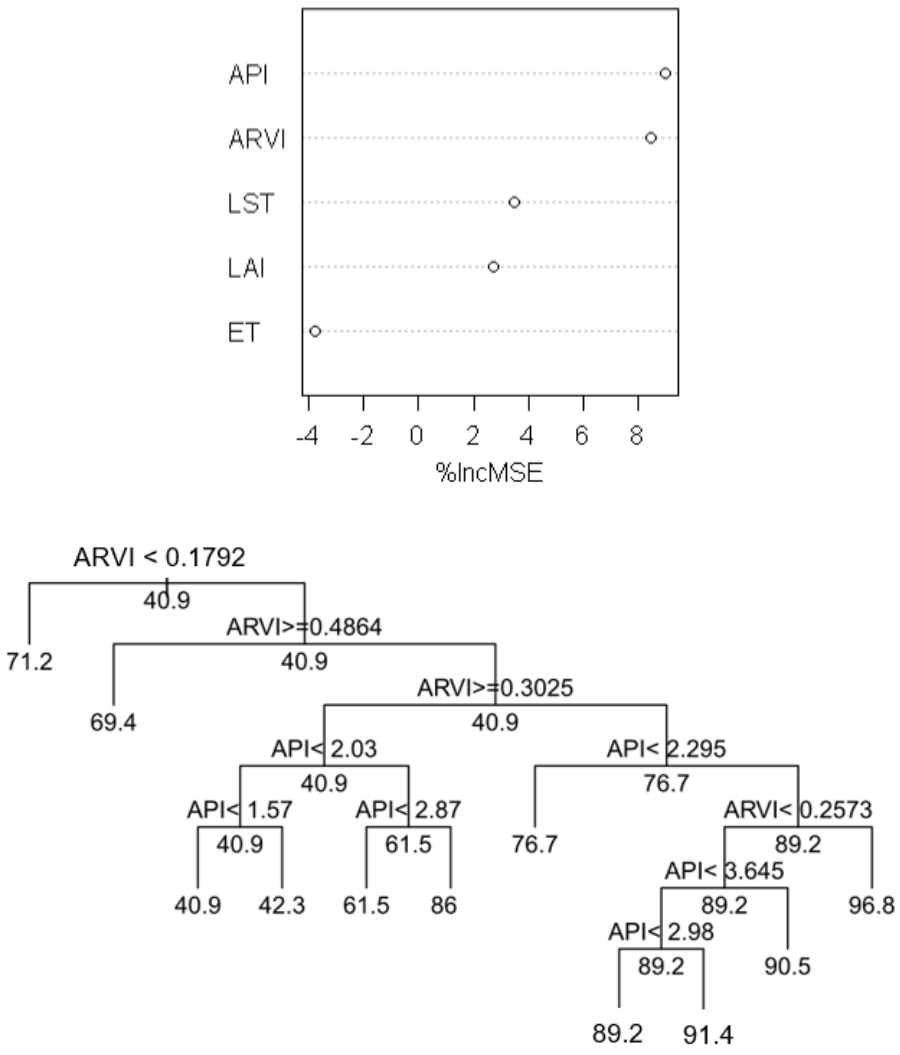

Fig 2. 6 Variable impact on curve number showing the percent mean square error (MSE) increase upon parameter shuffling and regression tree of the CN response variable (bottom) at HHM.

The application of the Regression Tree and Random Forest techniques to our dataset indicated that most of the variability in CN values at both sites could be explained by just two

parameters: Antecedent Precipitation Index (API) and the Atmospherically Resistant Vegetation Index, which quantifies vegetative cover, while the regression tree did not include any other variables in the splits (Fig 2. 6 - bottom). ARVI and API also produced the highest amount of prediction error upon shuffling (Fig 2. 6 – top). Further detail of how these two parameters were incorporated into the curve number calculation is described in the following section.

2.2.1 Antecedent Precipitation

The Antecedent Precipitation Index (API) provides an indication of the remaining soil moisture resulting from previous storm events. More antecedent soil moisture reduces the storage capacity of the soil, reducing the maximum storage potential and increasing runoff during a subsequent event. API was defined by Kohler and Linsley [12] as follows:

$$API_d = k * API_{d-1} + P_d \tag{2.3}$$

where, P_d is the daily rainfall (in inches) and k is an empirical decay parameter. This approach assumes that API decreases at a constant rate (k) for every dry day in between the previous and current storm event. The empirical decay parameter was calculated according to the methods proposed by Crow and Zhan [13], in which they relate the decay parameter with the day number of the year as follows:

$$k = \alpha + \beta \cos\left({}^{2\pi d_i}/_{365}\right) \tag{2.4}$$

where α and β are calibrated for each watershed

The calibrated values of α was 0.85 for all three watersheds. The calibrated value of β was 0.01 for HHN and Cain watershed but 0.025 for HHM. These values were obtained by trial and error method, with the objective function of producing the least error between the observed and predicted runoff. The k value was varying in accordance with the Julian day number (d_i) from the beginning of the year. The sampled onsite precipitation dataset did not have enough

preceding days data available to stabilize the API values for the first storm events in our dataset. Therefore, the Clinton Lake gage (ID: GHCND: USC00141612) precipitation dataset from Jan 2015 to Apr 2015 from the National Oceanic and Atmospheric Administration (NOAA) Climate Data Online repository [14] was used to supplement the observed onsite precipitation data. API was then calculated for the combined dataset (i.e., Jan – Nov).

2.2.2 Vegetation Coverage

To represent seasonal changes in vegetation coverage at the site without requiring direct measurements, a remotely sensed vegetation index was included in the model. The Normalized Density Vegetation Index (NDVI) has been widely used in the literature to quantify vegetation biomass through the satellite data obtained from Landsat images [15, 16]. Gonzalez et. al [7] developed a direct relationship between the NRCS CN and an NDVI-derived greenness fraction, and showed that this adjustment significantly improved model prediction capability for a specific watershed. The NDVI values are calculated using the near infra-red (NIR) and red reflectance bands from Landsat Images:

$$NDVI = \frac{NIR - Red}{NIR + Red} \tag{2.5}$$

However, due to the potential effect of aerosol scattering and absorption in remote sensing, additional vegetation indexes have been developed over the years to improve the efficiency of vegetation indexes in predicting land cover. One such index is Atmospherically Resistant Vegetation Index, which has been found to reduce effect of change in atmospheric opacity and depicts conditions on land with much better accuracy [17]. ARVI was developed by modifying Eq. 2.5 as follows [18]:

$$ARVI = \frac{NIR - RB}{NIR + RB} \tag{2.6}$$

Here, RB is the combination of reflectance obtained from Red and Blue band channels:

$$RB = Red - \gamma(B - Red), \tag{2.7}$$

where the value of gamma (ɣ) depends on the aerosol type but the general default value of 0.5 was used here. The difference between the shorter wavelength blue band and the relatively longer wavelength red band gives the indication of the atmospheric conditions present at a particular point in time [17].

ARVI were calculated using the reflectance bands from the USGS LANSAT 8 Operational Land Imager Collection 1 Level 1 datasets (Spatial Resolution: 30m). A Geographical Information System application (https://desktop.arcgis.com/en/arcmap/) was used to extract the ARVI values for every 16 days from 5/1/2015 to 11/9/2015. A simple linear transition of ARVI was assumed to assign values to storm events happening during the 16 days gap.

2.2.3 Developing an Adjusted Curve Number Equation

Since there is no pre-existing determination of the linearity of the relationship between our two parameters (API and ARVI) and CN, several different forms of equations were developed and then compared using the Akaike Information Criterion (AIC). The AIC is calculated as follows [19]:

$$AIC = 2k - 2\ln(L) \tag{2.8}$$

where k is the total number of predictor variables and L is the likelihood function, which can be defined as the probability of data being generated by the model with specific parameter values. A lower AIC value indicates that the model equation does a better job representing the relationship between the tested parameters and the curve number. This approach accounts for the expectation that more parameters will increase the fit by increasing the AIC value for each parameter added.

Only an increase in the likelihood of the model can overcome this penalty. The equations listed below were developed to test the different combinations of the API and ARVI. The complexity of the potential equations was restricted to cubic expressions.:

- $fit\ 1 \rightarrow\ CN = \text{a.API} + \text{b.ARVI} + \text{Intercept}$
- $fit\ 2 \rightarrow CN = \text{a.API} + \text{b.API}^2 + \text{c.ARVI} + \text{Intercept}$
- $fit\ 3 \rightarrow CN = \text{a.API} + \text{b.API}^2 + \text{c.API}^3 + \text{d.ARVI} + \text{Intercept}$
- $fit\ 4 \rightarrow\ CN = \text{a.API} + \text{b.ARVI} + \text{c.ARVI}^2 + \text{Intercept}$
- $fit\ 5 \rightarrow\ CN = \text{a.API} + \text{b.API}^2 + \text{Intercept}$
- $fit\ 6 \rightarrow\ CN = \text{a.ARVI} + \text{b.ARVI}^2 + \text{Intercept}$

For each form, the optimal values of the watershed calibration parameters were obtained by minimizing the sum of squared residuals, which can be calculated for both linear and nonlinear models [20]. The AIC_c differences (Δ_i) between the best fit model equation (i.e, the equation having the lowest AIC) and the rest of the individual equations are presented in Table 2. 1.

Table 2. 1 Computed values of Akaike's Information Criterion (AIC_c) and AIC_c differences (Δ_i).

Model	k	AIC	(Δ_i)
$fit\ 1$	2	80.78	1.85
$fit\ 2$	3	78.93	0
$fit\ 3$	4	80.35	1.42
$fit\ 4$	3	82.52	3.59
$fit\ 5$	2	93.15	14.22
$fit\ 6$	2	84.39	5.46

Generally, equation forms with $(\Delta_i) < 2$ are considered to have substantial validity, while values of (Δ_i) in between 2 and 10 are supposed to provide considerably less empirical support that the model represents the data and a value of $(\Delta_i) > 10$ generally represents a poor approximation [21]. Fit 2 produced the lowest overall AIC value, while both fits 1 and 3 showed an increase in AIC (Δ_i) of < 2, indicating substantial predictive power for CN. The increase in the degrees of freedom from fit 1 to fit 2 was justified by the lower AIC score of fit 2. Contrarily, going from fit 2 to fit 3, the increase in the degrees of freedom failed to increase the likelihood enough to compensate for the penalty and hence produced a higher AIC score. The two fits that included only API or ARVI (fits 5 and 6) had both the poorest AIC value and greatest increase in Δ_i compared to the best fit. Even when compared with fit 1, which has the same overall degrees of freedom, these fits more poorly represented the available data.

Based on these results, the adjusted curve number equation used for model calibration and validation was fit 2, reproduced below as Eq. 2.9:

$$CN = a.API^2 + b.API + c.ARVI + \mathrm{I} \tag{2.9}$$

where a, b, c and I are watershed-specific constants.

This predictive capability of Antecedent Precipitation Index has been tested before [22], with a Normalized Antecedent Precipitation Index (NAPI) used to predict the direct runoff from watersheds with area < 1000 acres. The predictive NAPI model was defined as:

$$\ln\left(1 - \frac{Q}{P}\right) = a + bP + cNAPI \tag{2.10}$$

where Q and P are the same as Eq. 2.1. Since Eq 2.10 doesn't incorporate the calculation of CNs, this equation was also used as an alternative approach to estimate the power of API as a direct predictor of runoff generation onsite.

To better isolate the impact of vegetative cover on runoff volumes from these sites, curve numbers were also calculated using fit 5, reproduced below as Eq. 2.11, which includes only the API parameter:

$$CN = a.API^2 + b.API + \mathrm{I} \tag{2.11}$$

These results were then contrasted with the results obtained from fit 1 since it has the ARVI parameter with an equal degree of freedom. Fit 1 is reproduced below as Eq. 2.12:

$$CN = a.API + b.ARVI + \mathrm{I} \tag{2.12}$$

2.3 Model Calibration and Validation

2.3.1 Storm Runoff Hydrographs

Hydrographs for each storm event were developed using HEC-HMS. The SCS dimensionless unit hydrograph method was used to develop the direct runoff hydrographs. The SCS method uses the time to peak (Tp) and peak flow (Qp) to develop the dimensionless unit hydrograph. Time to peak is calculated using the seasonal calibrated lag times and excess precipitation for each storm event. Peak flow is determined using the peak rate factor (PRF) and watershed area (A).

The standard SCS unit hydrograph equations use a peak rate factor of 484. Using this value for PRF, adjustments to the lag time were not sufficient for the model to match both the time to peak and the peak flow in the observed hydrographs from the field data (Fig 2. 7). Given the known flashy nature of these watersheds demonstrated in field data collected during the 2016-2018 field sampling [23], the peak rate factor was reduced from 484 to 100 for our model, which achieved the desired result of matching both the time and intensity of the peak flow in the model hydrographs to that observed onsite (Fig 2. 8 – bottom right). The dimensionless unit hydrograph coordinates (y = Q/Qp, x = T/Tp) for the new PRF were calculated by HEC-HMS,

but can also be manually determined using the equation described in [24]. The constructed unit hydrograph for each storm event was then used to produce the direct runoff hydrographs. Time base (tb) and duration of excess precipitation (D) for each hydrograph were also manually calculated using the standard SCS unit hydrograph method.

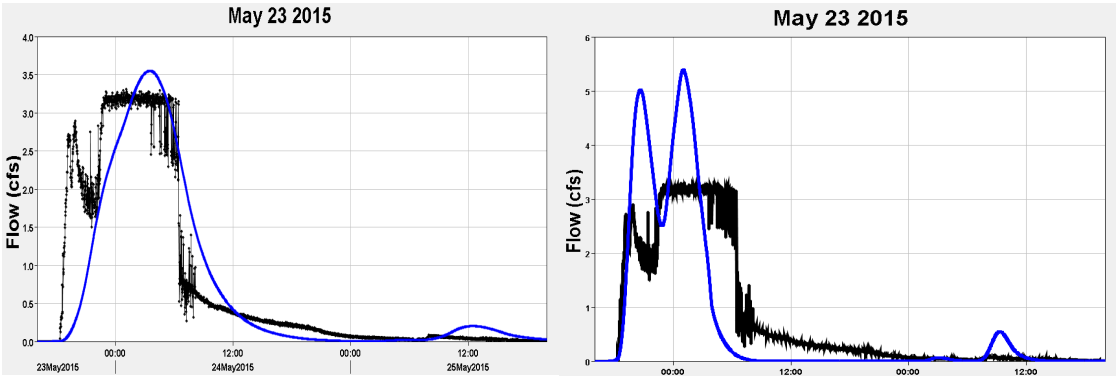

Fig 2. 7 Hydrographs observed (Black) vs predicted (Blue) for the storm event of May 23. Increasing the Lag time to 300 min (left) matches the observed peak flow but not the time to peak and reducing the Lag time to 100 min (right) does the opposite.

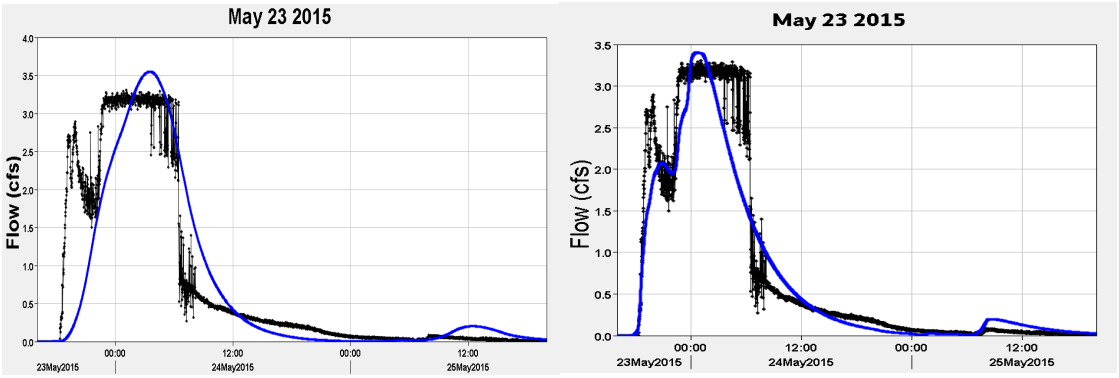

Fig 2. 8 Hydrographs observed (Black) vs predicted (Blue) for the storm event of May 23 (lag 300 min). Decreasing the PRF to 100 (right) matches the observed peak flow and the time to peak which is an improvement from the standard SCS PRF of 484 (left)

The observed hydrograph presented for the May 23rd storm event in Fig 2. 8 produced a flat peak flow which was particularly hard to simulate. This was not an isolated behavior and was consistent across several storm events across the year especially during high flow season. Several examples can be seen below in Fig 2. 9.

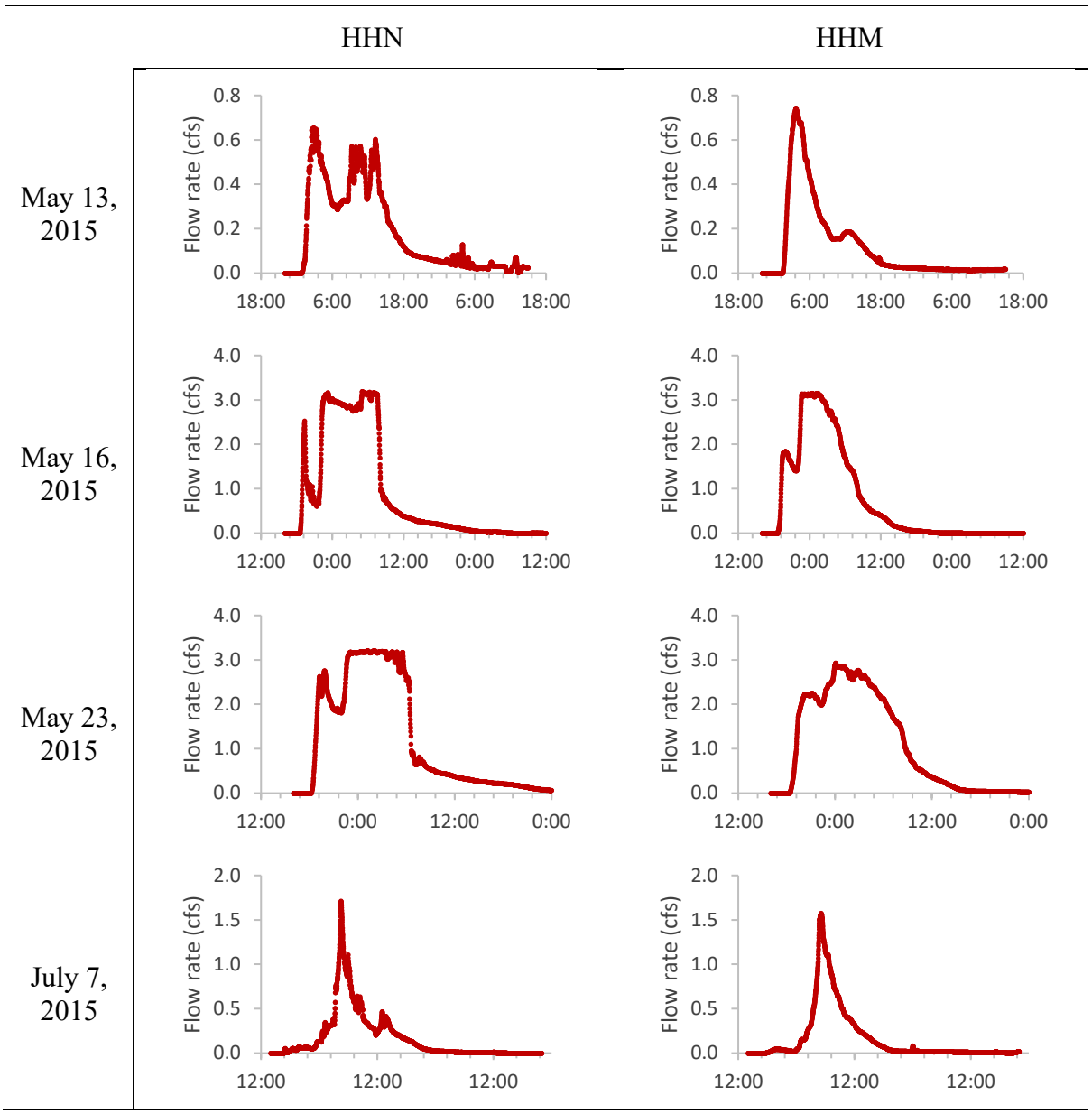

Fig 2. 9 Observed Runoff hydrographs for four storm events happening in 2015. Hydrographs represent 15 min average runoff.

The runoff hydrograph observed for May 16th and May 23rd storm event produced flat peaks at around 3 cfs at both sites. Contrarily, the av meter produced a smoothly curved peak for the storm event happening on May 13th, 3 days before the May 16th storm event. Since the two storm events happened so closely, the difference in peak shapes would most probably be because of the difference in peak flows and not because of the av meter malfunction.

One possibility might have been the maximum flow rate measurement capacity of the av meter sensor. However, the specifications for the av meter used on our site (ISCO AV750) indicate a maximum velocity measurement capacity of 20 ft/s [https://www.teledyneisco.com/en-us/waterandwastewater/Pages/750-Module.aspx]. This equates to a maximum influent flow rate of 6.98 cfs when flowing through an 8-inch diameter drain-pipe, as was the case on our sites. The second possibility is that, under full submergence conditions, the maximum velocity limit of the tile drain systems themselves is around 8.5 ft/s (3 cfs). Of these two possibilities, it is more likely that it is a site limitation under fully submerged conditions.

Since the purpose of the storm hydrograph simulation in this study was to match the time taken by the storm events to move off the watershed and enter the wetlands (see section 2.1), the particular issue of flat hydrograph peaks was not addressed further. The simulated hydrographs matched the total time base (tb) (i.e., the summation of peaking and receding limbs of the hydrograph) of the observed hydrographs (see Fig 2. 8). This was enough to calculate the average volumetric flow rate of the runoff water entering the wetlands.

2.3.2 The necessity of predicting CNs (limitation of the NAPI model - Eq 2.10):

Fig 2. 10 shows the results of using Eq. 2.10, which directly estimates runoff from antecedent precipitation, at the two model sites. The values for a, b and c in this equation were determined using the 2015 runoff data from the HHM site. The values for these calibration parameters were (a: 0.94, b: -0.82, c: -0.12). Note that this equation produced no runoff for some of the storm events on the two validation sites. This trend was due to the poor fit of Eq. 2.10 predicted values in the case of small storm events. While the CN-based models generated a unique initial abstraction (Ia) value for each predicted storm event, the direct runoff-estimation model maintained a constant calibrated initial abstraction depth, calculated as ($Ia = -a/b$).

Therefore, small storm events in the validation watersheds (P<Ia) produced no runoff with the direct prediction model. It should be noted that the NAPI model was never claimed to be validated on watersheds with crop types different than those from the calibration dataset. Therefore, the purpose of this discussion is not to identify its specific inaccuracy, but to point out the limitations of this more direct approach to calculating runoff based on antecedent precipitation.

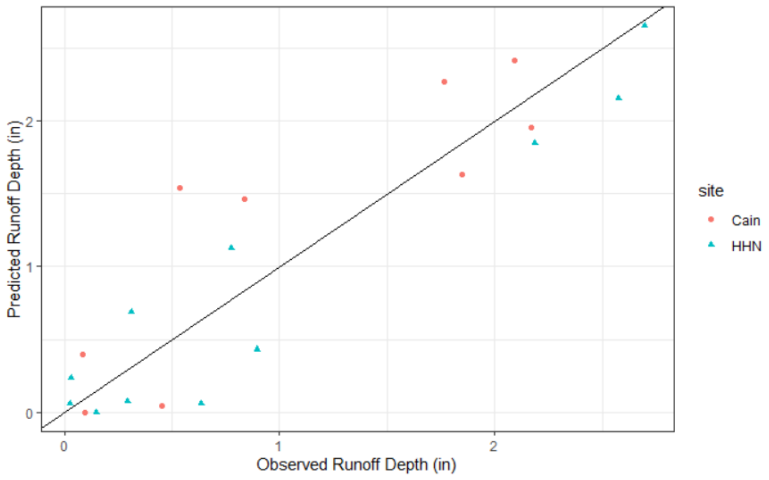

Fig 2. 10 Comparison of predicted and observed runoff depth for HHN and Cain watersheds using Eq. 2.10. The solid line shows 1:1 correlation.

2.3.3 Validation of the best fit equation (Eq 2.9):

The coefficient of determination (R^2) was calculated to determine the goodness of fit and the Nash Sutcliffe model efficiency coefficient (NSE) was used to quantify the performance of model prediction relative to observed measurements. R^2 measures the degree of linear relationship between the observed and simulated datasets. Therefore, a model which consistently over or under predicts can still produce a high R^2 value. NSE values, on the other hand, determine how well the plot of predicted vs observed data matches the 1:1 line. NSE, while incorporating the correlation, also takes the mean and variance between the two datasets into account. NSE values close to 1 represents better model performance.

For Eq. 2.9, the values of a, b, c and I were 34.11, -4.11, -91.06 and 46.58 respectively. The calibrated parameters were statistically significant with ($F(3,7) = 23.54$, $p < 0.0005$) and R^2 of 0.91. As previously mentioned, the calibration of the equation was performed at HHM site. The validation plots at the HHN and Cain site are presented below in Fig 2. 11. The statistical goodness of fit values is presented in Table 2. 2. The model equation produced good values for all three goodness of fit indicators.

The two sample Students t-test [25] was performed to test the assumption that the predicted and observed runoff values were statistically similar at each site (Table 2. 2). The p value was greater than 0.05, indicating that there is insufficient statistical evidence to reject the null hypothesis that the means of the observed and predicted values are same for the calibration and validation watersheds at 95% confidence.

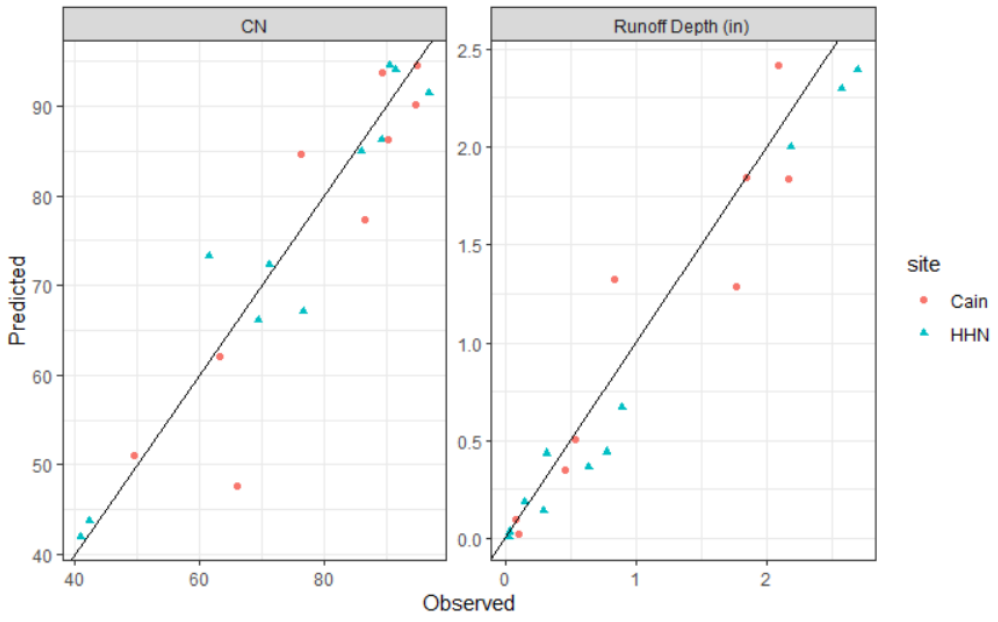

Fig 2. 11 Comparison of Predicted and Observed Curve Numbers (left) and runoff depth (right) for HHN and Cain watersheds using Eq. 2.9. The solid line shows 1:1 correlation

Table 2. 2 Statistical validation of the predicted runoff depths obtained using Eq. 2.9.

	R^2		P(T<=t) two-tail		NSE	
	HHN	Cain	HHN	Cain	HHN	Cain
Eq. 2.9	0.99	0.94	0.73	0.96	0.94	0.88

2.3.4 The necessity of ARVI (Eq 2.11 vs Eq 2.12)

The cropped portion of these watersheds is very high, at 78%, 95% and 88% for the HHN, HHM and Cain sites, respectively. As a result, vegetative cover at all three sites varies significantly over the course of the year. This produces a recurring pattern in which the ARVI values increase throughout the growing season and decrease in late fall (Fig 2. 12). However, the presence of green vegetation is often different for each site at a particular point in time. This difference produces a change in ARVI values as the larger presence of green vegetation decreases the signal in the red band and increases the signal in the NIR band, boosting up the ARVI value [18] (see Eq. 2.6). The sensitivity of the differences can be visualized by comparing the two neighboring Harvest Hills site. The differences are intensified at the peaks, representing the largest differences in green vegetation growth during the growing season (Fig 2. 13). Both seasonal and site-to-site variations in vegetative cover have a notable impact of runoff generation at these sites, as discussed later in the section.

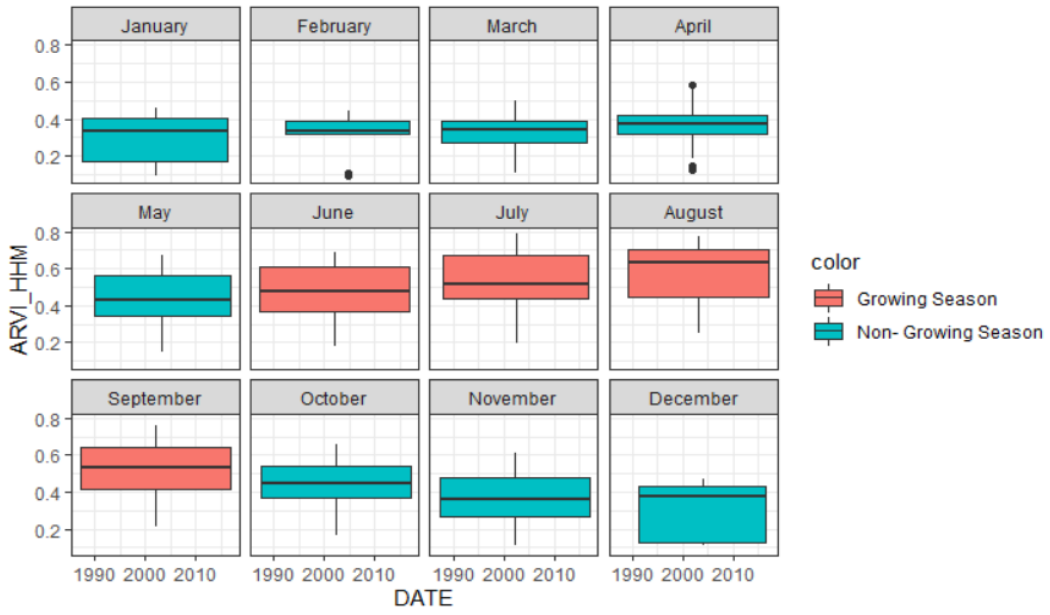

Fig 2. 12 ARVI pattern on HHM site from 1985-2018.

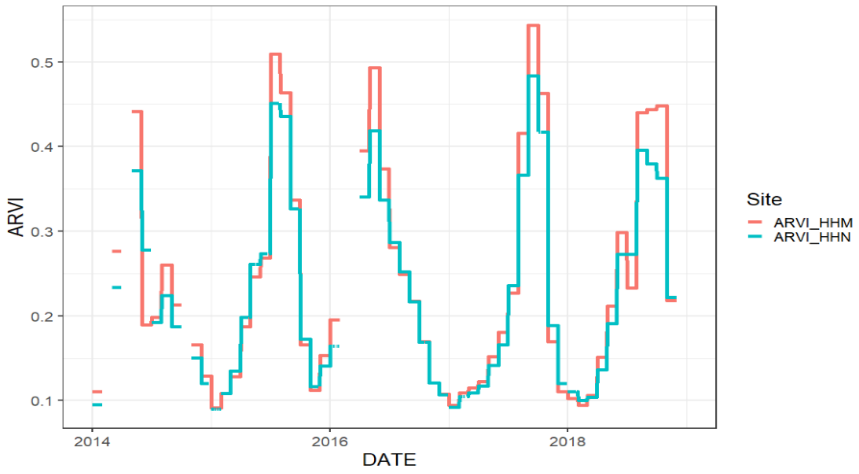

Fig 2. 13 ARVI values for HHN and HHM from 2014-2018.

The calibrated values for the constant terms in Eq. 2.11 and 2.12 for HHM based on 2015 runoff data from that site are shown in Table 2. 3. For Eq. 2.12, the calibrated parameters were statistically significant with ($F(2,8) = 34.65$, $p < 0.0005$) and R^2 of 0.90. Here the F statistic is the ratio between the Mean Sum of Squares (i.e., variation between the datasets) to the Error Mean Sum of Squares (i.e., variation within the datasets). Therefore, the F value of 23.54 at $p < 0.0005$ represents that there is a significant combined effect of API and ARVI on the CN

obtained at p <0.05 level. Similarly, for Eq. 2.11 the values of a, b and c were 8.62, 1.36 and 41.51 respectively with (F (2,8) = 5.81, p < 0.05) and R^2 of 0.59.

Table 2. 3 Calibration parameters for CN equations

Parameter	Eq. 2.11	Eq. 2.12
a	8.62	12.81
b	1.36	-82.79
I	41.51	68.09

Since the full dataset of storm events at HHM was used for model calibration, validation was carried out using data from the other two field sites. Curve numbers calculated using Eq. 2.11 and Eq. 2.12 with the values from Table 2. 3 were used to calculate the predicted runoff depth for the HHN and Cain site using Eq. 2.1. The comparison between the observed and predicted curve numbers and runoff values at both validation sites is shown in Fig 2. 14 for Eq 2.11 and Fig 2. 15 for Eq 2.12.

.

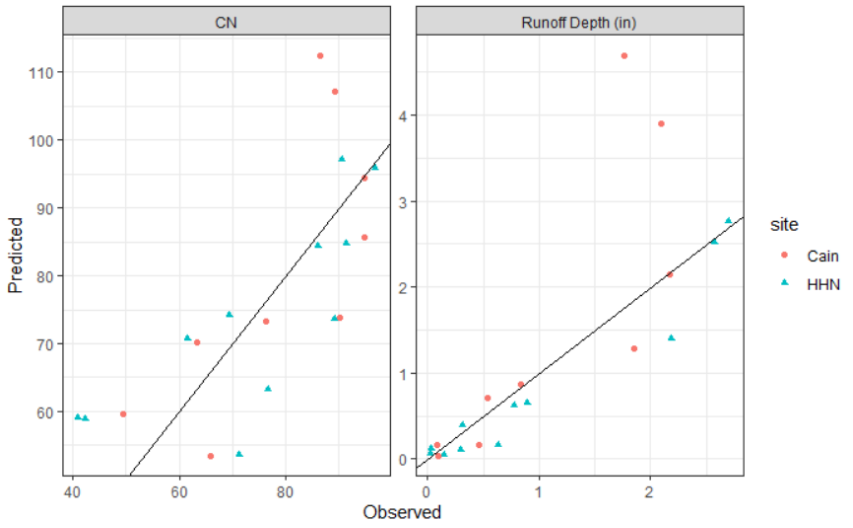

Fig 2. 14 Comparison of Predicted and Observed curve numbers (left) and runoff depth (right) for HHN and Cain watersheds using Eq. 2.11 (without ARVI). The solid line shows 1:1 correlation.

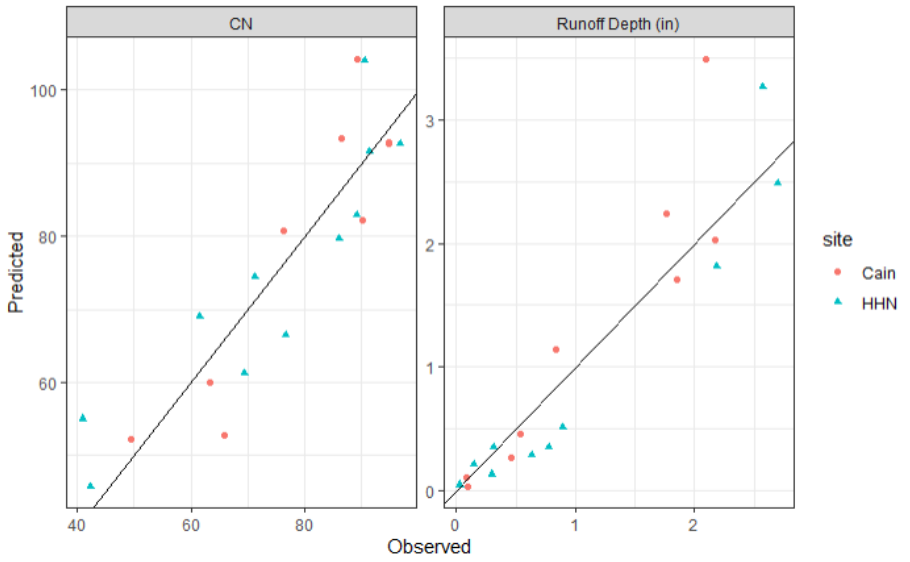

Fig 2. 15 Comparison of Predicted and Observed curve numbers (left) and runoff depth (right) for HHN and Cain watersheds using Eq. 2.12 (with ARVI). The solid line shows 1:1 correlation.

Fig 2. 15 shows that Eq. 2.12 was generally able to match both curve numbers and runoff depths recorded for individual storm events at the HHN and Cain sites. The model does appear to slightly over predict runoff depths for higher-volume storms (> 2 in runoff depths), but overall matches well across the range of events. A group of storm events at both sites have both model-calculated and observed curve numbers greater than 90, which is unusually high for agricultural sites. There are two major factors affecting these values. The first is the high slope at these terraced sites, which leads to greater runoff, particularly during high-intensity events. The second is timing: the majority of the high CN events occurred in a short period in May-June 2015. This occurred when crop cover was minimal and resulted in high residual soil saturation during this period.

Both Eq. 2.11 and 2.12 showed minimal difference in the ability to predict runoff from the HHN site, which is most similar to the calibration site in terms of soil conditions, size, and crop cover. However, both model equations produced CN > 100 for a couple of storm events. This shows the particular difficulty both model equations experience with high runoff storm

events. Since, neither of these two equations were selected as the best fit equation and will not be used for further analysis, this issue was not investigated further.

Removing the ARVI component (Eq 2.11) produces more variation between model-predicted and observed values for both CN and runoff depth, particularly at the Cain site (Fig 2. 14). This model appears to have particular difficulty with high runoff events at the Cain site. Three events that generated observed runoff of approximately 2 inches have model-predicted runoff values ranging from ~ 1.5 to 4 inches.

Table 2. 3 shows that both goodness of fit measures used to evaluate model performance for runoff depth (R^2 and NSE), were similar for both equations at the HHN site. However, both measures showed a decrease for the Cain site when using Eq 2-11. The presence of ARVI in Eq 2.11 in place of the API^2 present in Eq 2.12, produced better goodness of fit results. This greater effect of ARVI on model performance at Cain is likely due to the various differences present at Cain site, one of which is the change in crop type. HHN had the same crop planting in 2015 as the calibration site (corn), while soybeans were planted at Cain that year. Therefore, the change in crop type might have forced many other variations between the sites including the variations in the timing of the crop plantation and harvesting, differences in the ratio of bare soil patches to crop cover and others. However, the two Harvest Hill sites were farmed by the same operator, and therefore had nearly identical planting and harvesting times and crop management practices. The Cain site had a different operator, which resulted in some differences in farming practices. All of these differences could have played a role in producing lower goodness of fit values at the Cain site. While the variations among the HHM and Cain site was better captured by the model equation containing the ARVI term, it is therefore impossible to attribute this effect to a specific difference, such as crop type.

In all cases, the p value from the two sample student's t-test was greater than 0.05, indicating that there is insufficient statistical evidence to reject the null hypothesis that the means of the observed and predicted values are same for both watersheds at 95% confidence.

Table 2. 4 Statistical Comparison of the predicted runoff depths obtained using Eq. 2.11 and Eq. 2.12.

	R^2		P(T<=t) two-tail		NSE	
	HHN	Cain	HHN	Cain	HHN	Cain
Eq. 2.11	0.96	0.79	0.72	0.48	0.90	0.47
Eq. 2.12	0.96	0.92	0.78	0.39	0.91	0.79

2.3.5 Model Performance for 2016-2018 Storm Events

Observed velocity and precipitation data collected from the two Harvest Hills site in 2017-18 were used to validate the model performance. Maintaining the threshold of significant precipitation event (i.e., total rainfall > 1in) resulted in 3 storm events in HHM and 4 storm events in HHN. This low number of events reflects the relatively dry conditions, particularly in 2018, as well as some difficulties with the flow-monitoring equipment at HHM during 2017. ARVI and API values were calculated using the same procedure described before. The results obtained are plotted below in Fig 2. 16.

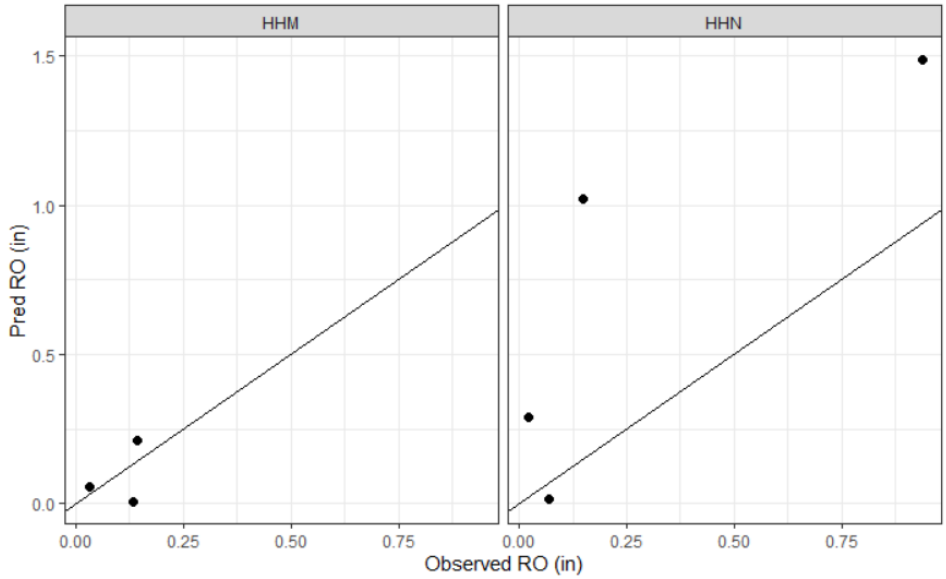

Fig 2. 16 Predicted vs observed runoff for HHM and HHN.

In total 5 of the 7 storm events (i.e., all 3 at HHM and 2 of 4 at HHN) produced satisfactory results (i.e., Predicted Runoff / Observed Runoff is close to 1:1 line). For the other two storm events, the model substantially over-predicted runoff relative to the observed runoff volumes. Both of these events occurred during 2018, which otherwise had very low rainfall. Compared to other storm events recorded from this site from 2014-17, the observed rainfall to runoff ratios for these two events in 2018 were unusually low compared to other storm events during the study periods, producing very high runoff than expected. This may indicate a change in soil or vegetation properties due to the extended low-rainfall period. This might have reduced the capacity of the dry soil to absorb moisture. These results suggest that there are limitations in applying the runoff model, calibrated during a wet year, to particularly dry conditions.

2.4 Model Application on Large Watershed

The incorporation of a vegetation index in the runoff prediction equation is not generally found in the literature. Given its successful implementation on our study sites, the next step was to test its utility on large watershed with heterogenous crop cover. Additionally, this watershed

allowed examination of the performance of the developed model equations (Eq 2.9 and 2.10) on a much larger spatial and temporal scale.

2.4.1 Site Description:

NASA Goddard Earth Sciences (GES) Data and Information Services Center (DISC) (Site Name: X240-Y104 of North American Land Data Assimilation System (NLDAS) NASA) (Stream gage location, Lat: 38.0625, Lon: -94.9375) was selected to evaluate the performance of the proposed model on large temporal (1990 – 2017) and spatial scale (Data Service URL: http://disc.sci.gsfc.nasa.gov/hydrology/data-holdings) (Accessed from: https://data.cuahsi.org/). The EPA watershed map alongside the stream flows and gage location is presented below in Fig 2. 17. The site was selected because of its location in proximity to the study site (~90 miles south of the Harvest Hills Watershed), which provides similar climate patterns. This site also had a similar land cover area with mostly grassed and cropped fields. Precipitation data was obtained from NLDAS-2 Forcing A 0.125-degree hourly dataset, while NLDAS-2 forcing NOAH model 0.125-degree hourly data was used to extract the surface runoff (non-infiltrating). NLDAS forcing data were generated using a range of individual variables including air temperature, specific humidity, wind speed, surface pressure, incoming solar radiation, incoming longwave radiation and precipitation [26].

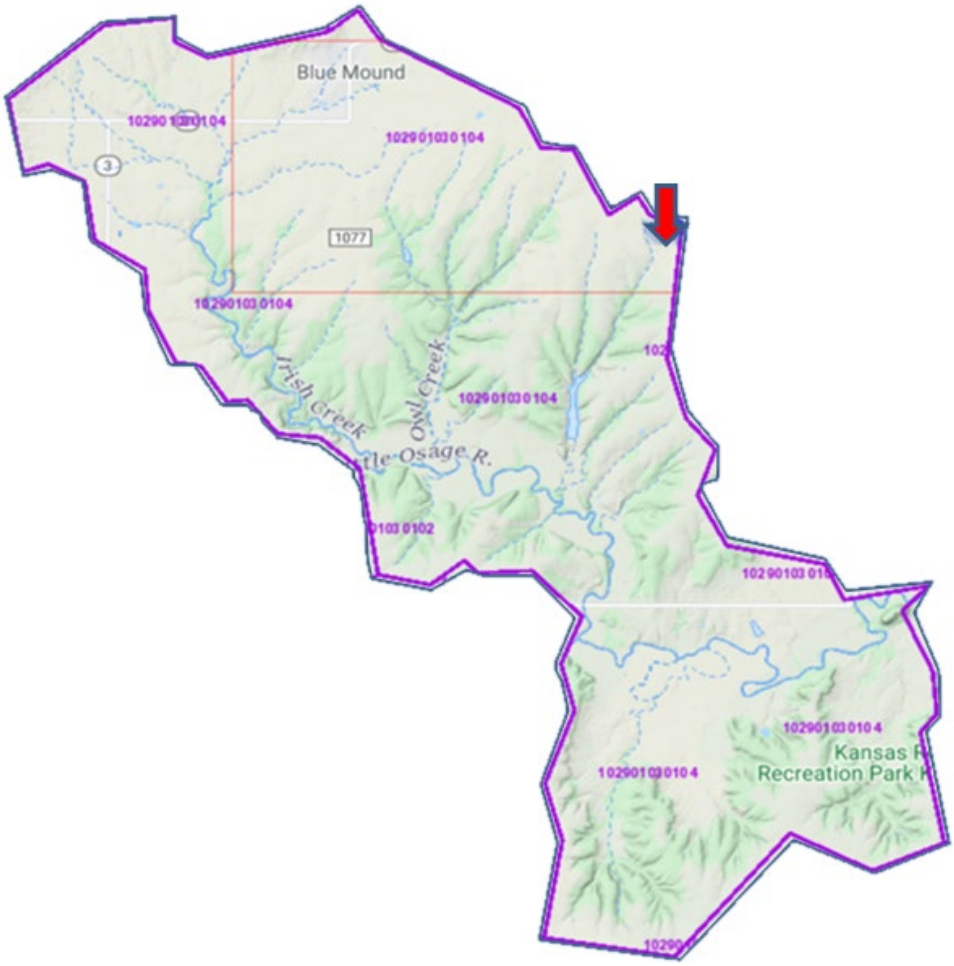

Fig 2. 17 Map of EPA Watershed boundary with the hydrological unit code (more info: https://www.epa.gov/wsio), drainage networks (more info: https://www.usgs.gov/core-science-systems/national-geospatial-program/national-map) and stream gage location (red arrow) (more info: https://waterwatch.usgs.gov/index.php?id=ww_current). Accessed from https://data.cuahsi.org/.

2.4.2 Methodology

The NLDAS-2 surface runoff dataset for 1990-1993 was used to calibrate the model equations. The calibrated equations were then used to generate runoff for the following fourteen years (1994-2017). This was done to evaluate the capability of the simple conceptual proposed model to match the relatively complex NLDAS-2 model generated runoff values.

As in Case 1, API and ARVI were calculated for the respective time periods. The hourly precipitation and runoff values were lumped into a monthly time scale and the initial curve

numbers for the year 1990-1993 were calculated using Eq. 2.1 (Fig 2. 18). The two model equations, Eq. 2.9 and Eq. 2.11 were calibrated using the calculated CNs.

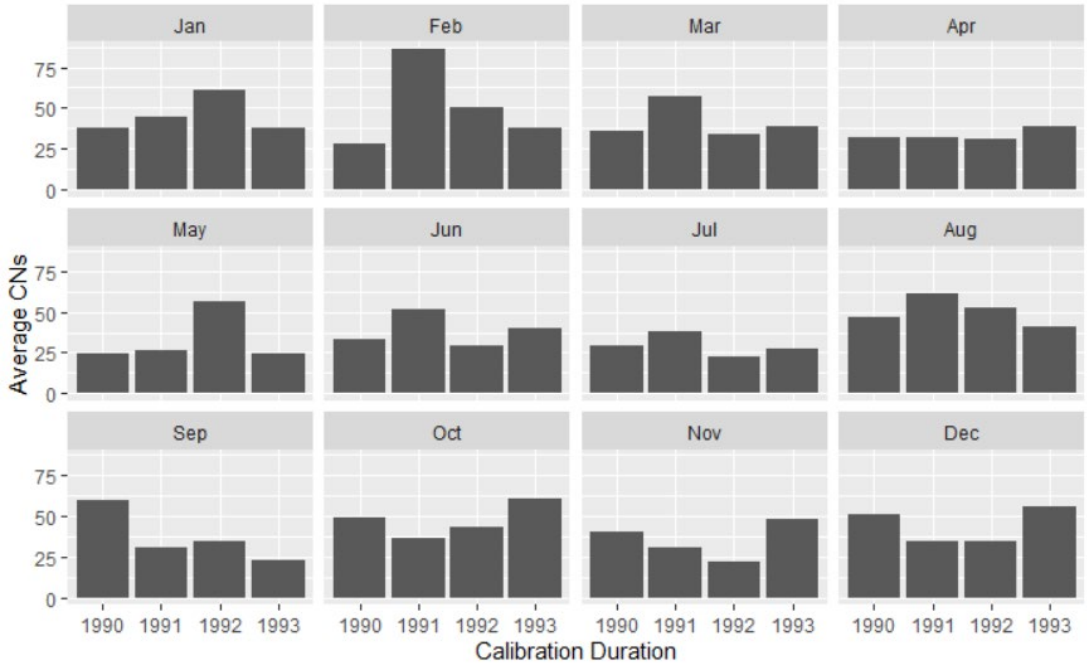

Fig 2. 18 Calculated watershed CNs for 1990-1993 (used to calibrate the model equation).

Afterwards, the two calibrated equations were tested for the AIC values against the calibration residuals. Eq. 2.9 was found to produce a higher AIC value (AIC= 167.108) against Eq. 2.11 (AIC= 165.62). This is counter to the small-scale watershed results, where inclusion of ARVI improved model performance. This is likely due to differences in the watershed size and heterogeneity. The study sites were small enough to contain monoculture crop cover during a given growing season. The larger watershed area at the NASA observation site covers land with heterogenous crop types and growth patterns. Under these conditions, a composite vegetation index did not manage to create any significant improvement on the model calibration. This might be due to the use of a monthly averaged ARVI value which failed to capture the spatial and temporal variations associated with the crop type and planting practices on individual

watersheds. Therefore, Eq. 2.9 was omitted from the analysis and the calibrated Eq. 2.11 was used to calculate the monthly runoff values for the following fourteen years (1994-2017).

The calculated CN for the calibration period showed high standard deviation which ranged from 6.46 for July to 25.35 for Feb. Therefore, to justify the requirement of a conceptual model utilizing environmental parameters to predict CN on such watersheds, the impact of CN variation was tested by using the four-year (1990-1993) monthly average CN during the calibration time period to predict the monthly runoff for the following fourteen years. These results were then compared with the results obtained from the conceptual model (Eq. 2.11). The NAPI model (Eq. 2.10) was not used here, since it was designed to calculate the runoff on watersheds <1000 acres.

2.4.3 Results:

The calibrated values of the watershed parameters a, b and c for Eq. 2.11 were found to be -40.88, 10.78 and 63.42 respectively. The parameters were statistically significant with ($F(2,45) = 30.41$, $p < 0.0001$) and an adjusted R2 of 0.57.

The goodness of fit, as represented by the R^2 values was significantly higher for Eq. 2.11 than for the average CNs approach, representing that there is insufficient statistical evidence to reject the null hypothesis that the means of the observed and predicted values are same for the observed and simulated datasets. The average CNs method failed to meet this standard, with a p value < 0.05 (Table 2. 5) indicating that the means of the observed and predicted data are significantly different.

The quality of predicted results was compared using the index of agreement (d) and Relative Biasness (RB) parameters. Eq. 2.11 produced a much closer value to 0 of RB, therefore producing a much better match to the NLDAS-2 model generated values than average CNs

method, which was found to be overpredicting. These results can be verified visually from Fig 2. 19, where Eq. 2.11 produces a significantly better fit to the NLDAS-2 model generated values than the average CNs method.

Table 2. 5 Validation metrics for Eq. 2.11 and averaged monthly CNs.

	R^2	P(T<=t) two-tail	RB
Eq. 2.11	0.75	0.24	0.07
Average CNs	0.03	2.50E-5	0.46

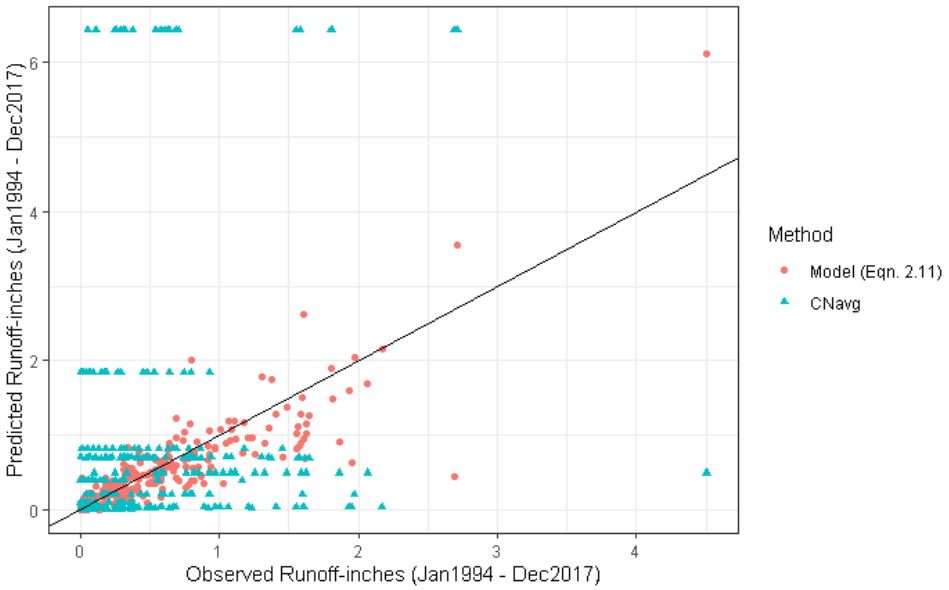

Fig 2. 19 Comparison of NLDAS-2 surface runoff and proposed runoff using; the proposed model Eq. 2.11 and the average monthly CNs for the years (1994-2017).

The monthly averaged CNs were not able to match the NLDAS-2 model generated runoff values during the validation period, while Eq. 2.11 produced a significantly better fit (Table 2. 5). Therefore, the lone presence of API was enough to produce significant improvement in the runoff predictions on the watersheds showing high monthly standard deviations in the runoff values across different years.

2.5 Summary and Model Application

Our initial studies showed that runoff patterns for these terraced watersheds are not well modeled by a direct application of a standard curve number approach, particularly when trying to estimate runoff volumes on a monthly or seasonal basis as is needed for an effective wetland water balance. The model development work presented here shows that there are two major factors that must be accounted for to improve these runoff models. The first is to account for antecedent precipitation, which affects the soil moisture, and therefore the storage capacity, of the watershed. The impact of soil moisture content in the curve number approach has long been recognized [6, 27, 28], although specific implementations to account for this factor vary. This model used a continuous calculation of API throughout the year, relying partially on precipitation data obtained from nearby weather stations for periods not covered by site-specific data.

The second major issue affecting runoff volume in these watersheds is the extent of vegetative cover. Our results found a strong impact of vegetative cover on the amount of runoff generated from storm events in these watersheds. This effect is likely amplified in small agricultural watersheds such as those tested here, where more than 75% of the watershed area is farmed.

2.5.1 Application Beyond this Study

In addition to providing input for the wetland hydrology model, a goal of developing this runoff model was to be able to better improve modeling of runoff from these small, terraced watersheds. The model ultimately developed uses several site-specific data inputs to determine curve number values and runoff volumes for the study locations. This sections briefly addresses how several of the major components of this model could be adapted to allow for use at similar sites:

2.5.1.1 Precipitation and Soil Moisture Content

Precipitation data can be downloaded for most sites across US from the nearby National Oceanic and Atmospheric Administration (NOAA) station from the Climate data online repository [https://www.ncdc.noaa.gov/cdo-web/search]. The highest resolution data available is at 15-minute timescale, which can be down-scaled to 1 min average rainfall if needed. However, 15 minute or higher resolution could be used, particularly if the goal is to provide general estimates for storm volumes. Precipitation data could be used to identify major storm events (in this case, P > 1 inch) and these storm events used in determination of peak runoff volumes from a given site.

The same precipitation data could be used to provide estimates for API values in calculation of curve numbers for specific runoff events. As discussed above, it is possible to maintain a continuous API index for a site over a given time period using these data, which would allow modeling of specific storm events or sequences of events. A daily decay constant (k) could be calculated for individual sites using the process defined in section 2.2.1 if site-specific runoff measurements are available. In the absence of these measurements, constant values have been recommended in the literature, such as a=0.85 and b = 0.10 [13].

2.5.1.2 Vegetation

The data source for the ARVI in this study, USGS Earth Explorer, maintains datasets for Landsat 8 Images from 2013 onwards, with 16-day intervals between images at a given location. These raster images are free to download from https://earthexplorer.usgs.gov/. The highest resolution available is 30 x 30 m which should be fine enough for most similar-sized agricultural fields in this region. Landsat images can then be used to calculate ARVI for a defined land area using a raster calculator available in commercially available geographic information system

programs, for instance, ARCMAP, ARCGIS, QGIS etc. While achievable, this process is labor intensive but necessary. As seen from the large-scale implementation of our model (section 2.4), the process of using a monthly averaged ARVI value on watersheds with spatial and temporal variations in crop cover was unsuccessful in improving the model predictive capabilities.

It should be noted, however, that the vegetation index used in the model quantifies the greenness of the vegetation present onsite. Photosynthetically active plants will reflect most of the NIR radiation and absorb red. This will result in a larger ARVI value. Conversely, dead vegetation will result in low ARVI values despite being present onsite. This can result in incorrect CN values because less green vegetation can still have significant effect on runoff generation. In these cases, some other index to quantify the amount of vegetation might become necessary.

2.5.1.3 Terrain

The slope of the study site will determine how fast the runoff water will move through it. The model does not require slope calculations, but some knowledge of the topography of the site is essential. Significant differences in slope would require adjustments to the peak rate factor, as seen in this study where the terraced field required a peak rate factor (PRF), lower than the standard SCS unit hydrograph value of 484. This allows replication of the flashy behavior of storm runoff hydrographs observed in these systems. A value of 100 could be used as a starting point, based on this study, but better results would be obtained by calibrating to site-specific runoff data.

Any natural or manmade storage units or major depressions on site will have an effect on the runoff drainage. These storage units can be modeled as a reservoir in HEC-HMS or any other rainfall runoff model. The topography of the storage unit is needed to calculate the lag. The

topography of the storage unit can be obtained from measuring elevations at 5 – 10 ft intervals on site using a survey-quality GPS or other appropriate instruments.

2.5.1.4 Geography

This model assumes general seasonal conditions similar to those found in northeastern Kansas. Substantial change in climate from the sites studied here may have an effect on the model performance. For instance, regions with snow cover for long portions of the year would need to incorporate snow hydrology into the model. This can drastically change the structure of the model proposed here.

2.6 References

1. Somes, N., J. Fabian, and T. Wong, *Tracking pollutant detention in constructed stormwater wetlands.* Urban Water, 2000. **2**(1): p. 29-37.
2. McNeish, D., *On using Bayesian methods to address small sample problems.* Structural Equation Modeling: A Multidisciplinary Journal, 2016. **23**(5): p. 750-773.
3. Peltier, E., et al., *Monitoring Effectiveness of Tile Outlet Terrace Fields with Constructed Wetlands for Sediment, Nutrient and Volume Reduction in Northeastern Kansas*. 2016, Kansas Water Office: Topeka, KS.
4. USDA, S., *Urban hydrology for small watersheds.* Technical release, 1986. **55**: p. 2-6.
5. Rietz, D. and R.H. Hawkins, *Effects of land use on runoff curve number*, in *Watershed Management and Operations Management 2000*. 2000. p. 1-11.
6. Hawkins, R.H., *Runoff curve numbers with varying site moisture.* Journal of the irrigation and drainage division, 1978. **104**(4): p. 389-398.
7. Gonzalez, A., M. Temimi, and R. Khanbilvardi, *Adjustment to the curve number (NRCS-CN) to account for the vegetation effect on hydrological processes.* Hydrological Sciences Journal, 2015. **60**(4): p. 591-605.
8. Huang, M., et al., *A modification to the Soil Conservation Service curve number method for steep slopes in the Loess Plateau of China.* Hydrological Processes: An International Journal, 2006. **20**(3): p. 579-589.
9. Survey, U.S.G. *EarthExplorer-Home*. 2018; Available from: https://earthexplorer.usgs.gov/.
10. Breiman, L., et al., *Classification and regression trees. Wadsworth Int.* Group, 1984. **37**(15): p. 237-251.
11. Liaw, A. and M. Wiener, *Classification and regression by randomForest.* R news, 2002. **2**(3): p. 18-22.
12. Kohler, M.A. and R.K. Linsley, *Predicting the runoff from storm rainfall*. Vol. 30. 1951: US Department of Commerce, Weather Bureau Washington, DC.

13. Crow, W.T. and X. Zhan, *Continental-scale evaluation of remotely sensed soil moisture products.* IEEE Geoscience and Remote Sensing Letters, 2007. **4**(3): p. 451-455.
14. Administration, N.O.a.A. *Climate Data Online.*; Available from: https://www.ncdc.noaa.gov/cdo-web/.
15. Zhu, X. and D. Liu, *Improving forest aboveground biomass estimation using seasonal Landsat NDVI time-series.* ISPRS Journal of Photogrammetry and Remote Sensing, 2015. **102**: p. 222-231.
16. Ke, Y., et al., *Characteristics of Landsat 8 OLI-derived NDVI by comparison with multiple satellite sensors and in-situ observations.* Remote Sensing of Environment, 2015. **164**: p. 298-313.
17. Liu, G.-R., et al., *Comparison of the NDVI, ARVI and AFRI vegetation index, along with their relations with the AOD using SPOT 4 vegetation data.* Terrestrial, Atmospheric and Oceanic Sciences, 2004. **15**(1): p. 15-31.
18. Kaufman, Y.J. and D. Tanre, *Atmospherically resistant vegetation index (ARVI) for EOS-MODIS.* IEEE transactions on Geoscience and Remote Sensing, 1992. **30**(2): p. 261-270.
19. Hurvich, C.M. and C.-L. Tsai, *Regression and time series model selection in small samples.* Biometrika, 1989. **76**(2): p. 297-307.
20. Snyder, W.M., *Fitting of distribution functions by nonlinear least squares.* Water Resources Research, 1972. **8**(6): p. 1423-1432.
21. Burnham, K.P. and D.R. Anderson, *A practical information-theoretic approach.* Model selection and multimodel inference, 2nd ed. Springer, New York, 2002.
22. Heggen, R.J., *Normalized antecedent precipitation index.* Journal of hydrologic Engineering, 2001. **6**(5): p. 377-381.
23. Peltier, E., et al., *Assessing the Water Quality Impacts of Constructed Wetlands on Tile Outlet Terrace Runoff (CD-97758901).* University of Kansas, 2020.
24. Agriculture, U.S.D.o., *Hydrographs - Chapter 16*, in *National Engineering Handbook Part 630- Hydrology. 1997*. National Resources Conservation Service: USDA: Washington, DC.
25. Student, *The probable error of a mean.* Biometrika, 1908: p. 1-25.
26. Xia, Y., et al., *Continental-scale water and energy flux analysis and validation for the North American Land Data Assimilation System project phase 2 (NLDAS-2): 1. Intercomparison and application of model products.* Journal of Geophysical Research: Atmospheres, 2012. **117**(D3).
27. Sahu, R., et al., *An advanced soil moisture accounting procedure for SCS curve number method.* Hydrological Processes: An International Journal, 2007. **21**(21): p. 2872-2881.
28. Brocca, L., et al., *Soil moisture temporal stability over experimental areas in Central Italy.* Geoderma, 2009. **148**(3-4): p. 364-374.

Chapter 3

Modelling Wetland Hydrology

Note: This chapter is adapted from a conference paper presented at the ASCE World Environmental and Resources Congress 2019 [1]

The hydraulic retention time is one of the dominant parameters determining nutrient removal efficiency in a treatment wetland [2]. Models for estimating nutrient removal in wetlands thus typically require the calculation of both water depth and retention times [3]. At a small scale, however, wetlands treating agricultural runoff are typically event-driven, meaning that both flow rates and total water volume will vary substantially over time. Under these conditions, wetlands can alternate between periods of flow-through regimes (similar to continuous-flow wetlands) and periods where water is held within the system for extended duration before release [4]. This alternation will depend on rainfall and climate patterns, conditions affecting runoff/rainfall ratios from the upland fields, and wetland parameters (size and layout, vegetation, outflow structure). Investigating the relationship between hydraulic parameters and treatment performance for these systems often requires construction of a full water budget to determine retention patterns.

This chapter describes our approach to determining hydraulic retention times at the wetland sites through the formation of a dynamic water budget model. Water budget models and retention time calculations were developed for the two Harvest Hills field sites (HHN and HHM) only. Cain site was not included in the analysis hereon. This was due to the combination of inconsistent observed dataset and unusual outflow structure at the site (see section 1.1.2 for more info). These models were first used to determine retention time for specific storm events during

the 2015 growing season, and then used to show the expected variation in wetland water storage throughout the year.

3.1 Retention Time Calculations

Hydraulic retention times for each wetland were determined for 10 storm events from the 2015 growing season (May – November) with precipitation greater than 1 inch. Data on these storm events are presented in [5]. Rainfall of less than 1 inch did not consistently result in substantial runoff from the terraced fields, depending on antecedent conditions, and was therefore not included in this assessment. Retention time (t) inside the wetland was calculated by using Eq. 3.1, below [4].

$$t = ehA/Q_{in} \tag{3.1}$$

where Q_{in} is the inlet volumetric flow rate (assumed to dominated by discharge from the tile system), h is water depth, A is the water surface area inside the wetland, calculated using the stage-storage relationship (Fig 3. 1), and e is the volumetric efficiency of the wetland. The volumetric efficiency is based on the wetland length:width aspect ratio as defined by [6]:

$$e = 0.84\left[1 - exp(-0.59 * \frac{L}{W})\right] \tag{3.2}$$

Table 3. 1 lists all of the required input parameters for this retention time analysis. Variables defined as independent (volumetric efficiency and precipitation) are those that are not required for determination of Q_{in} or h and are thus determined directly from site measurements. Q_{in} is calculated for an individual storm event from the upland flow model described in chapter 2, while water depth (h) is calculated from a water budget model developed for this assessment.

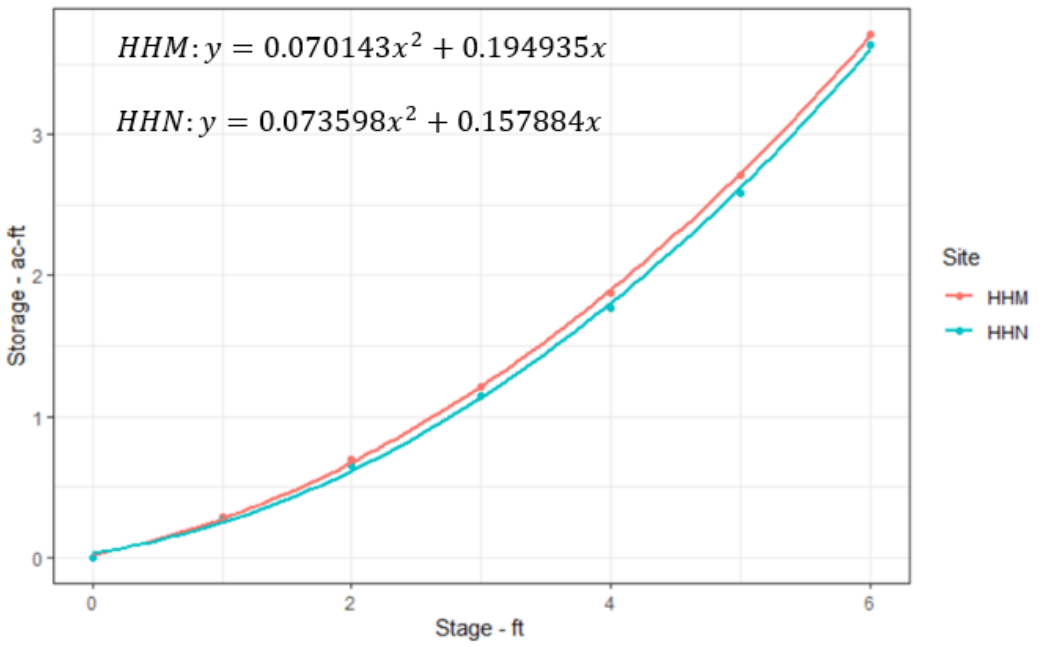

Fig 3. 1 Stage Storage Relationship for HHM and HHN wetlands [5]

Table 3. 1 Input variables for retention time analysis.

Input Variables	Unit	Type	Nature	Source
Inflow (Q_{in})	ac-ft/hr.	Continuous	Dependent	Upland model
Precipitation (P)	in	Continuous	Independent	Gage Data
Lag time (Lag)	min	Continuous	Dependent	Upland model
Duration of excess rainfall (D)	min	Continuous	Dependent	Upland model
Level of water in the wetland (h)	ft	Continuous	Dependent	Water budget model
Wetland Volumetric Efficiency (e)		Fixed	Independent	Aspect ratio
Peak Rate Factor		Fixed	Dependent	Upland model

3.2 Water Budget Model

A wetland water budget model was developed to predict the wetland water level (h) immediately preceding each storm event. This water budget balances input flows (Q_{in}) calculated from the upland model with water losses from surface outflow, evaporation, and seepage. Surface inflows and outflows were converted into inflow and outflow (h_{out}) depths by using the stage-storage discharge relationship of each wetland from Fig 3. 1. Evaporation (E) and seepage (S) losses were calculated using a bulk aerodynamic method presented by Anderson et al. [7], as cited in [8].

$$E = f(u)(e_o - e_a) \tag{3.3}$$

Here, e_o is the saturation vapor pressure, e_a is vapor pressure of the air, f(u) = coefficient of proportionality calculated as $f(u) = a + Nu^n$, where a and n are constants specific to the water body, N is the mass transfer coefficient and u is the wind speed.

Wind speed, air and dew-point temperatures were obtained from the nearby Philip Billard municipal station (39.07°N, 95.64°W) [https://www.wunderground.com/history/monthly/us/ks/topeka/KTOP/date/2015-12] . The value of 'n' is assumed to be one in lakes and 'a' is zero if the wind speed is measured near the center of an open water body [8]. Since these wetlands were expected to have a different flow pattern than a standard lake, a sensitivity analysis was performed to calibrate the value of 'n' to produce the best fit match between the observed and predicted water levels while keeping the other variables constant. For both wetlands, n= 0.97 produced the best agreement between observed and predicted water levels. Due to the lack of site measurements, water temperatures were assumed to be at the same temperature as the air above them. The value of variable 'a' was assumed to be zero. The mass transfer coefficient (N) and seepage loss (S) are the slope and

intercept, respectively, of the linear relationship between change in observed water levels (Δh_{obs}) and the product term, $u(e_o - e_a)$ (Fig 3. 2).

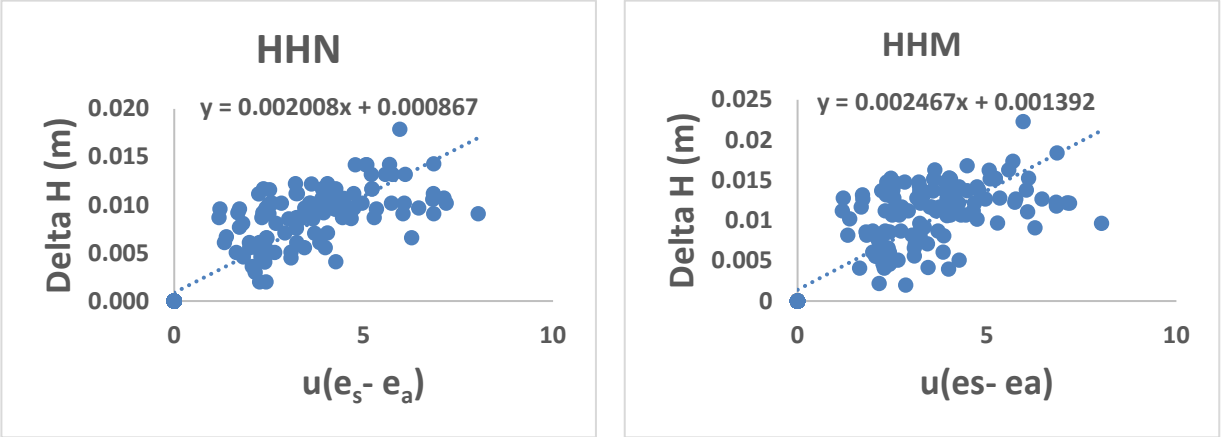

Fig 3. 2 Relationship between change in observed water levels (Δh_{obs}) and the product term, $u(e_o - e_a)$.

As with the surface inflow and outflow, the direct precipitation (P_d), evaporation, and seepage terms were converted to changes in water levels using the stage-storage relationship from Fig 3. 1. A daily continuous change in water level inside the wetland was then determined using the equation:

$$\Delta h/\Delta t = h_{in} + P_d - h_{out} - E - S \tag{3.4}$$

The water budget model was used to determine the starting water level at the beginning of each storm event, which was then used in the retention time equation. The step by step process of the model calculations for both outflow and water levels are described below.

3.2.1 Model Description (Outflow)

A surface outflow model was developed to predict depth of water leaving the wetland following a storm event. This outflow model balances the present water level inside the wetland with the amount of storm runoff coming into the wetland as surface inflow and direct precipitation (P_d). Since both wetlands have rectangular weir boxes controlling effluent flow, outflows were modelled using the rectangular sharp-edged weir equation [9].

$$Q_{out} = 3.33LH^{3/2} \quad (3.5)$$

where Q_{out} is flow in cfs, L is the length of the weir in ft, H is the head above weir crest in ft and 3.33 is the product of the constant terms when the coefficient of discharge is assumed to be 0.62.

Outflows were modelled for individual storm event. Inflows at 1-min interval from each major storm event were obtained from the direct runoff hydrographs generated in the watershed upland model which was then used to calculate the 1-min outflow. The outflows were then summed up to get the accumulated outflow for each storm event.

Since this approach converts the volume of inflow to the stage at every one-minute interval, the magnitude of the total stage adding or decreasing from the wetland is not an accurate representation of the change in water depth. Instead, the true change in wetland stage would be obtained by converting the total volume of water entered to the wetland depth following a storm event. However, modelling outflow using this true change in wetland depth would not be sensitive to the change in flowrates throughout the inflow duration. This would overestimate the total outflow from the wetland and would not satisfy the water balance. The actual approach used is presented in Fig 3. 3. A brief description of each step in the process, as noted by the marked letters A-D in the figure, is presented below.

A. Wetland inflow from the upland model, based on the measured precipitation from the storm event, was added to the preceding minute water level. The outflow depth generated on the preceding minute was then subtracted to obtain the present minute water level.
B. The obtained water level was then subtracted from the weir crest height to obtain the total head of water going over the weir (H).
C. The water head (H) and the weir width (L) were used to calculate the 1-min outflow in cfs using Eq. 3.5.

D. The outflow was then converted to the volume and depth of water going out of the wetland on 1-min intervals using stage storage discharge relationship (SSR) of each wetland from Fig 3. 1. The total outflow following a storm event was then obtained by summing up the individual 1-min outflow depths.

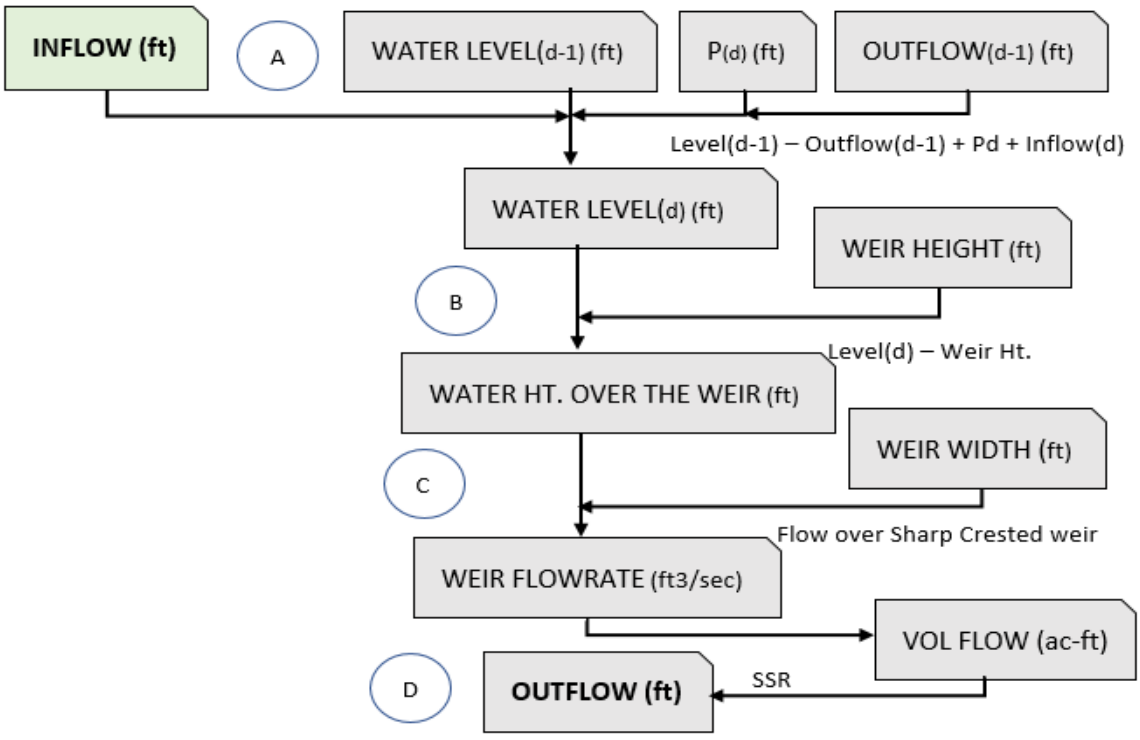

Fig 3. 3 Outflow model flow chart.

3.2.2 Model Development (Water level)

Once outflow can be calculated, the next step is to calculate water levels inside the wetlands. A description of the model flow diagram for this step is presented in Fig 3. 4. Again, a brief description of each step in the process, as noted by the marked letters A-F in the figure, is presented below.

A. If the preceding water level was greater than the weir height, the change in water level inside the wetland will be the difference between inflow and outflow. Otherwise outflow would be zero and the present-day level would be the sum of the preceding day level and the runoff inflow. (*This step considers the water level present in the wetland before the*

present-day runoff enters it. Therefore, the outflow would only be calculated if the preceding level was initially above the weir height).

B. If the change in water level is zero, then the present-day level would be the weir height as this indicates that there was no flow going through the system. If not, the calculated difference would be added to the preceding day level.

C. Since the outflow was initially ignored, this step checks to see if the resulting present-day level is now above the weir height. If this is true, the initial assumption no longer holds true and the outflow is then subtracted from the level. If not, the level remains the same.

D. After subtracting the outflow if the resulting level is now below the weir height, the level is raised back up to the weir height, as this situation is practically impossible without including other losses like evaporation or seepage, which occur on a much slower time scale. If the present-day level is still greater than the weir height in the presence of a positive outflow, the level will remain the same.

E. If there was no outflow present at the first place, the level will remain the same.

F. The surface inflow/outflow balance water level obtained from step D is then adjusted for total drawdown (Evaporation + Seepage) and direct precipitation for the present-day to obtain the ‘end of day’ water level inside the wetland.

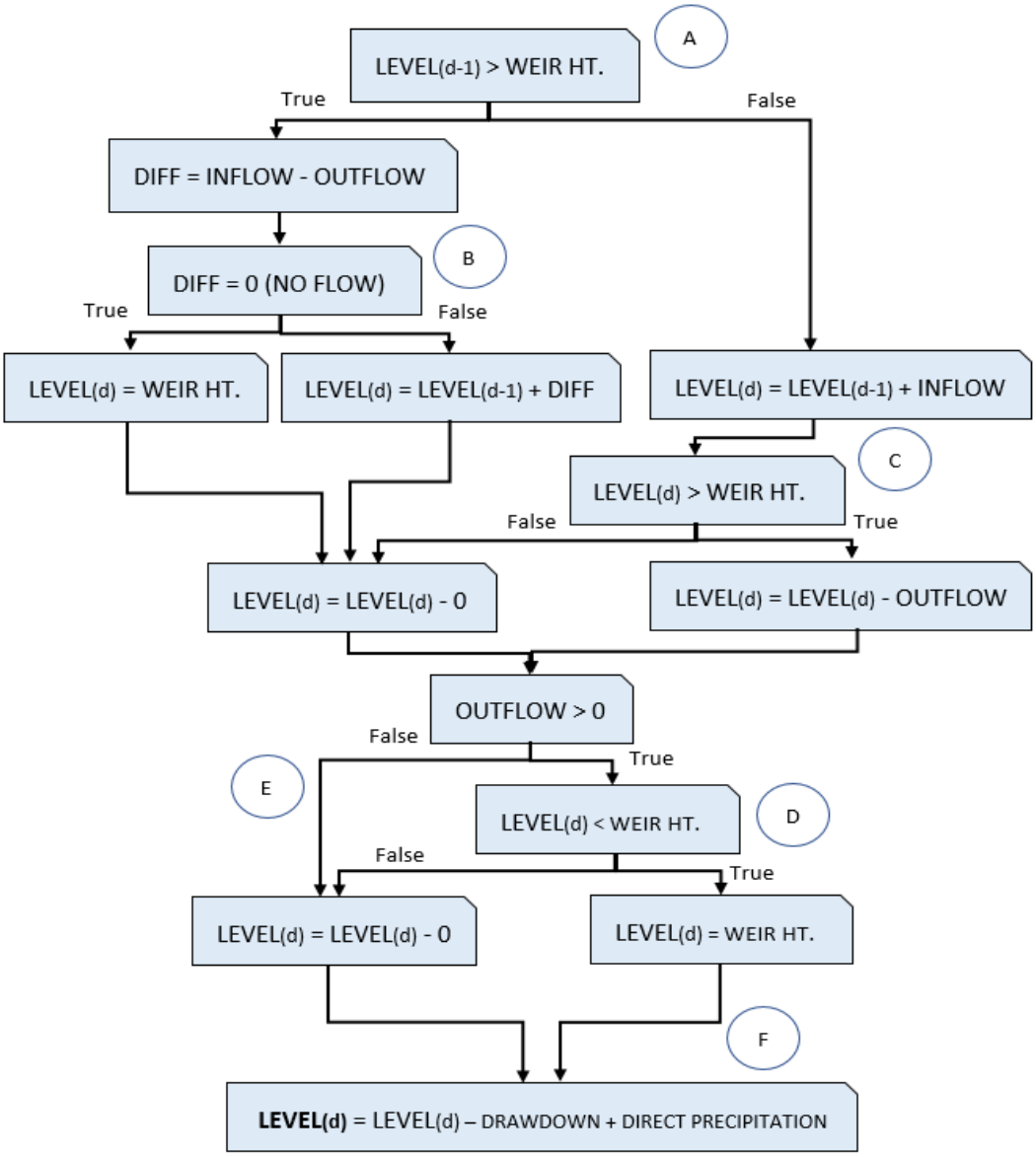

Fig 3. 4 Water balance model flow chart.

3.3 Model Results

The daily evaporation and seepage were calculated for each of the two wetlands over the 2015 growing season by comparison to measured stage data (Fig 3. 5). The seepage (S) value obtained using the aerodynamic method is assumed to remain constant throughout the year while the evaporation changes daily with the changing environmental conditions (i.e., temperature,

vapor pressure, and wind speed). For HHM and HHN, seepage was calculated to be 0.055 in/day and 0.034 in/day respectively.

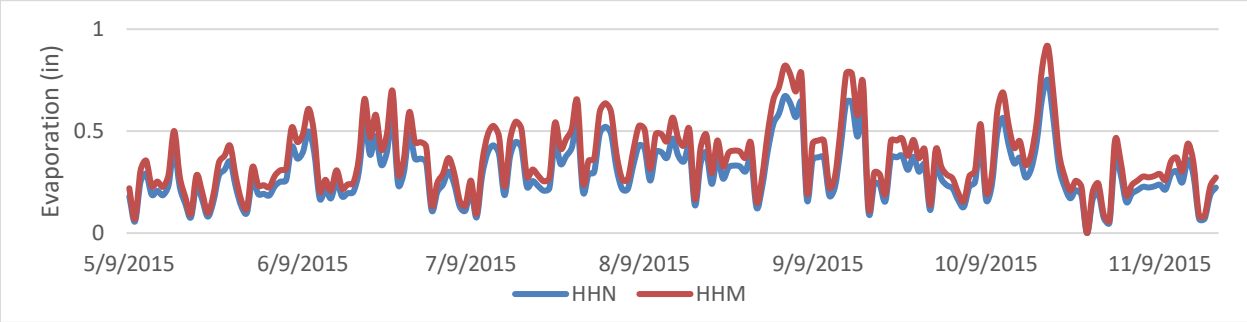

Fig 3. 5 Daily evaporation from HHN and HHM wetlands.

The daily water balance was then obtained for both wetlands and compared to the observed water levels from 2015. As can be seen in Fig 3. 6, this approach was successful at tracking the major trend of water level changes in both wetlands over the 2015 growing season. For the most part, the model even tracks the rapid changes in water depth observed during storm events.

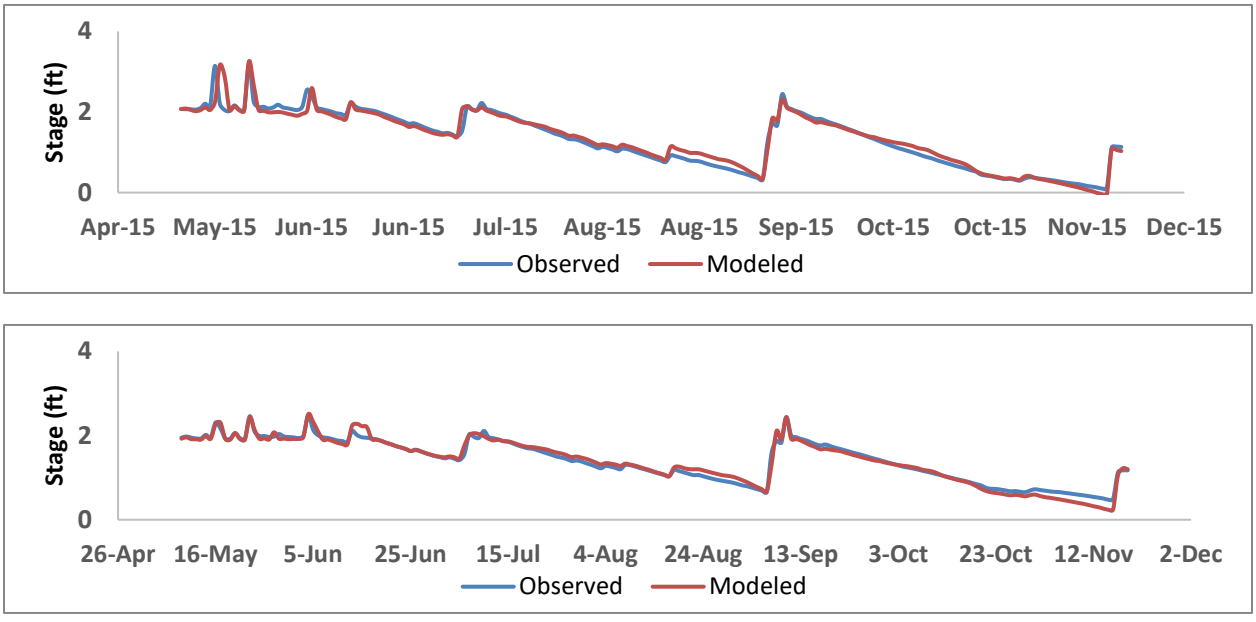

Fig 3. 6 Calibrated and observed water balance for HHN [10] and HHM (bottom).

Using the predicted values of volumetric stormwater runoff (Q_{in}) from the upland model and daily water level from the water budget model, the retention time was calculated using Eq. 3.1 for the ten individual storm events with > 1 inch of precipitation, ranging across 6 months in the year 2015 (Fig 3. 7). Retention times in the HHN wetland were both longer and more variable across these 10 storm events, with a median retention time of 10 hrs 31 min compared to 8 hrs 2 min for HHM.

The longer retention times in HHN corresponds to better removal efficiency for total nitrogen, dissolved nitrogen and dissolved phosphorus observed in this wetland during the 2015 sampling season (Table 3. 2).

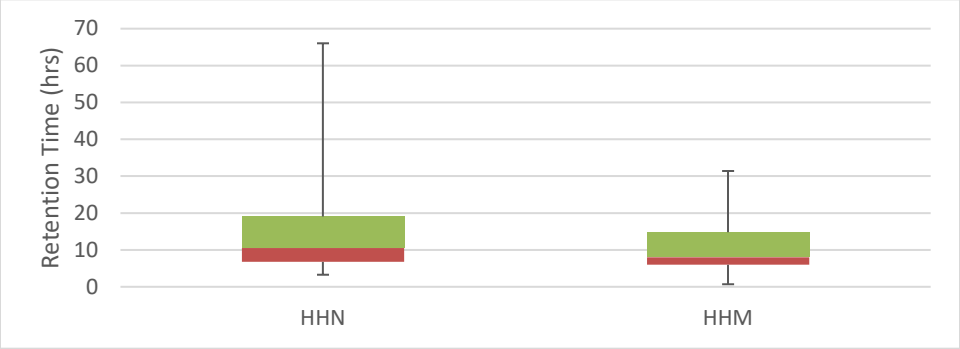

Fig 3. 7 Box plots of simulated retention time for ten storm events.

Table 3. 2 Observed removal efficiency of HHM and HHN wetlands [5].

	Concentration Based Removal (%)					
	TN	TP	TDN	TN	TP	TDN
HHN	32	38	21	21	39	23
HHM	17	40	15	3	38	2

Note: TN = Total Nitrogen, TP = Total Phosphorus, TDN= Total Dissolved Nitrogen, TDP = Total Dissolved Phosphorus.

Total phosphorus was not notably affected by the difference in retention times between the two wetlands. However, the majority of total phosphorus in these systems was particulate-associated and would have been removed with suspended solids. It is possible that TSS removal in these systems (which was > 65%) was sufficiently rapid that the difference in retention times had little effect. Further analysis of the relationship between retention time and nutrient removal is presented in chapter 4.

3.4 Simulating HHN and HHM Retention Time Performance

Following this initial analysis, a Monte Carlo simulation was performed to examine the likely range of retention times at both sites over a wider range of potential storm events. The key variables for this analysis can be divided into two types: rainfall variables (precipitation, lag time and duration) and site variables (existing water level, antecedent moisture (AVI) and vegetative cover [10]). Ranges for each variable in the simulation were determined by the average, minimum, and maximum values recorded during the 10 precipitation events in 2015 (Table 3. 3).

Table 3. 3 Calculated ranges for continuous variables at both sites.

		HHN			**HHM**		
Variable	**Unit**	**Min**	**Avg**	**Max**	**Min**	**Avg**	**Max**
Water Level (h)	ft	0.22	1.43	1.92	0.12	1.44	2.05
Duration of excess rainfall (D)	min	30	187	437	50	174	420
Lag time	min	25	70	170	30	59	90
Precipitation (P)	in	1.04	1.81	3.16	1.06	1.85	2.91
ARVI	-	0.12	0.31	0.48	0.09	0.31	0.52
API	in	1.41	3.20	5.31	1.40	3.01	4.65

These ranges were used to generate 10,000 unique combinations of values using the min, avg and max values for each parameter. From these values, a uniform distribution was used to calculate a probability density function and cumulative density function for retention times at these sites (Fig 3. 8).

As seen in Fig 3. 8, the retention time distributions and both HHN and HHM have a strong positive skew. This indicates that a high number of simulations resulted in low detention times (< 5 hours). This suggests that storm events of the magnitude simulated here will stress the ability of the existing wetlands to significantly detain and treat field runoff. It should be noted that 2015 was a wet year- using a drier year to set the range of input values could affect these results. Still, these simulations show that the amount of runoff generated from these sites can easily meet or exceed the storage capacity of their wetlands on a regular basis during high rainfall periods.

The second notable result of these simulations is that they show higher detention time in the HHM wetland at the higher end of the cumulative distribution function. At a cumulative probability of 90%, the detention time for HHM (10hrs 41min) was 1.56 times the detention time for HHN (6hrs 52min). This difference disappeared at the cumulative probability of 50% with HHN (3hr 2min) having a detention time similar to HHM (3hr 21min). This indicates that the storm events with moderate to low runoff rates tends to spend much more time in HHM wetland probably due to the larger depth, than in HHN. On the other hand, the two systems will perform similarly during periods of frequent precipitation and high runoff, when both wetland's performances approximate that of flow through systems.

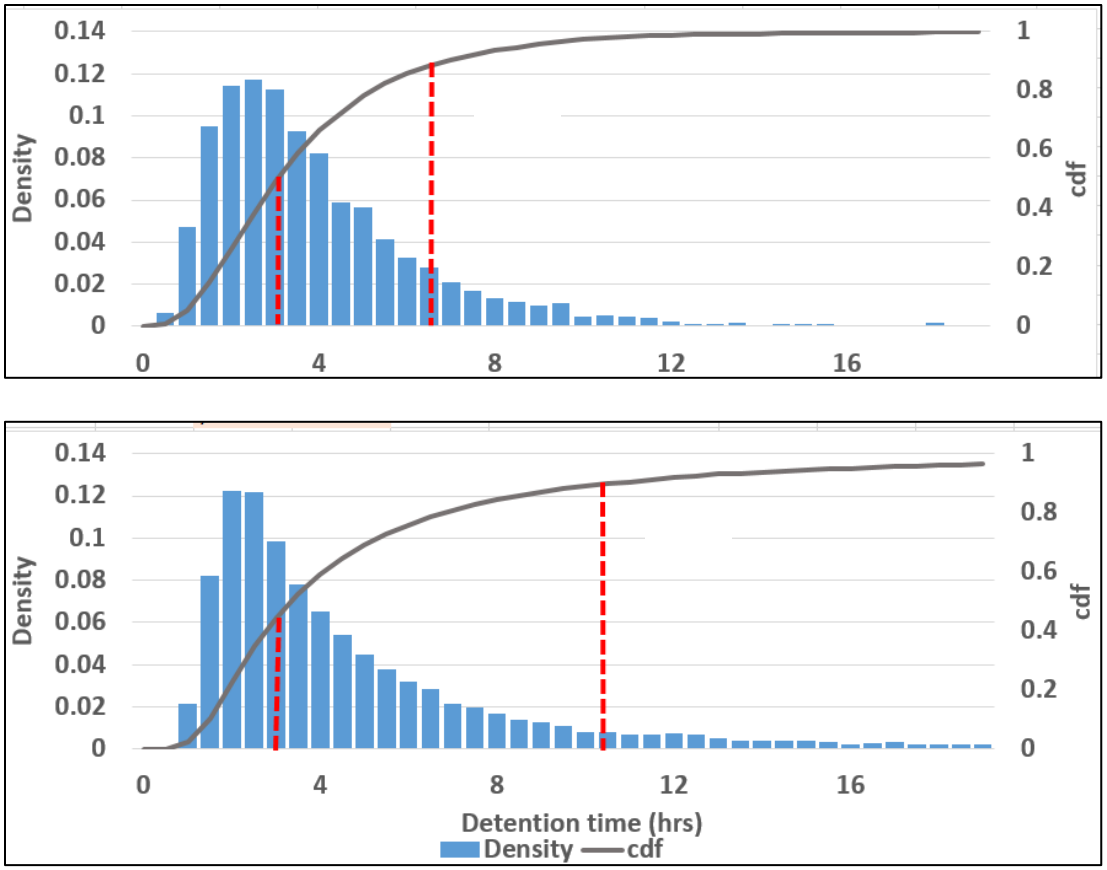

Fig 3. 8 Monte Carlo simulation results for HHN and HHM (bottom).

The retention time distributions determined by this simulation include both the effects of fixed differences in the wetlands (surface area, stage-storage relationship) and the continuous variables described above. To test the relative impact of the individual variables in defining the overall wetland retention time, a sensitivity analysis was conducted to examine the impact of each individual variable on calculated retention time (Fig 3. 9). For this analysis, each variable was tested at its minimum and maximum value from Table 3. 3, while keeping the other variables fixed at their average value.

The retention time for HHM wetland was found to be more sensitive than HHN to each of the tested continuous variables. API was the single most dominant variable in defining the retention time in both systems. This was due to the direct correlation of API with the influent

volumetric runoff into the wetland. Greater antecedent precipitation leads to lower soil capacity for rainfall retention in the upland fields, and thus higher levels of influent runoff. This result was in general agreement with Somes et al. [2], who also found significant impact on retention time due to changes in influent volume to wetland storage ratios. The much greater range of retention times due to API variation at HHM is a result of a generally lower ratio of runoff to rainfall at that site, which increases the impact of less soil moisture storage on decreasing inflow volumes and eventually produces large retention times.

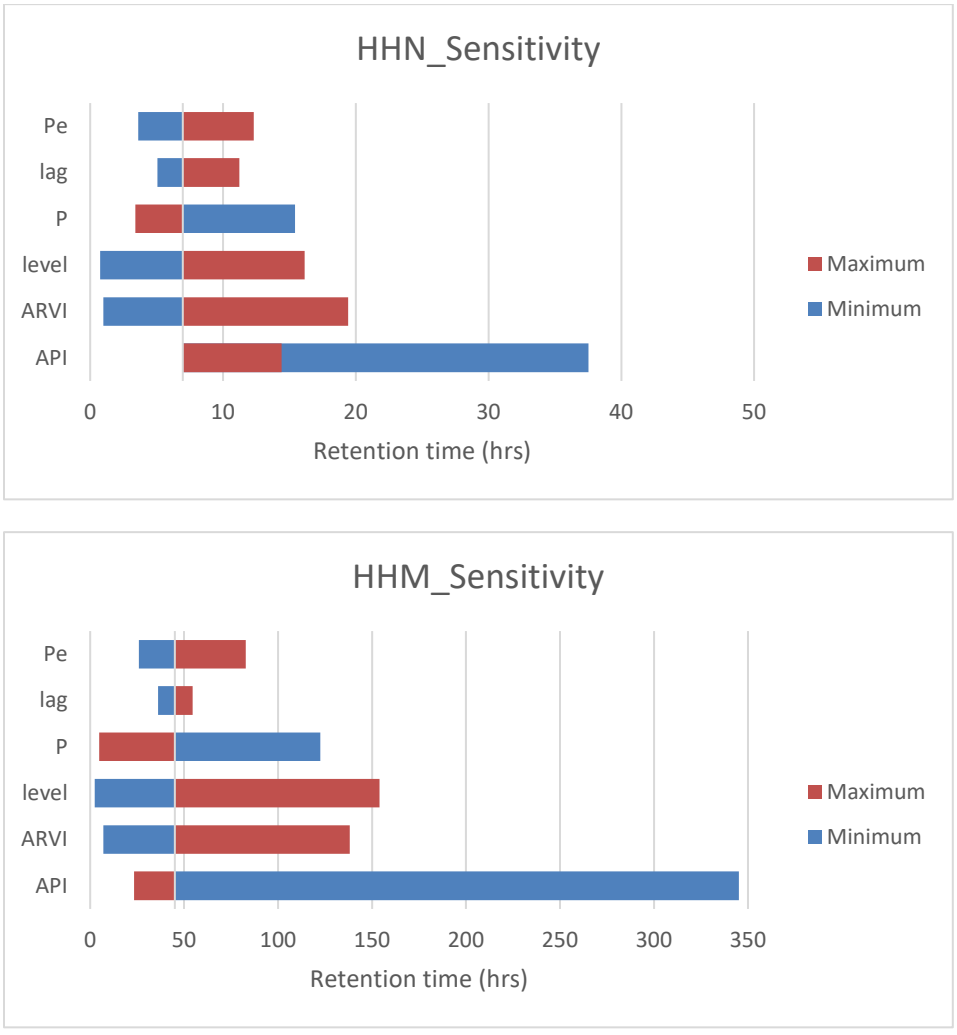

Fig 3. 9 Sensitivity analysis of input variables for HHN and HHM (bottom).

Although the sensitivity analysis helped to identify the significant parameters influencing wetland retention time, it does not reflect interdependence between some of the input variables. In actual operation, some combinations of variable values are more likely to occur than others. For instance, a low API value indicates relatively low recent rainfall, which makes it less likely that the initial water level will be high. In addition, at very low water levels, the wetland will have excess storage available before discharge begins, which is not fully accounted for in this approach. Thus, some of the more extreme retention times indicated by this simulation are unlikely to occur in practice.

3.5 Seasonal Patterns of Water Retention

The previous analysis addresses retention times during and after individual storm events. While this is a key parameter in assessing pollutant removal, it is not the full story of wetland water storage. At these sites, rainfall events are relatively frequent during the early part of the growing season (April - mid June), and water levels are primarily driven by surface inflows during these events. From mid-June through November, however, rainfall becomes less common, and water levels fluctuate based on evapotranspiration and isolated storm events (Fig 3. 5 and Fig 3. 6). The effect of these seasonal change on wetland water retention is important to determining nutrient removal and transformation processes during this period. To quantitatively evaluate changes in water storage in these wetlands across different months, an aggregate retention time was calculated for each month, following the same procedure as discussed before, with one exception. Rather than using data from individual storm events, average monthly values for the variables in Table 3. 1 were determined over each of the 6 months in which a storm event was measured and used in the retention time calculation. This approach incorporates the impact

of dry days between storm events and gives an indication of the impact of seasonal rainfall patterns on water retention patterns.

To quantitatively evaluate changes in water storage in these wetlands across different months, the wetland turnover time was calculated for each of the 6 months in which a storm event was recorded during 2015 (Fig 3. 10). The turnover time is defined as the amount of time required to completely change out all water in the wetland [11]. The lower the turnover time, the more frequently water is exchanged through inflow-outflow processes. It is therefore similar to a detention time but applies across a longer time period than a single storm event and incorporates periods without precipitation. In this case, turnover times were calculated on a monthly basis.

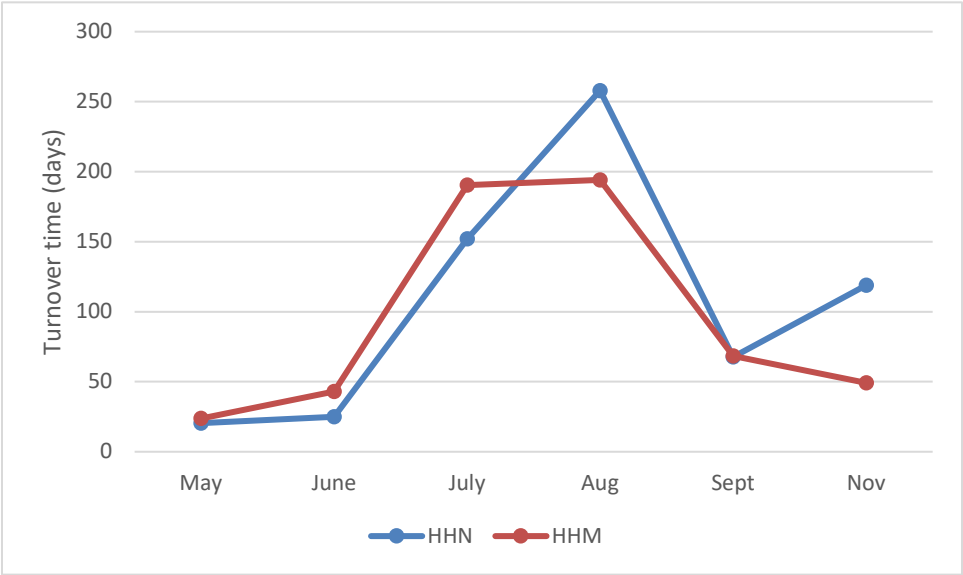

Fig 3. 10 Turnover rate for HHN and HHM wetlands.

Turnover times in spring and late fall were low, with minimum times of < 30 days in May (Fig 3. 10). This implied that if the wetlands were to be fed throughout the year at the rate observed during May, the total volume of water inside both wetlands would get flushed around 14 times per year. This is comparable to yearly turnover rates for freshwater marshes, which are considered relatively open systems that import and export nutrients at a higher rate [11]. By

contrast, turnover times at HHM were around 200 days in mid to late summer and reached > 250 days for HHN in August. This means that, for both wetlands, water would be fully exchanged around 1 time per year or less if wetlands were fed consistently at the late-summer rate. These high turnover times correlate with the much higher detention time obtained for 90% cdf range in both wetlands (Fig 3. 9). The rate of water renewal during these months is more typical of low-nutrient systems such as peat bogs [11], where low levels of surface input means that available nutrients are more extensively removed from the water column. This result would be expected to affect nutrient export as well, as wetland water quality results from the 2017-18 field sampling show that nutrient concentrations in the water column tend to decrease during summer months when the water spends more time in the wetland [10].Similar trends in both hydrology and nutrient concentrations have been recently reported for prairie pothole wetlands receiving farm runoff [12], emphasizing the important role that seasonality plays in wetland performance.

3.6 Conclusion

Water budget and runoff models were developed to assess retention time distributions in two storm water wetlands receiving runoff from agricultural watersheds with tile outlet terraced systems. Results for 10 major storm events (precipitation > 1 inch) showed a longer median residence time for the HHN wetland than the HHM. This difference corresponds to a greater efficiency of total nitrogen and dissolved N and P removal in the HHN wetland during the same year. Sensitivity analysis performed to test the impact of individual model input variables on predicted retention times indicated that the most significant impact was from the amount of antecedent moisture, which affected input runoff flows. Monthly aggregates showed a significant seasonal difference in water retention in both wetlands, with much greater rates of water

exchange in May-June compared to July - November. These seasonal impacts should have a substantial impact on retention of nitrogen and phosphorus in these systems.

3.7 References

1. Siddiqui, D.A., et al. *Modelling Influent Runoff and Retention Time in Storm Water Wetland Systems*. in *World Environmental and Water Resources Congress 2019: Watershed Management, Irrigation and Drainage, and Water Resources Planning and Management*. 2019. American Society of Civil Engineers Reston, VA.
2. Somes, N., J. Fabian, and T. Wong, *Tracking pollutant detention in constructed stormwater wetlands.* Urban Water, 2000. **2**(1): p. 29-37.
3. Merriman, L., et al., *Adapting the Relaxed Tanks-in-Series Model for Stormwater Wetland Water Quality Performance.* Water, 2017. **9**(9): p. 691.
4. Kadlec, R.H. and S. Wallace, *Treatment Wetlands*. 2nd ed. 2009, Boca Raton, FL: CRC Press.
5. Peltier, E., et al., *Monitoring Effectiveness of Tile Outlet Terrace Fields with Constructed Wetlands for Sediment, Nutrient and Volume Reduction in Northeastern Kansas*. 2016, Kansas Water Office: Topeka, KS.
6. Thackston, E.L., F.D. Shields Jr, and P.R. Schroeder, *Residence time distributions of shallow basins.* Journal of Environmental Engineering, 1987. **113**(6): p. 1319-1332.
7. Anderson, E.R., L. Anderson, and J. Marciano, *A review of evaporation theory and development of instrumentation.* US Navy Electronics Laboratory Rep, 1950. **159**: p. 71.
8. Winter, T.C., *Uncertainties in estimating the water balance of lakes 1.* JAWRA Journal of the American Water Resources Association, 1981. **17**(1): p. 82-115.
9. Ramamurthy, A.S., U.S. Tim, and M. Rao, *Flow over sharp-crested plate weirs.* Journal of irrigation and drainage Engineering, 1987. **113**(2): p. 163-172.
10. Peltier, E., et al., *Assessing the Water Quality Impacts of Constructed Wetlands on Tile Outlet Terrace Runoff (CD-97758901).* University of Kansas, 2020.
11. Mitsch, W. and J. Gosselink, *Wetlands. 5th*. 2015, Wiley Press.
12. Martin, A.R., M.L. Soupir, and A.L. Kaleita, *Seasonal and intra-event nutrient levels in farmed prairie potholes of the Des Moines Lobe.* Transactions of the ASABE, 2019. **62**(6): p. 1607-1617.

Chapter 4

Modeling Nutrient Removal

Multiple efforts have been made to develop models to assess nutrient removal in constructed wetlands, at a range of complexities [1, 2]. Most of these models are developed for constant (or at least consistent) flow systems, and often assume the presence of either perfect plug flow conditions in the wetland, completely mixed conditions or a combination of both. In general, wetland modeling literature indicates that neither a plug-flow nor a well-mixed model describe most real wetland conditions [3]. Stormwater treatment wetlands, in particular, often experience a number of different flow regimes throughout the year. These flow regimes are influenced by varying precipitation patterns, vegetation presence, water level and other environmental conditions, all of which have been shown in previous chapters to influence the current study sites. As a result, effective treatment models typically incorporate considerations of a variety of site-specific knowledge, including:

- Influent and effluent concentrations of the pollutants under study.
- Influent velocities of the storm water runoff entering the wetlands.
- Wetland hydraulics including the flow hydrodynamics and sometimes vegetation patterns.
- Wetland dimensions and size

Incorporation of more detailed wetland information can improve model performance and increase our knowledge of wetland processes, but also adds complexity to the model and requires additional data collection. This chapter addresses the problems associated with using traditional approaches to model nutrient removal, develop and calibrate a modified tank in series model

using 2015 sampling data for the Harvest Hills wetlands, and use the results to assess the likely performance of these wetlands for nitrogen and phosphorus removal under various conditions.

4.1 Model Development

A common approach to modelling nutrient removal in wetlands is to assume first-order kinetics for each constituent [4, 5]. The model equation is generally given as [6]:

$$q\frac{dC}{dx} = -k(C - C^*) \tag{4.1}$$

where,

q is the hydraulic loading rate (m/yr),

x is the distance water travels from inlet to the outlet,

C is the pollutant concentration,

C* is the background pollutant concentration and

k is the areal rate constant (m/yr).

While the k-C* model has been used for a variety of wetland applications, it does have limitations in application to variable-flow or event-driven systems [7], such as those in this study. The k-C* model was developed and is best suited for steady flow conditions with constant water flow and pollutant concentrations and nonideal mixing patterns has been shown to cause large errors in the estimation of the rate constant [8]. Departures from the steady flow conditions, as in the case of stormwater wetlands, will result in inaccuracies in the predicted runoffs. The uncertainty would be the combined effect of intermittent nature of rainfall intensity, rainfall duration, rate of pollutant accumulation and preceding conditions onsite [5]. Secondly, the model assumes a linear plug flow conditions, with the rate of decrease of each pollutant determined as a linear function of the concentration along the length of the wetland. This theory is well criticized

in the literature as most of the removal generally happens near the influent of the wetlands [9, 10].

Finally, the reaction rate constant k in the model is an areal rate constant, making pollutant removal independent of wetland depth. For example, Kadlec & Knight [11] used depths ranging from 0.15m to 0.45m to calculate the detention times, since most of the constant flow wastewater treatment are not expected to have large depths. This becomes a problem when dealing with stormwater event driven wetlands as their depth ranges are expected to be much wider than those in wastewater wetlands with more consistent flow.

For this work, a relaxed tank in series model combining the first order k-C* model with a series of continuously stirred tank reactors (CSTR) was used to calibrate the hydraulic parameters of each wetland. This unified model approach was first proposed by Kadlec [12] and was later tested on several stormwater treatment facilities [13] and constructed wetlands of various sizes located in urban and agricultural watersheds [14]. The three-parameter model (i.e. p, k, C*) provides an efficient tradeoff between treating a wetland as a 'black box' system with ideal plug flow conditions and a complex dynamic model requiring time flow data for each pollutant at the inlet and outlet of the wetland. The fundamental equation for nutrient removal in this mode is:

$$\frac{(C_{out} - C^*)}{(C_{in} - C^*)} = \left(1 + \frac{kt}{Ph}\right)^{-P} \tag{4.2}$$

where,

C_{out} = effluent concentration (mg/L)

C_{in} = influent concentration (mg/L)

C* = background concentration (mg/L)

k = modified reaction rate constant (m/yr.),

t = detention time (days)

h = wetland water level (m)

P = apparent number of tanks

Nutrient removal models were developed for the two Harvest Hills wetlands (HHN and HHM) based on data available in the previous report on these sites [15]. The Cain site was not included in this modelling for two reasons: the additional time and complexity of developing a model for this site, which has an unusual outlet flow structure, and the fact that nutrient removal in that wetland appeared to be dominated by sediment settling processes. In addition, a focus of this study was to assess why the HHN and HHM sites had notable differences in nitrogen removal despite similar watersheds, planting practices, and wetland design.

Modeling in this work focused on the subset of events with positive nitrogen removal. This threshold had a significant impact on HHM site as 44% of the observed storm water quality events recorded for TN and 46% of the events recorded for TDN showed negative removals. Contrarily, HHN had none of the events showing negative removal for TN and only 18% for TDN. The majority of the storm events resulting in negative removals had very high influent flow rates. For instance, all three negative removal events for TDN in 2015 at the HHM site happened during the high flow season in May with recorded curve numbers (89.2, 91.4 and 90.5) in the top 70^{th} percentile. These fast-moving storm events, which added large volumes of water to the pond over a short time, may have resulted in an influx of dissolved oxygen that suppressed denitrification. In addition, the high flow rates likely led to scouring of the sediment surface. This scouring could release nitrogen, both as re-suspended particles and as pore water nitrogen that exchanged with the surface waters. HHN had fewer negative removal events. This may be due to the high levels of TSS and particulate nitrogen in the influent to that wetland. While the

same processes may have released dissolved nitrogen and reduced denitrification at HHN, this was balanced out in most cases by the settling of influent particles, which removed particulate nitrogen at the same time. Solids settling processes are more rapid and much less susceptible to the high flow runoff. Since this effect of particulate settling did not impact the TDN removal rates, 18% of the total storm events at HHN showed negative removal. Therefore, to reduce the impact of total nitrogen removal through settling, the events producing negative removals were removed from the analysis.

The calibration datasets used for model development included flow volumes and composite influent and effluent concentrations for N, P and TSS obtained from the recorded storm events in 2015. Influent and effluent concentrations for Total Nitrogen (TN), Total Dissolved Nitrogen (TDN), Total Phosphorus (TP) and Total Suspended Solids (TSS) were modelled. Total dissolved phosphorus (TDP) was not addressed, as both influent and effluent values for this parameter were near detection limits. Reduction in pollutant concentrations were non uniform but consistent across the range of influent concentration observed (Fig 4. 1). A summary of the overall removal observed for each of these pollutants in the previous study is also presented in Table 4. 1.

The background concentration, C*, represents the 'irreducible concentration' below which it is not possible to consistently remove a given pollutant from the water column in a biological treatment process, such as a wetland [16]. This behavior is found most often for nutrients such as carbon and nitrogen that are cycled between organic and inorganic forms and between the abiotic and biotic components of the system. However, TSS concentrations in a wetland are also unlikely to reach zero, as wetland processes generate new suspended solid material even as they remove influent solids [6]. For this model, C* values were set at the

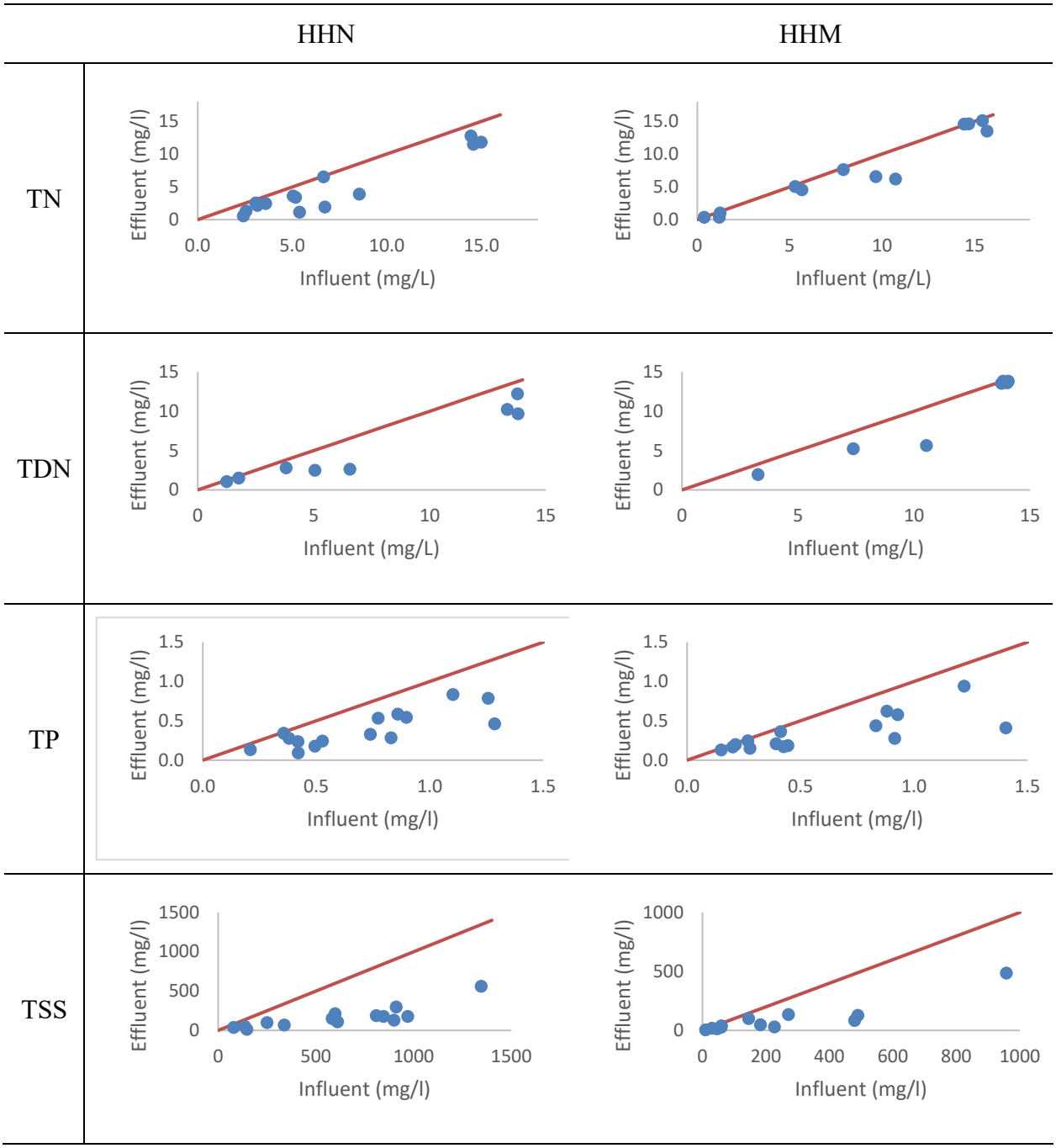

Fig 4. 1 Observed influent vs effluent concentrations for calibration dataset in Harvest Hills North (HHN) and Harvest Hills Middle (HHM) wetlands. The data points only represent the events that showed positive removal. TN: Total Nitrogen, TDN: Total Dissolved Nitrogen, TP: Total Phosphorus, TSS: Total Suspended Solids. Solid line represents no change in concentration.

threshold value below which no consistent decrease in concentration of that constituent was observed at the three study sites from 2014-15, as presented in [17]. This resulted in the

following C* values of TSS: 10mg/L, TN: 1mg/L, TDN: 1mg/L. For total phosphorus, C* was set to zero, as some effluent samples were below detection limit in the previous study.

Table 4. 1 Mean observed concentration-based removal percentages of modelled parameters at Harvest Hills North (HHN) and Harvest Hills Middle (HHM) wetlands in 2015.

	TN	TDN	TP	TSS
HHN	27.7	24.4	36.6	70.9
HHM	8.4	4.1	27.7	53.5

Detention times were calculated using a theoretical method described in Kadlec and Wallace [6].

$$t = ehA/Q_{in} \tag{4.3}$$

where A is the surface area of the wetland, calculated using the stage storage relationship from Fig 3. 1, h was taken to be the preceding day water level and e is the volumetric efficiency. For each storm event, runoff depths from the upland model were converted to volumetric flowrates entering the wetland using the time base of the produced runoff hydrographs. The volumetric efficiency can be calculated using the aspect ratio of the wetland as described in section 3.1.

Treated stormwater runoff exiting from the wetland is expected to have entered from a tenth to four times the nominal detention times earlier [6]. However, detention times in stormwater constructed wetlands tend to vary throughout the year depending on seasonal precipitation patterns. Shorter times are observed during wetter periods, when the wetlands remain near capacity. During low-precipitation periods, the wetlands experience drawdown from peak water level, which leads to longer detention times during the less frequent storm events. A single averaged value of detention times over a growing season or year will therefore incorporate

a bias towards high-rainfall seasons (when more events occur) and produce inaccurate results. Ideally, a dynamic model using the time series data for the flow and concentration of each pollutant should be used to calibrate the value of 'k' for each wetland. In the absence of these chemographs, the next best option was to use the range of detention time distributions developed in the previous chapter to represent the likely time period that storm runoff will spend in the respective wetland. This range was obtained from the Monte Carlo analysis performed for the two wetlands detention time calculations in chapter 3.

4.2 Model Calibration (dynamic water levels)

Calibration of the relaxed tank in series model requires simultaneous fitting of values for k (the reaction rate) and P (the # of tanks or mixing parameter) from Eq. 4.2 over the range of flow and pollutant conditions observed in the sample data. The Shuffled Complex Evolution (SCE-UA) algorithm developed at the University of Arizona [18] was used to calibrate the *k* and *P* model parameters. The SCE global search optimization algorithm was designed to provide an optimization process that was both robust to a variety of starting conditions and also efficient at finding optimal solutions for hydrological modeling problems [19, 20]. This approach has proved to be a significant improvement on accuracy while being computationally more efficient than several existing optimization models when tested on wide range of hydrological applications including rainfall-runoff modeling [21, 22] and water quality catchment models [23]. The model combines a simple search optimization method with algorithms for complex shuffling and competitive evolution and provides access to controlled random search [24]. The Root Mean Square Error (RMSE) between the observed and predicted parameter values was used to minimize the objective function. The optimization model was run to search the best fit value of *P* and *k* within the upper and lower bounds of (1-10) tanks and (0-50) m/year respectively.

Initial calibration results forced the *P* value to fall towards the lower bound (*P* = 1) for all four pollutants. This result indicates significant mixing along the main flow path between the inlet and outlet at both wetlands and suggest that water moves rapidly through the wetlands during most storm events. This finding reinforces the necessity of the unified model approach as compared to a single parameter k-C* model, which will over-predict removal as flow conditions deviate from ideal plug flow. The presence of a single 'tank' also indicates that the wetlands are operating with low hydraulic efficiency. In general, larger total wetland area would be required to achieve high levels of pollutant removal in a low P wetland compared to one which exhibits more plug flow-like conditions [6].

Low P values might also be an indication of significant weathering of nitrogen and phosphorus (i.e., decomposition into individual forms) occurring inside the wetlands. Since the tested pollutants (total N and total P) are mixtures rather than individual components, a change in composition is expected as water moves along the wetlands and different components get reduced at different rates. For instance, TN consist of individual components like nitrate and ammonia and sub mixtures including particulate nitrogen and organic nitrogen. Similarly, TP includes particulate-associated, soluble reactive, and dissolved organic forms of phosphorus. Chemical and biological processes within the wetland will act at different rates on these individual components, changing the makeup and reactivity of 'total nitrogen' or 'total phosphorus' as it moves through the system. Since the model assumes a single rate of reactivity (k) for TN and TP, these effects will be represented as lower values for the mixing parameter [6].

Best-fit values for k obtained at different detention times and for P =1-3 are presented in Table 4. 2. Values for the reactivity constants follow the removal trend expected from the experimental results (Table 4. 1): given an identical detention time, higher values are obtained

for constituents with higher overall removal rates (TSS and TP). Given the high level of total phosphorus association with suspended solids, both compounds are likely removed primarily by settling processes. As settling often occurs near the wetland inlet, these processes are often less sensitive to hydraulic flow and mixing patterns.

For a given pollutant, the optimal value of k decreased with increasing retention time. Without spatially resolved data on pollutant concentrations within the wetland, the system essentially treats internal wetland processes as a black box, with the model trying to achieve a given level of total removal between wetland inlet and outlet. Thus, retention time and reactivity (k) should have an inverse relationship when fitting the model. At a shorter detention time, a higher reactivity is required to achieve the same level of contaminant removal, requiring a higher value of k. This relationship is linear, and values for k at intermediate retention times can be calculated by a simple interpolation.

Table 4. 2 Calibration results for k as a function of detention times and P.

	HHN				HHM			
	t	P=1	P=2	P=3	t	P=1	P=2	P=3
TN	50% cdf (3.04 hrs)	1.34	1.23	1.20	50% cdf (3.35 hrs)	0.41	0.40	0.40
	70% cdf (4.28 hrs)	0.95	0.87	0.85	70% cdf (5.15 hrs)	0.27	0.26	0.26
	90% cdf (6.87 hrs)	0.59	0.54	0.53	90% cdf (10.69 hrs)	0.13	0.12	0.12
TDN	50% cdf	1.33	1.22	1.19	50% cdf	0.34	0.33	0.33
	70% cdf	0.94	0.87	0.84	70% cdf	0.22	0.22	0.22
	90% cdf	0.59	0.54	0.52	90% cdf	0.11	0.10	0.10
TP	50% cdf	2.65	2.25	2.14	50% cdf	3.23	2.67	2.51
	70% cdf	1.88	1.60	1.52	70% cdf	2.10	1.74	1.63
	90% cdf	1.17	0.99	0.94	90% cdf	1.01	0.84	0.79
TSS	50% cdf	11.32	7.82	6.96	50% cdf	5.08	3.92	3.61
	70% cdf	8.04	5.55	4.95	70% cdf	3.30	2.55	2.35
	90% cdf	5.01	3.46	3.08	90% cdf	1.59	1.23	1.13

Table 4. 2 also shows that the number of 'tanks' used in the model (again, a measure of how much mixing occurs in the wetland) did not have a significant impact on the value of k for total or dissolved nitrogen. For these constituents, only the total time for reaction, as measured by detention time, has a significant effect. TSS and TP showed greater decreases in k as P increased from 1 to 3 tanks, particularly at HHN. The effect was largest at lower retention times. However, the root-mean squared error (RMSE), which measures the goodness of fit, increased slightly as P increased from 1 to 3 for a specific pollutant. For instance, the best objective function for TP with 1 CSTR in HHN wetland was achieved with an RMSE of 0.137, which rose

to 0.140 with 2 CSTRs and to 0.142 with 3 CSTRs. While individual changes are not statistically significant, there was an increasing trend in RMSE across pollutants as P increased. This further suggests that both wetlands experience substantial mixing.

The k values obtained here were on the lower end of those found by Merriman et al [14], who used a similar model to fit nutrient removal data across 10 constructed wetlands. The mean rate constants for that study were 44.2 m/yr for TN, 38.0 m/yr for TP and 128.6 m/yr for TSS. However, the observed mean removal of contaminants from the ten wetlands (i.e., TN: 28%, TP: 33%, TSS: 42%) were similar to what was observed here (Table 4. 1).

The average free water depths used by Merriman et al. [14] was much lower than what was used here. The water depths for the ten wetlands studied ranged from 0.33 ft to 0.98ft. Despite the much shallower systems and similar surface area (ranging from 0.17 ac to 0.49 ac for five out of the ten wetlands as compared to 0.43 ac for HHM and 0.27 ac for HHN), that study reported much higher 'k' values. For instance, the five sites which were geometrically similar to our study sites resulted in k values of between 5.1 m/yr to 61.6 m/yr for TN. However, a similar study done by Carleton et al. [25] reported much lower reaction rates for stormwater wetlands. The reaction rate constant ranged between -9.6 m/yr to 57.1 m/yr with the mean value of 15.2 m/yr for NO_3. Additionally, three out of the twenty-two wetlands studied produced reaction rate below 1 m/yr. For TP, the reaction rate obtained for sixteen out of the thirty-seven wetlands in that study were at or below 5 m/yr which aligns closely to the results obtained for our site.

One significant difference between these two studies is that the Merriman study used the constant design free water depth to represent 'h'. By contrast, here the water budget model was used to produce different water depth values for h for different storm events. This was due to the fact that the depth of water in the Harvest Hills wetlands varied substantially over the 2015

growing season, from 0.22 to 2.51 feet at HHN and 0.10 to 3.17 ft at HHM. This variation may have increased the weight placed on detention time, rather than k, in fitting the calibration data using the tank in series model.

4.3 Model Calibration (constant water depth)

To further investigate the effects of water depth assumptions on the apparent reaction rate constant (k), the data were re-fit using a different approach. The wetland water level (h) in Eq. 4.2 and 4.3 was replaced with the maximum wetland free water depth available for each wetland (i.e., HHM = 2.07 ft, HHN = 1.94 ft), and left as a constant value. This resulted in new retention time distributions with the 50% cdf values of 3hrs 54min for HHN and 5hrs 56min for HHM. Unlike the Merriman et al assumption, these constant depths were equivalent to the weir height controlling the outflow at both sites. While this does not represent the full hydraulic pattern of the stormwater wetlands during storm events, setting a higher water level does reflect the fact that discharge from the wetland will only occur once the water level has exceeded a minimum depth that allows flow over the effluent weir.

4.3.1 Split Dataset

The observed 2014-15 inlet and outlet concentration dataset was merged, for each site separately, and then split in half after being shuffled randomly to make calibration and validation subsets. The calibration results obtained for k and P while holding water depth constant are presented in Fig 4. 2.

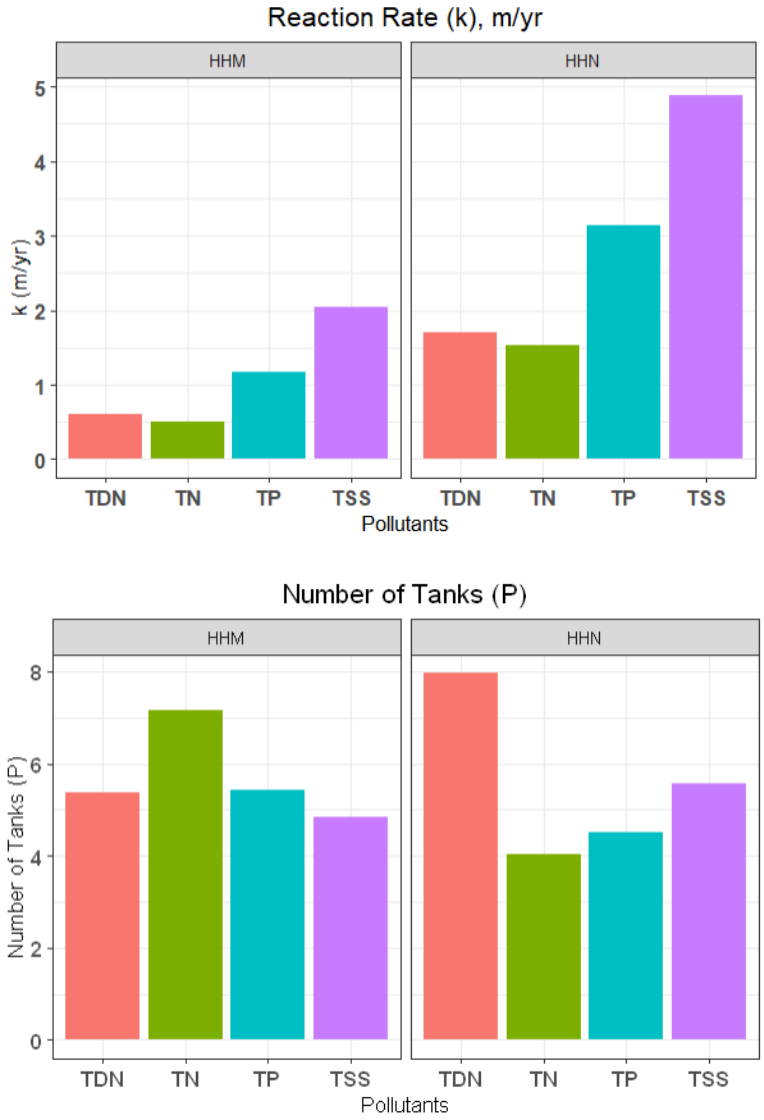

Fig 4. 2 Calibrated k and P values using the randomly shuffled 50% portion of the combined 2014-15 dataset.

Using the constant free water depth and the 50% cdf retention time values of 'k' and 'P' shown in Fig 4. 2, calibration and validation plots of the observed and predicted effluent concentrations were developed for the HHN and HHM wetlands (Fig 4. 3). Relative biasness is a measure of overprediction (RB>0) or underprediction (RB<0) of the predicted values. It is given as:

$$RB = \frac{1}{N}\sum_{i=1}^{N}\frac{(P_i - O_i)}{O_i} \tag{4.4}$$

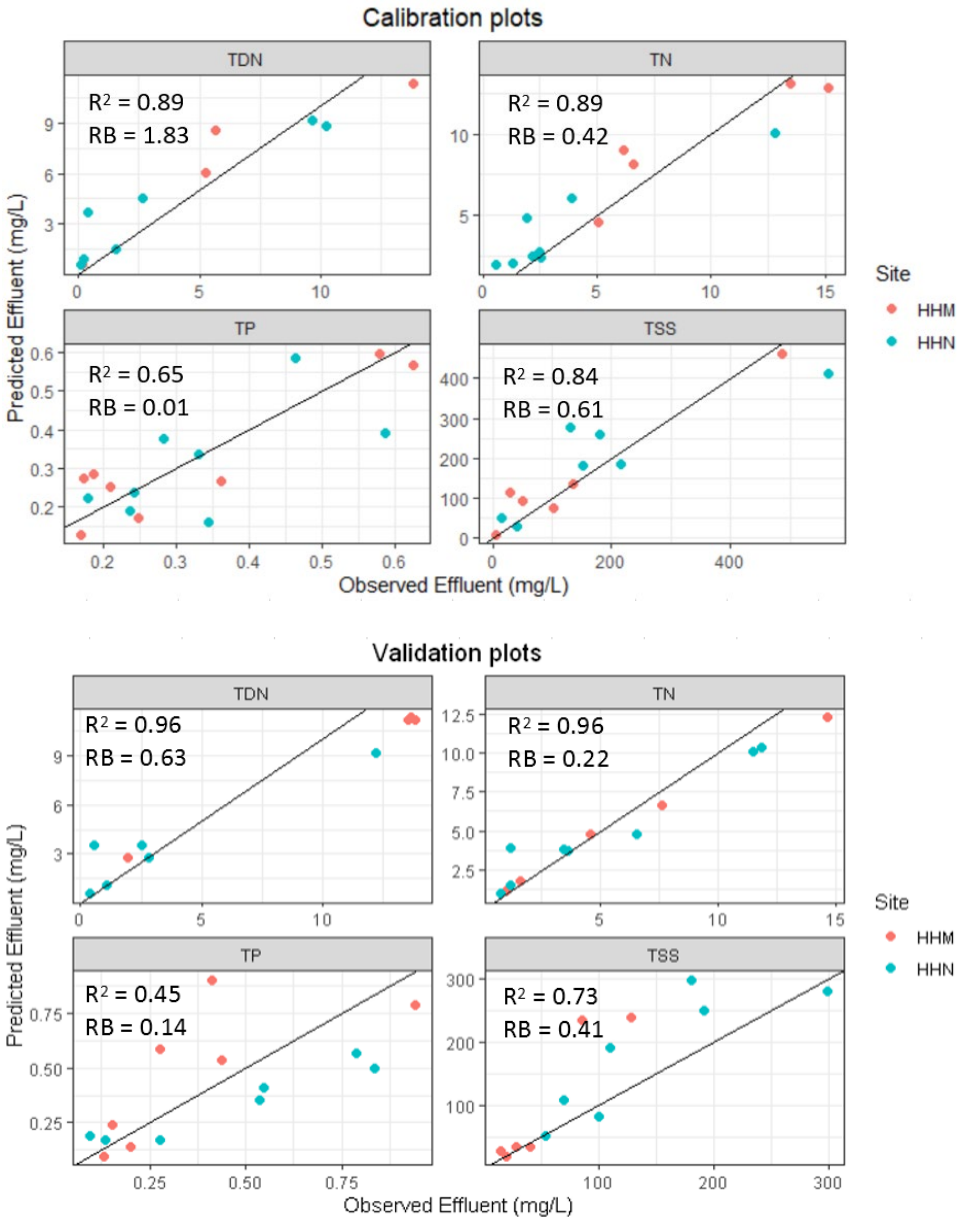

Fig 4. 3 Calibration and Validation plots for HHM and HHN. R^2 represents Pearson correlation measure and RB is the relative bias.

Predicted effluent concentrations of all pollutant mixtures were in close agreement to the observed concentrations except for TP, which showed the most scatter, but the least bias (RB). The model also generally underpredicted concentrations for high concentration effluent events. These high effluent concentrations do not necessarily a result of high influent concentrations. For example, Table 4. 3 shows that a relatively high influent TSS concentration of 227 mg/L on May

7th in HHM produced 87% removal while another storm event with similar influent concentration of 271 mg/L on May 26th only produced 50% removal.

Table 4. 3 Observed inflow concentrations and removal for TSS at HHM and HHN.

	HHN		HHM	
Date	Inflow Conc (mg/L)	Removal (%)	Inflow Conc (mg/L)	Removal (%)
6/10/2014	900.00	85.55	NA	NA
6/13/2014	NA	NA	10.00	50.00
9/3/2014	610.00	81.97	60.00	33.33
10/11/2014	970.00	81.44	NA	NA
10/14/2014	80.00	50.00	NA	NA
10/23/2014	250.00	60.00	30.00	33.33
5/7/2015	337.50	79.41	226.50	86.75
5/8/2015	146.50	89.76	59.00	52.54
5/14/2015	135.50	59.78	46.50	66.67
5/17/2015	910.50	67.22	479.50	82.17
5/21/2015	583.00	73.93	183.00	72.68
5/26/2015	597.50	64.10	270.50	50.09
6/7/2015	1346.00	58.17	957.50	49.24
6/15/2015	808.50	76.31	489.50	73.75
7/7/2015	846.00	78.61	145.50	30.24

Therefore, the high observed effluent concentrations in Fig 4. 3 can be a result of poor removal performance in the wetland for that event, which is dependent upon the performance of the specific processes responsible for the removal of the specific pollutant, rather than solely depending on influent water quality.

Although the calibrated values produced decent validation results as presented in Fig 4. 3, the small number of observed data points (can be visualized from Fig 4. 1) and the possible effect of seasonal variation on the removal performance of the wetland was expected to decrease the robustness of the calibrated parameter values. To test this proposal, the parameters were calibrated 10 times, each after the dataset was randomly shuffled and split in half. This also allowed the visualization of the spread of the calibrated parameter values and the results are presented below in Fig 4. 4.

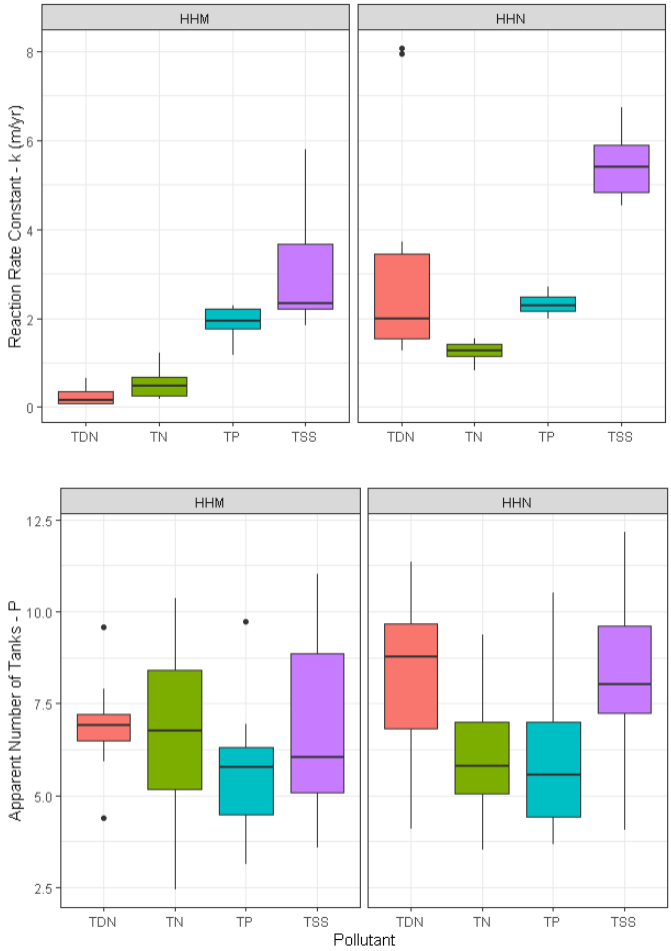

Fig 4. 4 Calibration spread of reaction rate (k) and apparent number of tanks (P).

The calibrated reaction rate values produced a large spread for TSS at both sites and HHN in addition, showed large TDN spread. This was due to the combination of the small

number of observed data points (see Fig 4. 1) and the variability in the observed removal efficiencies for the pollutants. For instance, TSS showed high variations in concentration removal across the year (see Table 4.2), this is reflected here in the high spread of the calibrated k values from the randomly shuffled data points. Additionally, the number of tanks varied significantly for all pollutants and at both sites.

4.3.2 Full Dataset

To strengthen the calibration of k and P parameter for the Bayesian analysis in the following section, the model was also calibrated using the whole of the 2014-15 dataset. The results for k and P are presented below in Fig 4. 5 and the calibration plots are shown in Fig 4. 6 . These values will be used for further analysis hereon.

Fig 4. 5 Reaction rate (k) and number of tanks (P) calculated using a fixed water depth.

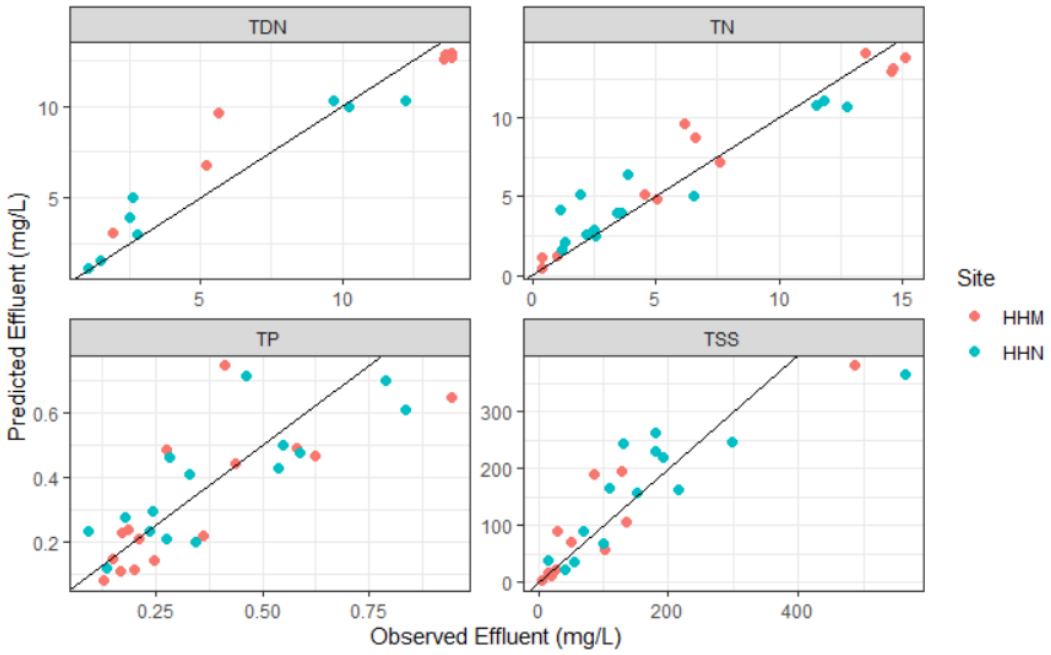

Fig 4. 6 Combined wetlands calibration plots for TN, TDN, TP and TSS using all of 2014-15 dataset.

TN, TDN and TSS showed high Pearson correlation (R^2) and Nash-Sutcliffe Efficiency (NSE) with TP having the poorest fit based on both measures (Table 4. 4). In general, phosphorus loadings entering and leaving the wetland were quite low, with mean influent concentration of 0.65 mg/l and mean outlet concentration of 0.37 mg/l. While the background concentration for TP was set at $C^* = 0$ mg/l, it is quite likely that removal becomes inconsistent at the lower range of influent values observed here.TN and TSS had more positive RB scores than TDN and TP, indicating that the model tends to over-predict effluent concentrations of these constituents relative to observed values. In all cases, there was no consistent difference in predictive capacity between the two wetlands.

Table 4. 4 Combined wetland calibration statistics using observed and predicted effluent data.

	R^2	NSE	RB
TN	0.92	0.90	0.36
TDN	0.92	0.89	0.19
TP	0.62	0.57	0.04
TSS	0.78	0.74	0.18

4.3.3 Discussion

The fixed water depth assumption had a significant impact on the mixing term (P) for both systems. This new range of values (i.e., 2 to 7 tanks), indicates substantially less mixing than was suggested by the earlier version of the model. In general, these results are more consistent with previous results published by Merriman et al. [14] and with other results obtained for a variety of free surface treatment wetlands [3, 26].

In addition to changes in apparent mixing, the k values with the fixed depth assumption decreased slightly from the original k values (Table 4. 2). The constant free water depth used in Eq 4.2 was lower than the water depth obtained during high flow season storm events, with a maximum height reaching 2.51ft in HHN and 3.17 ft in HHM. Since increase in water depth increases the calculated reaction rate values in Eq 4.2, using the constant free water depth equivalent to the weir height (i.e., HHM = 2.07 ft, HHN = 1.94 ft) produced lower reaction rate values than those obtained previously.

The low k values for total and dissolved nitrogen are representative of the inefficient biogeochemical process happening inside the wetland. The major removal pathway for nitrogen from stormwater constructed wetlands (i.e., denitrification), depends upon many factors including microbial flora, organic carbon source, plant species residue, amount of dissolved

oxygen, soil moisture, redox potential, pH values and water levels [27, 28].The lack of incorporation of the temperature effect in our model would have also affected the produced reaction rate values. Removal rates for nitrate have been found to be 2-4 times higher in summer than in winter [29], a distinction that would not be noted in our approach. It is also possible that the lack of macrophyte activity due to the limitation of carbon and/or phosphorus supply and other physical obstructions presence contributed to the lower reaction rates. Denitrification rates have been found to increase by adding supplemental carbon [30] especially in agricultural watersheds with tile drain systems installed [31]. This will be discussed further in detail in chapter 5.

The most significant difference between the study wetlands and sites in the comparative studies was the much lower average detention times. The detention time term 't' in Eq 4.2 from Merriman et al. was 2 days for four of the five wetlands as compared to the 3hrs 54min for HHN and 5hrs 56min for HHM. Carleton et al. also consistently reported detention times > 2 days for most of their wetlands. This low retention time would have had a significantly higher impact on the nitrogen removal processes in our wetland than on the processes responsible for solids removal. This can be seen in the much higher observed removal for the solids obtained in our systems for the same storm events (see Fig 4.1 and Table 4.1). TSS and TP was mostly removed through settling which mainly happens around the wetland inlet and are thus much less susceptible to hydraulic loading rate and wetland retention time. The general agreement upon the minimum retention time required for nitrate removal in wetlands receiving agricultural runoff has been around two days [32, 33] with recommendations of around two weeks present [34]. Additionally, the variability of storm water runoff has the tendency of overwhelming the nitrate removal processes in wetlands during the high flow seasons [35].

The most probable reason for the larger detention time at the comparison sites would be a slower influent flow rate. The flashy behavior of the runoff hydrographs combined with the high storm runoff volumes observed here produced CN > 90 for 45% and 27% of the storm events at HHN and HHM respectively (chapter 2). By comparison, the average CN reported by Merriman et al. for the ten wetlands was 77.5 with none above 90. This resulted in much lower retention times in both of our study wetlands as the inflow high velocity water flow through the systems.

HHM showed much lower reaction rate values than HHN. This was expected as HHM was acting as a nitrogen source for > 40% of the observed storm events in 2014-15 for both TN and TDN as documented in section 4.1 above. Additionally, the storm events where wetlands were acting as a net nitrogen sink, also showed very little removal efficiencies with median removal rate of 14% for TN and 3% for TDN for the combined 2014-15 storm events. This is much lower than the median removal rates of 31% for TN and 25% for TDN at HHN for events showing positive removal. Since, the retention time for both wetlands are similar at 50% cdf (see section 3.4), this change in removal efficiency can be directly attributed to the biogeochemical and hydraulic differences between the two sites. For instance, HHN had a much larger solids associated nitrogen. This would have boosted up the TN removal efficiency, courtesy of a much more efficient solids removal performance of the wetland. Additionally, HHM had a much lower aspect ratio than HHN (0.99 vs 1.84). This might have resulted in the short-circuiting of the influent water at a much higher rate at HHM. Therefore, even though the two sites showed similar retention time distributions, the narrower aspect ratio at HHN, might have allowed for better mixing patterns which would have promoted the necessary sediment water contact required for denitrification. This will be discussed in more detail in section 5.1.

4.4 Bayesian Analysis of Reaction Rate Constants

The modeling approach outlined above provides important information about the major factors influencing nutrient removal. However, using an annual average value of k and P to address the nutrient removal capacity of the wetlands is not ideal, as it obscures the likely effects of both seasonal and storm-to-storm variation on wetland performance. To better address the uncertainty in the modeled parameters, particularly the reaction rate constant k, a Bayesian approach was also developed. Bayesian analysis works on the fundamental assumption that all parameters have random values and therefore must have a distribution, while the dataset used to calculate the parameters are fixed. This approach is directly in contrast to the frequentist method (for example: SCE method described above) which assumes the dataset to be a random sample of a population and calculates fixed parameter values to represent the underlying process. So, in short, the Bayesian approach can be used to address the likely range of one or more parameters assuming that the full dataset is collected, and the experiment is not to be repeated.

The Bayesian method relies upon the Bayes theorem [36], which is given as:

$$P(\theta/D) = \frac{P(D/\theta)\ P(\theta)}{P(D)} \tag{4.5}$$

where,

$P(\theta)$ = Prior; Strength in truth of parameter 'θ' without data 'D'

$P(\theta/D)$ = Posterior; Strength in truth of parameter 'θ' given data 'D'

$P(D/\theta)$ = Likelihood; Probability that data could be generated by model with parameter values 'θ'.

$P(D)$ = Evidence; Probability of data according to the model.

The prior distribution, or the estimate of how the parameter should behave, is defined by the user based on some existing knowledge about the phenomenon under investigation. The

likelihood distribution, on the other hand, is dependent upon the information stored in the observed dataset. In small sized datasets, as is the case here, the contribution of the prior assumption to the posterior distribution becomes much more significant than the likelihood function [37]. Therefore, the use of an informative prior (i.e., one that represents the specific underlying process being studied, rather than a random value or set of values) is crucial to determine the correct posterior distribution.

For this study, the Bayesian method was used to calculate the posterior distribution of k and P parameters used in Eq 4.2. A 50% detention time cdf value was used for the time parameter 't' for each wetland, and the height was set to the maximum water level (i.e., the outflow weir crest height) for that wetland (i.e., HHM = 2.07 ft, HHN = 1.94 ft).

Since likelihood distribution should be based on the observed data, the response variable (C_{out}) was tested for different distributions (uniform, normal and gamma) and the gamma distribution was selected for all constituents, as this distribution produced the lowest Akaike information criterion (AIC) value. This choice can also be validated by comparing the empirical cumulative distribution function of C_{out} with the theoretical CDF of each distribution, as shown in Fig 4. 6 for TSS. As can be seen, the cumulative distribution function for the gamma distibution aligns much better with the emperical cdf of the outflow concentration (C_{out}). Similar patterns were observed for the remaining three pollutant mixes.

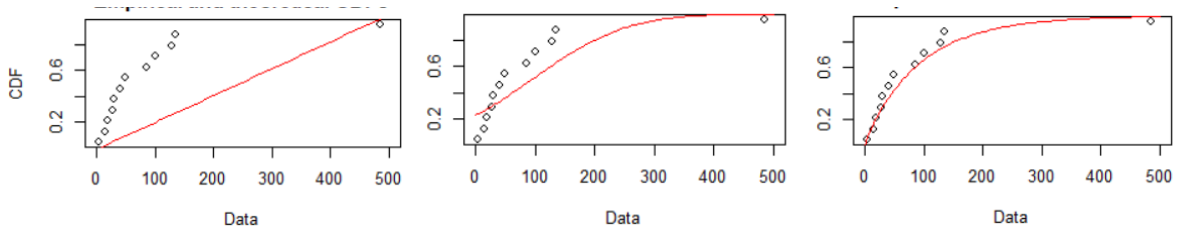

Fig 4. 7 Calculated (red line) vs emperical CDF for effleunt TSS (black dots) for uniform distribution (left), normal distibution (center) and gamma distribution (right).

Two approaches were used to determine the prior distribution for P and k. A ‘strong’ prior was set by assuming that the mean value for both ‘k’ and ‘P’ would be equal to the values obtained using the SCE method for each constituent at a retention time equal to 50% of the cdf. The prior was assumed to be normally distributed around these mean values. This meets the recommendation to provide additional information about system behavior for a small sized dataset [38]. A second ‘weak’ prior that used no system-specific knowledge was also tested. For this weak prior, mean values of both k and P were assumed to be equal to 1 for each constituent.

The mean k and P values of the posterior distribution produced using the strong prior Bayesian method (Fig 4. 7) were similar to values produced using the SCE method for both HHN and HHM for TN, TDN and TP. For TSS, the strong prior Bayesian analysis suggested that the mean value of both k and P was somewhat higher than that calculated by the SCE method. Significantly, the weak prior method did not produce similar results - instead the mean value for TN, TDN and TP using the weak priors were close to their originally guessed values of 1 for both k and P. Once again, TSS is the exception, with higher k and P values than its prior means. Overall, this suggests that relatively more information is available in the observed dataset for TSS, which allowed the posterior distribution to divert from the prior distribution by increasing the contribution of the likelihood. Contrarily, mean results of the posterior distributions for the other three parameters are dominated by the intial assumptions regardless of the strength of the prior.

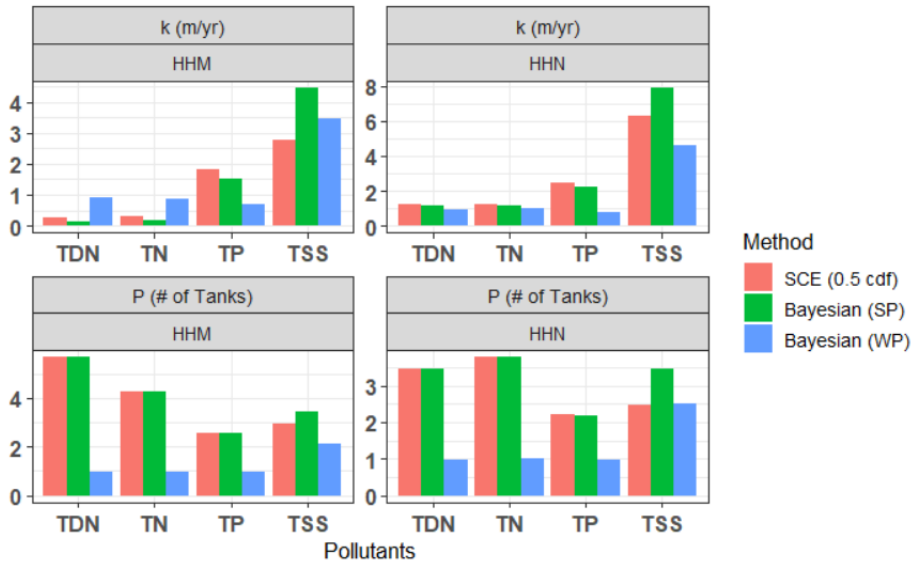

Fig 4. 8 Mean Reaction Rate constant, k (m/yr) and Mixing Term (P) using Bayesian analysis with a Strong Prior (SP) and Weak Prior (WP) distribution.

The results presented above verified the significant impact of using the informative prior for small sized datasets as it was found to dictate the resulting mean value of the posterior distribution of the parameters modeled. The value of the Bayesian approach in this case is therefore not to provide an independent estimate of the mean values for k and P. Given the small size of this dataset, those values must be obtained independently, in this case through the SCE analysis. The Bayesian analysis, however, does provide information on the uncertainities associated with these two parameters. The range of likely values obatined from the posterior distributions for k and P for each constituent are plotted in Fig 4. 9 and Fig 4. 10 for the HHM and HHN wetlands, respectively. Essentially, this approach provides us with a method for quantifying the likely range of reaction rate constants that we could expect to observe in these wetlands under a wider range of storm events during the 2014-15 period.

	k (m/yr)	P
TN	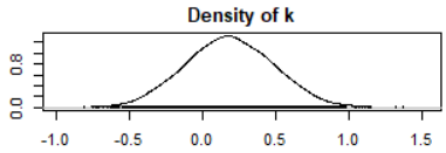 Mean = 0.18, SD = 0.30	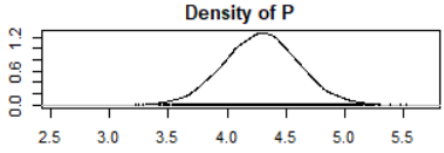 Mean = 4.29. SD = 0.32
TDN	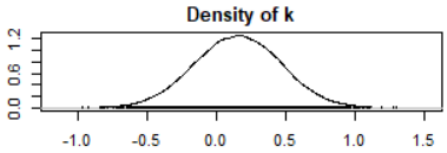 Mean = 1.15, SD = 0.31	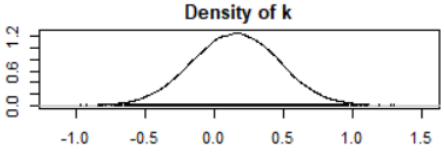 Mean = 5.68, SD = 0.32
TP	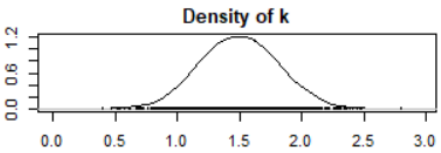 Mean = 1.50, SD = 0.32	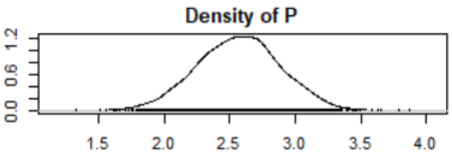 Mean = 2.57, SD = 0.32
TSS	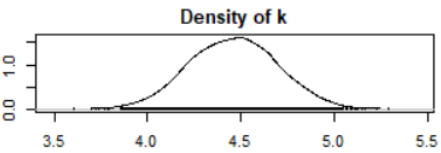 Mean = 4.46, SD = 0.24	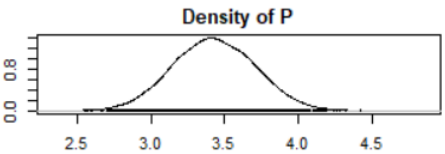 Mean = 3.43, SD = 0.28

Fig 4. 9 Posterior distributions for ‘k’ and ‘P’ parameter values at HHM obtained using the strong prior Bayesian method.

	k (m/yr)	P
TN	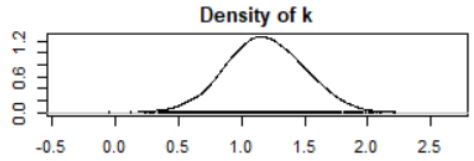 Mean = 1.19, SD = 0.32	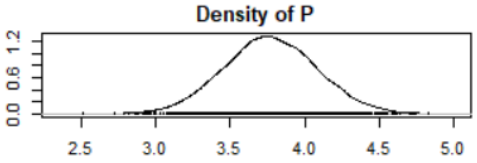 Mean = 3.77. SD = 0.31
TDN	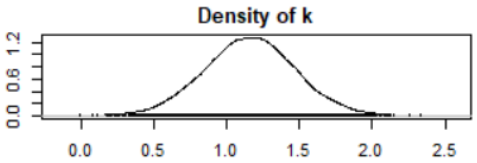 Mean = 1.16, SD = 0.31	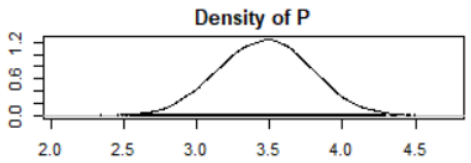 Mean = 3.47, SD = 0.32
TP	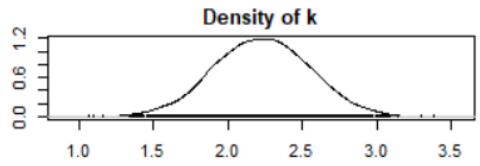 Mean = 2.23, SD = 0.32	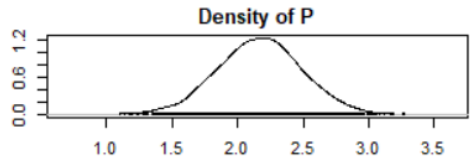 Mean = 2.17, SD = 0.32
TSS	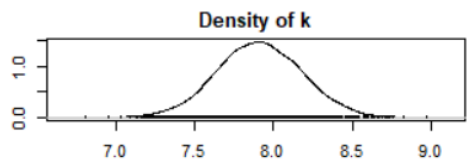 Mean = 7.91, SD = 0.27	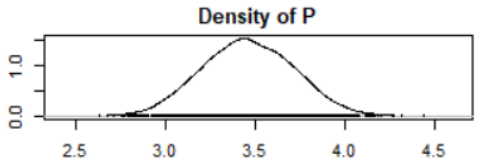 Mean = 3.46, SD = 0.26

Fig 4. 10 Posterior distributions for 'k' and 'P' parameter values at HHN obtained using the strong prior Bayesian method.

4.5 Estimating Wetland Nutrient Removal

The utility of this Bayesian analysis can be seen by using the information obtained on the range of reaction rate constants and mixing values to estimate removal of individual constituents across a range of influent concentrations. To explore this observed change in predicted effluent concentration due to uncertainties associated with the parameters, the expected removal was determined for the minimum and maximum observed influent concentrations for all four pollutants using the 2.5% and 97.5% quantile values determined for k and P (listed as min and

max values in Table 4. 5). These values provide a range for the expected extent of pollutant removal at each site across the likely influent conditions.

Table 4. 5 Minimum and maximum ranges for observed influent concentrations and the k and P values obtained from the posterior distributions.

		HHM			HHN		
		Inflow (mg/L)	k (m/yr)	P (# of tanks)	Inflow (mg/L)	k (m/yr)	P (# of tanks)
TN	Min	0.38	-0.40	3.67	1.85	0.57	3.16
	Max	15.67	0.77	4.93	14.99	1.81	4.39
TDN	Min	3.30	-0.46	5.06	1.25	0.54	2.85
	Max	14.10	0.76	6.31	13.81	1.78	4.08
TP	Min	0.15	0.88	1.93	0.21	1.59	1.52
	Max	1.40	2.11	3.18	1.29	2.86	2.80
TSS	Min	10.00	3.99	2.89	80.00	7.38	2.97
	Max	958.00	4.93	3.98	1346.00	8.44	3.97

Fig 4. 10 shows the expected range of wetland performance with respect to removal of TSS, TP, TN and TDN. In each case, the pollutant removal percentage increased significantly when comparing the parameter values at the 97.5% quantile to the 2.5% quantile. This figure emphasizes that, while providing a useful reference point, a single value for removal is too simplistic to accurately represent the performance of these systems. The wetlands are dynamic systems that are exposed to different hydraulic patterns throughout the year, which influence their pollutant removal capabilities. Therefore, it is more realistic to report a range of probable removal rates that better reflect the uncertainty associated with the parameters used to model wetland performance.

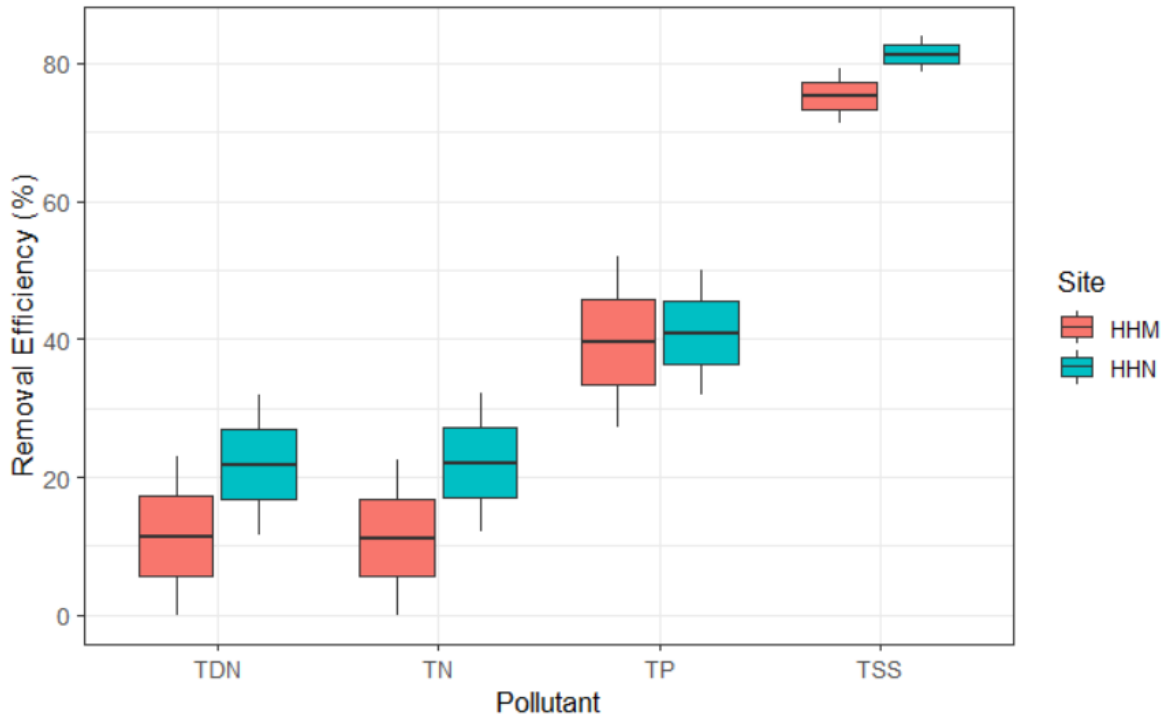

Fig 4. 11 Confidence interval (95%) of pollutant removal percentages at the Harvest Hills sites.

Fig 4. 11 shows that both sites are expected to be very effective at solids removal, with at least 78% and 71% removal for HHN and HHM, respectively, under typical site conditions. The difference in removals between these two sites for TSS is likely driven by erosion effects in the HHN watershed. This leads to higher influent TSS concentrations, and likely to larger, more easily settled solids. The two wetlands are most similar with respect to phosphorus removal, with both wetlands expected to achieve a 30-50% reduction in influent TP. Consistent with the observed results from 2014-15, the model predicts that the biggest difference in wetland performance will be in nitrogen removal. The distribution for HHM includes an expectation that some storm events will see little to no removal of either TN or TDN at 'typical' conditions (median detention time), while HHN will generally achieve up to 30% removal. Removal percentages for TN and TDN are very similar in both systems, as nitrogen removal is driven more by biogeochemical processes than by particulate settling.

Comparison of the expected range to the overall observed removal rates from 2015 (Table 4. 1) shows that the actual removal of TSS and TP was at or below the low end of expected values shown in Fig 4. 11. A substantial portion of the recorded storm events in that year occurred under continuous-flow conditions in May to early June, with detention times below the median value used for the calculations. TN and TDN removals during 2015 were more in-line with the ranges predicted here. Nitrogen removal processes, particularly denitrification, require longer times, and are thus less sensitive to smaller differences in detention time below the median value. Conversely, we would expect that nitrogen removal would improve more during low-rainfall periods, when detention times are longer.

4.6 Summary

The relaxed tank in series model proved to be an effective approach for modeling nutrient removal at the two Harvest Hills study sites. In general, results indicated that these wetlands have a relatively high level of mixing. Higher levels of mixing would contribute to less time for removal of dissolved constituents, particularly nitrogen. In this model, the reaction rate constant k value is strongly impacted by the low observed removal. This low observed removal was predicted to be the direct result of the suboptimal execution of the biogeochemical processes responsible for nitrogen removal. Several approaches were taken to address this inter-dependence, all of which suggested that reaction rates for these systems are near the low end of that observed in similar studies. A Bayesian analysis was used to provide a better picture of the range of contaminant removals that could be expected in these wetlands during actual performance. The results indicate that these wetlands will be effective for TSS and TP removal under most conditions, but that nitrogen removal is likely to vary substantially. During high rainfall periods, short detention times and low reaction rates will result in nitrogen removal of

20-30% at HHN and < 15% at HHM for most events. During low rainfall periods, however, longer times for reaction should lead to greater removal of influent nitrogen.

4.7 References:

1. Kumar, J. and Y. Zhao, *A review on numerous modeling approaches for effective, economical and ecological treatment wetlands.* Journal of environmental management, 2011. **92**(3): p. 400-406.
2. Meyer, D., et al., *Modelling constructed wetlands: Scopes and aims–a comparative review.* Ecological Engineering, 2015. **80**: p. 205-213.
3. Kadlec, R.H. and S. Wallace, *Treatment Wetlands*. 2008: CRC Press.
4. Rousseau, D.P., P.A. Vanrolleghem, and N. De Pauw, *Model-based design of horizontal subsurface flow constructed treatment wetlands: a review.* Water research, 2004. **38**(6): p. 1484-1493.
5. Wong, T. and W. Geiger, *Adaptation of wastewater surface flow wetland formulae for application in constructed stormwater wetlands.* Ecological Engineering, 1997. **9**(3-4): p. 187-202.
6. Kadlec, R. and S. Wallace, *Treatment wetlands. CRC Press Taylor & Francis Group.* Boca Raton, London, New York, 2009: p. 267-347.
7. Kadlec, R.H., *The inadequacy of first-order treatment wetland models.* Ecological Engineering, 2000. **15**(1-2): p. 105-119.
8. Kadlec, R., W. Bastiaens, and D. Urban, *Hydrological Design of Free Water Surface Treatment Wetlands, Constructed Wetland for Water Quality Improvement, GA. Moshiri ed*. 1983, Lewis publishers.
9. Hathaway, J. and W.F. Hunt. *An evaluation of stormwater wetlands in series*. in *World Environmental and Water Resources Congress 2009: Great Rivers*. 2009.
10. Merriman, L., W. Hunt, and K. Bass, *Development/ripening of ecosystems services in the first two growing seasons of a regional-scale constructed stormwater wetland on the coast of North Carolina.* Ecological Engineering, 2016. **94**: p. 393-405.
11. Kadlec, R. and R. Knight, *Treatment Wetlands–CRC Press, Inc.* Boca Raton, FloridaUSA, 1996.
12. Kadlec, R.H., *Effects of pollutant speciation in treatment wetlands design.* Ecological Engineering, 2003. **20**(1): p. 1-16.
13. Wong, T.H., et al., *Modelling urban stormwater treatment—A unified approach.* Ecological Engineering, 2006. **27**(1): p. 58-70.
14. Merriman, L.S., et al., *Adapting the relaxed tanks-in-series model for stormwater wetland water quality performance.* Water, 2017. **9**(9): p. 691.
15. Peltier, E., et al., *Monitoring Effectiveness of Tile Outlet Terrace Fields with Constructed Wetlands for Sediment, Nutrient and Volume Reduction in Northeastern Kansas*. 2016, Kansas Water Office: Topeka, KS.
16. Schueler, T.R., *Irreducible Pollutant Discharge Concentrations Discharged from Stormwater Practices.* Watershed Protection Techniques, 1996: p. 369-372.

17. Lee, H., *Nutrient Removal in Constructed Wetlands Treating Agricultural Tile Drainage*. 2016, University of Kansas.
18. Duan, Q., S. Sorooshian, and V. Gupta, *Effective and efficient global optimization for conceptual rainfall-runoff models.* Water resources research, 1992. **28**(4): p. 1015-1031.
19. Duan, Q., V.K. Gupta, and S. Sorooshian, *Shuffled complex evolution approach for effective and efficient global minimization.* Journal of optimization theory and applications, 1993. **76**(3): p. 501-521.
20. Duan, Q., S. Sorooshian, and V.K. Gupta, *Optimal use of the SCE-UA global optimization method for calibrating watershed models.* Journal of hydrology, 1994. **158**(3-4): p. 265-284.
21. Cooper, V., V. Nguyen, and J. Nicell, *Evaluation of global optimization methods for conceptual rainfall-runoff model calibration.* Water Science and Technology, 1997. **36**(5): p. 53-60.
22. Franchini, M., G. Galeati, and S. Berra, *Global optimization techniques for the calibration of conceptual rainfall-runoff models.* Hydrological Sciences Journal, 1998. **43**(3): p. 443-458.
23. Van Griensven, A. and T. Meixner, *A global and efficient multi-objective auto-calibration and uncertainty estimation method for water quality catchment models.* Journal of Hydroinformatics, 2007. **9**(4): p. 277-291.
24. Seong, C., Y. Her, and B.L. Benham, *Automatic calibration tool for Hydrologic Simulation Program-FORTRAN using a shuffled complex evolution algorithm.* Water, 2015. **7**(2): p. 503-527.
25. Carleton, J., et al., *Factors affecting the performance of stormwater treatment wetlands.* Water Research, 2001. **35**(6): p. 1552-1562.
26. Persson, J., N.L. Somes, and T. Wong, *Hydraulics efficiency of constructed wetlands and ponds.* Water science and technology, 1999. **40**(3): p. 291-300.
27. Sirivedhin, T. and K.A. Gray, *Factors affecting denitrification rates in experimental wetlands: field and laboratory studies.* Ecological Engineering, 2006. **26**(2): p. 167-181.
28. Bastviken, S.K., et al., *Potential denitrification in wetland sediments with different plant species detritus.* Ecological Engineering, 2005. **25**(2): p. 183-190.
29. Beutel, M.W., et al., *Nitrate removal in surface-flow constructed wetlands treating dilute agricultural runoff in the lower Yakima Basin, Washington.* Ecological Engineering, 2009. **35**(10): p. 1538-1546.
30. Killingstad, M.W., M.A. Widdowson, and R.L. Smith, *Modeling enhanced in situ denitrification in groundwater.* Journal of Environmental Engineering, 2002. **128**(6): p. 491-504.
31. Grebliunas, B.D. and W.L. Perry, *The role of C: N: P stoichiometry in affecting denitrification in sediments from agricultural surface and tile-water wetlands.* SpringerPlus, 2016. **5**(1): p. 359.
32. Hey, D.L., A.L. Kenimer, and K.R. Barrett, *Water quality improvement by four experimental wetlands.* Ecological Engineering, 1994. **3**(4): p. 381-397.
33. Phipps, R.G. and W.G. Crumpton, *Factors affecting nitrogen loss in experimental wetlands with different hydrologic loads.* Ecological Engineering, 1994. **3**(4): p. 399-408.

34. Woltemade, C., *Ability of restored wetlands to reduce nitrogen and phosphorus concentrations in agricultural drainage water.* Journal of Soil and Water Conservation, 2000. **55**(3): p. 303-309.
35. Kovacic, D.A., et al., *Effectiveness of constructed wetlands in reducing nitrogen and phosphorus export from agricultural tile drainage.* Journal of environmental quality, 2000. **29**(4): p. 1262-1274.
36. Bayes, T., *An essay toward solving a problem in the doctrine of chances. By the late Rev. Mr. Bayes, FRS communicated by Mr. Price, in a letter to John Canton, AMFRS.* Philosophical Transactions, 1763: p. 1683-1775.
37. Van de Schoot, R., et al., *A gentle introduction to Bayesian analysis: Applications to developmental research.* Child development, 2014. **85**(3): p. 842-860.
38. McNeish, D., *On using Bayesian methods to address small sample problems.* Structural Equation Modeling: A Multidisciplinary Journal, 2016. **23**(5): p. 750-773.

Chapter 5

Potential Design Improvements

This chapter focuses on improving the removal efficiencies of total and dissolved inorganic nitrogen, including NO_3, NO_2, NH_3 and NH_4. Since the study wetlands performed relatively well in removing solids and phosphorus (which were mostly particle associated), specific focus will be placed here on the nitrogen dynamics. Specifically, water quality and hydrological models developed in the previous chapters were used to examine the improvement in the removal efficiencies by inducing changes in wetland design.

Nitrate (NO_3) has been found to be the dominant form of nitrogen in agricultural runoff, as well as the most mobile state in well drained soils [1, 2]. Wetlands treating NO_3-N from agricultural watersheds have been shown to produce variable degrees of success [3-5] . Nitrogen removal in these studies has been found to be influenced by factors such as wetland to watershed ratio, residence time, temperature and seasonal variation in water discharge [6, 7]. In almost all of the cases, the major pathway of $NO_3 - N$ removal has been through denitrification and plant uptake [8, 9]. Therefore, the wetland design analysis will focus on changes to parameters that could improve the process of denitrification.

The governing equation used in this study (Eq 4.2) to model pollutant concentration removal uses hydraulic retention time (HRT) as a key predictor of system performance. Longer HRT has been found to produce better conditions for nutrient removal in constructed wetlands [10]. When tested on wetlands with similar vegetation type and surface area but different retention time (i.e., 0.8 days and 9.3 days), both ammonium (NH_4)-N and nitrate (NO_3)-N removal efficiencies increased, from 29.2% to 87% and from 29.8% to 85.6%, respectively [8]. With a retention time of 1 week, constructed wetlands receiving agricultural runoff from tile

drain systems upstream of the Embarras River in southeastern Illinois have been shown to achieve 37% removal of total nitrogen and up to 28% of Nitrate (NO_3) [11].

Retention time in our model is described by Eq. 5.1, and can be affected by changing any of the four components in the equation: wetland volumetric efficiency (e), wetland depth (h), wetland surface area (A), or influent flow rate (Qin)

$$t = ehA/Q_{in} \tag{5.1}$$

The wetland volumetric efficiency, which represents the ratio of effective to total volume within the wetland, can be affected by a number of site design choices. Kadlec and Wallace define this efficiency as [12]:

$$e = \frac{\mathcal{E}\eta h}{h_{nominal}} \tag{5.2}$$

where,

$\mathcal{E}$ = fraction of volume occupied by water

η = gross aerial efficiency

h = water depth, m

$h_{nominal}$ = nominal water depth, m

In free water surface wetlands, the wetland volume will be occupied by plants stems and litter therefore $\mathcal{E} < 1$. The gross areal efficiency (η) can be calculated as (Active flow area / total flow area) since there would most probably be stagnant pockets in the wetlands. Therefore $\eta < 1$. Since wetland bathymetry can vary along the length of the wetland, mean depth (h) can have uncertainty associated with it, specifically for large wetlands.

Due to the nature of the models developed in chapters 2-4, which ignore internal wetland flow patterns, we can only adjust the outer boundary aspect ratio of the wetlands to investigate

the effect of changing volumetric/hydraulic efficiency [13]. It should be noted however that the length to width ratio has been found to have the most impact on the hydraulic efficiency [14]

$$\lambda/e = 0.84\left[1 - exp(-0.59 * \frac{L}{W})\right] \tag{5.3}$$

Therefore, to examine the detailed impact of all the design variables upon wetland retention time and nutrient removal, the changes in various factors needs to be studied, which includes but not limited to:

- The volume of the wetland
- The shape of the wetland
- Upland/watershed properties
- Inlet and Outlet structures
- Vegetation type, density and spatial distribution
- Bathymetry

This chapter uses sensitivity analysis to explore the various ways some of the design features of these constructed wetlands can influence the wetland retention time and/or the nutrient removal performance. It also addresses the existing literature to identify the impacts of these parameters, and to discuss additional design issues that should be considered but cannot be directly represented using this model. Since this section focuses on improving the wetland design, modifications to the upland watershed are not addressed.

5.1 Improving Hydraulic Efficiency

Flow through wetlands is generally non-uniform [15]. This creates low velocity zones inside the wetland, which in turn decreases the volume utilization and hence the treatment efficiency [14]. Short circuiting, where a portion of the influent flows rapidly along the shortest

flow path through the center of the wetland, also influences the distribution of the hydraulic retention times [16]. Both of these factors result in only a portion of the total wetland volume being effectively utilized. This produces lower nutrient removal and sedimentation settling than would be expected based on the full wetland volume [17]. Using the full wetland surface area in the retention time equation with no modification for non-uniform flow would result in lower apparent values for the reaction rate (k).

This non-ideal wetland hydrodynamic behavior is usually quantified using a hydraulic efficiency parameter (λ). This parameteris primarily influenced by the wetland shape, inlet and outlet configurations, vegetation patterns and basin morphology [18]. Specific focus will be placed in this section in improving the hydraulic efficiency by modifying the wetland shape and the configurations of the inlet and outlet structures.

Before exploring the literature about the potential ways to improve the hydraulic efficiency of the wetland, it is first important to distinguish between hydraulic efficiency and volumetric efficiency/effective volume:

Hydraulic efficiency is defined as [18]:

$$\lambda = \frac{T_p}{T_n} \tag{5.4}$$

where T_p is the time taken to observe the peak concentration of a non-reactive tracer at the wetland outlet and T_n is the nominal retention time calculated from the ratio of volume of the wetland to the influent flow rate. On the other hand, volumetric efficiency is represented as:

$$e = \frac{T_m}{T_n} \tag{5.5}$$

where T_m is the mean retention time of the retention time distribution (RTD) curve.

Hydraulic efficiency and volumetric efficiency are related by the number of CSTRs (N) [18], which quantifies the mixing criterion in the wetlands (see section 4.1 for more details):

$$\lambda = e\left(1 - \frac{1}{N}\right) \tag{5.6}$$

Increasing the number of tanks (simulating plug flow) will result in more similar values for hydraulic and volumetric efficiency. Hydraulic efficiency has been used in the majority of studies as it also incorporates the shape of the RTD curve. However, the only way to directly calculate the number of tanks using this relationship is to find the parameters T_p and T_m using a tracer study. Since a tracer study could not be completed at these sites due to lack of water volume and flow during the 2018 drought, the method presented by Thackston et al. [13] (Eq 5.3), was used, which does not distinguish between the two. Afterwards, the equation presented in Kadlec & Wallace [12] (Eq 5.1) was used to calculate the actual retention time.

Since most of the literature has been concerned with increasing the hydraulic efficiency (λ) of the wetland, that term will be used for this chapter. Unless otherwise mentioned, this is assumed to be equivalent to volumetric efficiency (e).

5.1.1 Implementation on Study Site

Simulations were conducted using the models developed in chapters 3-4 where the aspect ratio of the study wetlands was increased artificially to 5 to examine the impact on retention time and pollutant removal. Table 5. 1 shows the impact of this aspect ratio increase on volumetric efficiency and retention time. The increase in retention time was greater at HHM, which had a lower actual aspect ratio (0.99 vs 1.84).

The obtained 50% retention times (t_{50}) from increasing the aspect ratios were then used to calculate the outflow concentrations using Eq 4.2. The reaction rate constant and the number

of tanks were kept constant to evaluate the sensitivity of the effect of increased aspect ratio on the removal efficiency of the wetland (Fig 5. 1).

Table 5. 1 Actual and Increased Aspect Ratios with the calculated 50% cdf retention time.

	AR	e	t_{50} (hrs)
HHN	1.84	0.77	3.90
	5.00	0.84	4.16
HHM	0.99	0.62	5.93
	5.00	0.84	8.30

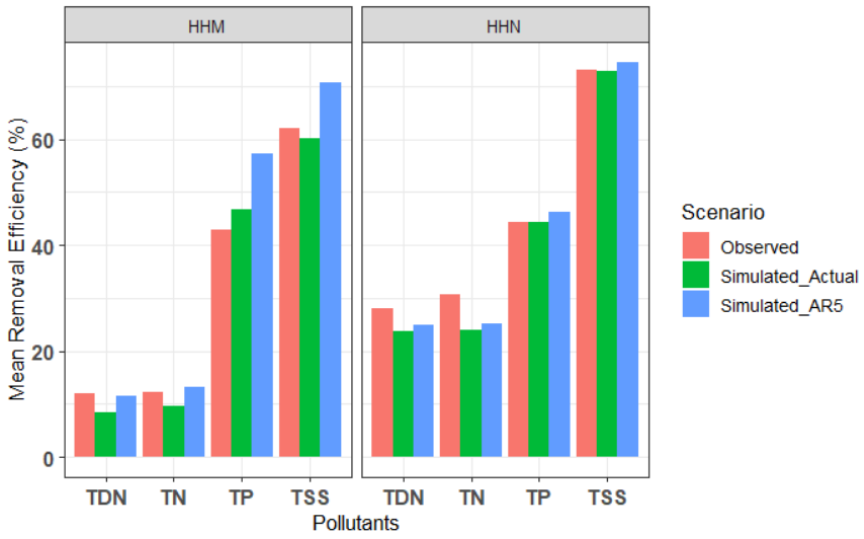

Fig 5. 1 Mean Removal efficiency obtained using the observed, simulated and increased aspect ratios of the wetland.

The increase in removal efficiencies with increased aspect ratio (AR5) was higher in HHM than in HHN. This was expected due to larger change in t_{50} obtained in HHM as discussed above. Overall, the change is aspect ratios had a larger impact on removal of TSS and TP as compared to TN and TDN. Even at the higher aspect ratio, the simulated removal efficiencies for TN and TDN were still lower than the actually observed values in three out of four cases. This comparison shows that the increase in aspect ratio was not enough to boost the

nitrogen removal in our study wetlands. This could be due to several reasons. The wetlands can be severely undersized on an areal basis. This topic is addressed in section 5.3. The mere increase in aspect ratio without the identification of low velocity zones may also not optimize the impact on removal efficiency. Additional specific design measures used in the literature to optimize pollutant removal through improving hydraulic efficiency are described below.

5.1.2 Changing Aspect Ratio through Baffles

Wörman and Kronnäs [16] found that narrower wetlands removed nitrogen three times more effectively than wider wetlands due to better hydraulic efficiency. This effect of low hydraulic efficiency is more elaborate in deep water wetlands [19]. The use of baffles inside the wetlands has been found to successfully increase the hydraulic efficiency by decreasing the ineffective wetland segments [20, 21]. Despite this evidence, the use of baffles in any kind of sedimentation basin remains infrequent. This is primarily due to the lack of specification and guidelines available for their general usage [22].

For wetland design, the question of the selection of emergent or submerged baffles needs to be addressed. From the recent studies on this topic, the usage of emergent baffles seems to be highly recommended. For instance, Chang et al. [21] found no improvement in hydraulic efficiency with submerged obstructions due to the overtopping of the flow and recommended the usage of emergent obstructions. There is evidence, though, that too many emergent obstructions can have a negative effect on the hydraulic efficiency [14]. This happens due to the decrease in total volume of the wetland occupied by the water which counteracts the benefits of improved effective volume ratio.

To optimally install baffles in wetlands, Su et al. [14] provided a regression equation relating the hydraulic efficiency to the total number of obstructions needed, obstruction width

and wetland width. Keeping the rest of the variables constant, the total number of baffles needed to achieve the desired hydraulic efficiency can be determined:

$$\lambda = 0.63 - 0.02n_{ob} + 0.64\frac{w_{ob}}{w_w} \tag{5.7}$$

Where, n_{ob} is the number of baffles, w_{ob} is the width of baffles and w_w is the width of wetland.

Secondly, the spacing and configuration of baffles placement should aim to optimize their potential benefit. Su et al. [14] demonstrated that using baffles to achieve an aspect ratio of 5 will achieve a 90% hydraulic efficiency. Achieving an aspect ratio of greater than 5 by employing more baffles may not be economically feasible as the rate of increase in hydraulic efficiency decreases quite sharply afterwards. These results were obtained from ideal shapes of wetlands using numerical simulations and should only be taken as general guidelines as the actual impact of the aspect ratio on the hydraulic efficiency can be a bit more conservative [23].

5.1.3 Configuration of Inlet and Outlet

The configuration of the wetland inlet and outlet has a direct impact on the hydraulic and treatment efficiency inside the wetland [18, 24]. Su et al. [14] demonstrated through numerical simulations that changing the location of inlet and outlet from corner-corner to uniform-midpoint in a wetland with aspect ratio < 2 increased the hydraulic efficiency from 0.65 to 0.88. Optimizing for the location of the inlet was found to have a much lesser impact on wetlands with aspect ratio > 4 [20]. This is because the elongated shape of the wetland already acts to minimize short circuiting of the flow. Sabokrouhiyeh et al. [25] recently found that the corner to corner configuration of inlet and outlet produced the least dead zones, highest hydraulic efficiency and least dispersion when compared to center to center and corner to center configurations. Similar to Su et al. [14], the study also concluded that the use of multiple inlets further increased all of the

efficiency metrics in most configurations (with the exception of corner outlets), and also resulted in a more uniform velocity field.

5.1.4 Vegetation Patterns

In most cases, addressing the impact of aspect ratios will be enough to address the actual hydraulic conductivity of the wetland. This also includes wetlands with banded vegetation placed across the wetland as all of the flow path will pass through the banded vegetations. Minor changes can be expected for flow rate but the hydraulic efficiencies may well be very close to the non-vegetated wetlands [26].

This is not the case, though, in wetlands with high density of riparian or fringing vegetation. In the presence of fringing/riparian vegetation, the effect of recirculation zones near the inlet and low mixing zones near the outlet will be diminished. Most of these zones will fall inside the riparian vegetation section and the water will short circuit through the middle non vegetated area of the wetland, reducing the effective area of the wetland. This will also produce a long tail in retention time distribution curves due to the significant drag produced by the vegetation on the remaining flow. Therefore, even wetlands with large L:W ratios could have lower hydraulic efficiencies in this case, as the impact of increased L:W ratio will decrease.

To best determine the effects of vegetation, a tracer study should be done to find out the time it takes for the tracer to reach the peak concentration at the outlet (Tp). This can then be used to calculate the plug flow hydraulic efficiency (λ_p) which is the ratio of peak concentration of tracer at the outlet under plug flow conditions (Tp) and nominal retention time (Tn). Here, λ_p decreases with the density and coverage of fringing vegetation.

Incorporation of this factor into the relationship between aspect ratio and hydraulic efficiency of the wetland is given below [26]:

$$\lambda = 0.96\lambda_p \left[1 - exp\left(-\left(0.58 - 0.36\lambda_p\right)\frac{L}{W}\right)\right] \quad (5.8)$$

Here, as λ_p decreases the impact of L:W ratio on increasing the hydraulic efficiency (λ) decreases. Again, the hydraulic efficiency (λ) can be replaced by volumetric efficiency (e) as per our assumptions for the studies where tracer test results are not available.

5.2 Improving Denitrification

Denitrification has generally been found to be the most significant process for nitrogen removal in treatment wetlands, and in most cases might be the only pathway for permanent N removal from the aquatic environment [27]. Additionally, organic carbon and phosphorus has been found to most often be the limiting element in the process of denitrification [28] and wetland vegetation usually acts as a key source of organic C for the denitrifying bacteria [29].

5.2.1 Vegetation Configuration

Wetland vegetation can be configured into three major forms: emergent, submerged and floating. Changing water depth has been found to dictate the dominant presence of the type of vegetation in the wetland [30, 31]. As with hydraulic effects, however, the effect of vegetation type on nitrogen removal also has contradictory conclusions in literature.

Weisner and Thiere [32] demonstrated that having a homogenous emergent plant species will produce better nitrogen removal rates due to their ability to produce large amount of organic matter and larger litter surface area for attachment of biofilms. This high productivity is also more suitable to developing anaerobic conditions for denitrification. Contrarily, Weisner et al. [33] found that submerged vegetation has been found to produce more readily decomposed litter than emergent macrophytes and that the release of dissolved organic carbon from submerged vegetation can be higher during certain time period of the year. This led them to suggest a hybrid

water depth model of wetland with shallow parts favoring submerged vegetation growth and deeper parts favoring emergent vegetation growth for optimal nitrogen removal.

Similar contradictions are present in the case of sparse and dense vegetation cover. Bodin et al. [34] showed that the tracer recoveries and effective volume ratio were lower in wetlands with dense emergent vegetation which will influence the hydraulic efficiency of the wetlands and nutrient removal. On the other hand, Liu et al. [29] found that higher plant cover would positively affect the denitrification rates by providing sufficient amount of organic matter.

5.2.2 Phosphorus content in soil

Availability of dissolved phosphorus aids in plant production particularly during the vegetation growing season [35]. The improved plant productivity can directly boost nitrogen removal in wetlands by enhanced plant nutrient uptake [36].

The contribution of phosphorus in promoting denitrification directly was described by White and Reddy [37], in a study that found the availability of phosphorus in soils to be the primary limiting factor for denitrification in wetlands with organically rich soils and high initial NO_3 concentrations. The study implied that wetlands in agricultural setting will generally have ample amount of NO_3 available which will be supplemented by mineralization of organic nitrogen and nitrification of NH_4. Organic carbon is usually the other common limiting element which is present in abundance in organically rich soils like peat [38]. Given these conditions, phosphorus availability becomes the primary factor to improve nitrogen removal. (However, the presence of carbon rich peatlands does not guarantee higher denitrification rates, due to the presence of phenolic compounds in peat which can inhibit the reduction of nitrate by denitrifiers and also slow down the microbial decomposition under anaerobic conditions [39].)

Kim et al. [40] showed that the relationship between phosphorus and denitrification is not always positive and is highly dependent on carbon availability. When both carbon and nitrogen were added in the presence of high phosphorus, the wetlands were found to have increased quantities of NO_2, therefore significantly affecting the first step of denitrification.

5.2.3 Dissolved Organic Carbon content

Dissolved Organic Carbon (DOC) limitation in wetlands significantly hinders denitrification, particularly in agricultural wetlands with tile drain systems receiving high NO_3 concentrations [41]. Additionally, denitrification has been found to be much higher in permanently flooded wetlands than dry or intermittently flooded wetlands [42]. The flooded conditions of agricultural wetlands during late spring-early summer when combined with high NO_3 inputs boost the requirement for DOC to perform denitrification. DOC produced through wetlands plants is very often insufficient to remove the high NO_3 concentrations received by these systems [43]. This is mainly due to the limited size of wetlands relative to the agricultural watersheds that limits the production of autochthonous DOC from the wetland plant communities [41]. The other main source of DOC input to wetlands is allochthonous DOC, from the agricultural watersheds. Royer and David [44] found that the amount of allochthonous DOC generated from the agricultural watersheds in Illinois, USA, was dictated by the storm hydrographs, with major amounts entering the wetlands after a storm event. The study also determined that the total amount of DOC drained from the watershed was much lower than the amount present in the soil, and that only 18% of the drained DOC was bioavailable.

The optimal range of C:N ratio to achieve highest removal efficiency of NO_3-N has been reported to be around 5:1 in both surface flow constructed wetlands [45] and subsurface flow constructed wetlands [46]. C:N ratios as low as 2.5:1 to as high as 10:1 has been measured in

vertical flow constructed wetlands [47, 48] indicating that the C:N ratios producing optimal N removal efficiencies might also be affected by other factors like pH, temperature and dissolved oxygen [49].

To overcome this deficiency of DOC supply, artificial sources have been used to supply sufficient carbon for the optimal performance of denitrification process. Improved denitrification results have been reported through the addition of cornstalks, soybean oil, woodchips, cardboard fibers [50], sweet factory wastewater [51], methanol [52] and other materials. However, the use of alternative carbon sources might not be feasible in every situation. Organic matter in the soils might be able to provide sufficient DOC for denitrification, even in the case of sandy soils and the addition of alternate carbon source might not provide any additional benefits [53].

5.2.4 Implementation on Study Site

The model developed in the previous chapters does not address specific pathways for nitrogen removal through denitrification, and data (such as DOC concentrations) that could address these issues were not collected in the field study. Therefore, this section examines the impacts of changes in the overall reaction rate (k) on removal of total and dissolved nitrogen without specifying the processes responsible for these changes. It is uncertain which (if any) design approaches would be most effective at producing increased k values for nitrogen removal.

Similar to the approach taken with the watershed to wetland area ratios, a sensitivity analysis was performed and is presented in Fig 5.2 below. The resulting outflow concentrations from the relaxed tank in series model equation (Eq. 4.2) at different values of k was then used to calculate pollutant removal efficiency in the wetlands. The higher end of the increased reaction rate values aligns with the general values reported in literature for stormwater wetlands (see

section 4.2). As per the previous approaches, the retention time (t_{50}), number of tanks (P) and water depth (h) were kept constant at their actual simulated values.

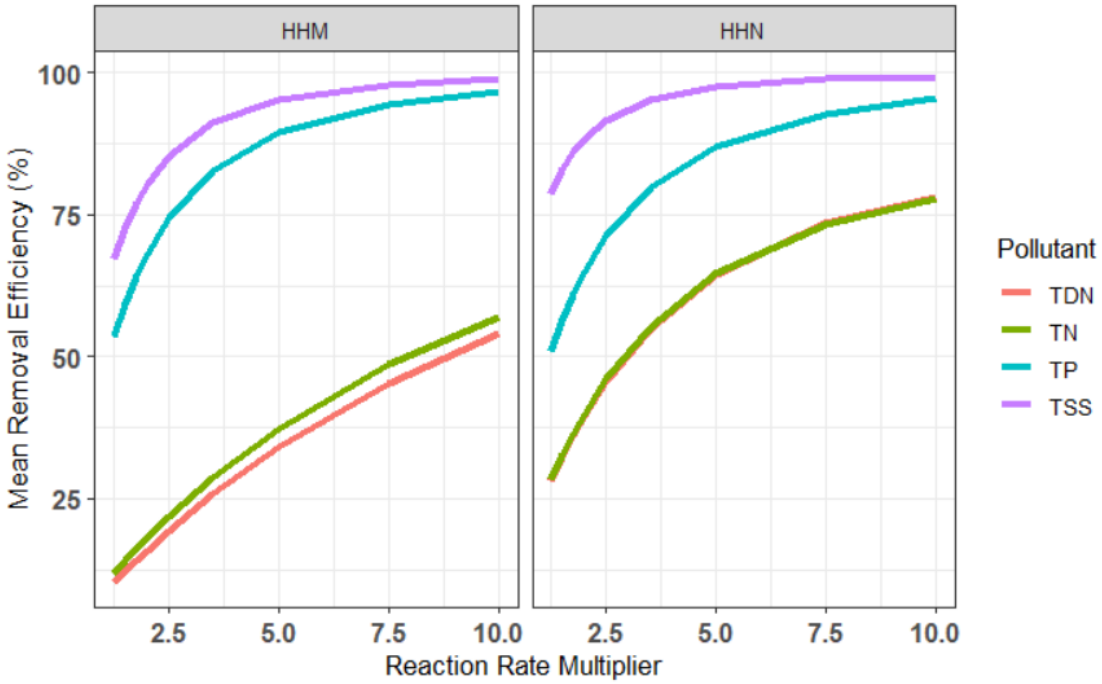

Fig 5. 2 The rate of increase in the mean removal efficiency of the all four pollutants with the increased reaction rate multiplier.

The rate of increase in the removal efficiencies with the increase in k was much higher for TSS and TP on both sites than for dissolved or total nitrogen. Also, TN and TDN curves were much flatter at HHM than at HHN. This is partly due to the much lower initially calibrated k values obtained in HHM. These low values were a direct result of the low removal efficiencies observed on HHM site for the two nitrogen pollutants. The practical reason due to this difference between the two sites would be largely due to the differences in the design structures of the wetlands. Although the limitation of this study does not allow to specify the causes, possible contributors would be the change in vegetation configuration (see section 5.2.1), differences in the aspect ratios (see section 5.1.1) and differences in the influent flow rates (see chapter 2).

5.3.1 Increasing Wetland Water Depth

Wetland depth is a direct contributor to the wetland volume, which significantly affects the wetland retention time. For instance, changing water levels produced significantly different retention time distribution (RTD) curves for a tracer study done during a natural storm events on a FWS wetland [54]. The RTD curves produced for storm events with high water levels reached peak outlet concentration much faster and therefore also had much lower minimum retention times.

This is found to have a direct impact on pollutant removal. For instance, linear modelling of nitrogen removal in shallow surface-flow wetlands on agricultural landscape produced negative removal with hydraulic residence time of < 2 days [6]. These observations have the tendency to lead towards increasing the wetland depth to increase the hydraulic retention time and therefore achieve higher N removal efficiencies. However, the actual scenario has more complexity and the relationship is not so directly proportional.

Lie et al. [55] found that with increasing water depth, the effective volume ratio (i.e., effective volume (V_e) / total volume) decreased linearly, even though the absolute total effective volume increased. This showed that the ratio of dead zone volume to total volume in the wetland ponds increases with increasing water depth. The study also showed that by combining the negative linear regression equation of effective volume ratio and water depth with the general effective volume equation (i.e., $V_e = (effective\ volume\ ratio) * h * A_t$), a quadratic equation can be developed. This equation can then be used to produce the depth required to achieve the maximum effective volume of the wetland. Producing wetland depths below this will produce layered flow paths for the pollutants producing multiple peaks of the RTD curves. This

phenomenon of multiple peaks is an indication of short circuiting of some portion of the influent pollutants at the shallower depths or near surface segments and/or mixing of the pollutants at the deeper segments of the wetland. Both of these phenomena will contribute to decreasing the hydraulic efficiency of the wetland by either decreasing the hydraulic residence time or increasing dispersion, which will decrease the concentration gradient and lower the reaction rate.

Song et al. [10] provided an explanation for this contradiction in a study where they concluded that deeper wetlands will produce higher residence times and hence, higher nitrogen removal but shallower wetlands will end up producing more emergent vegetation than deep wetlands and therefore will promote denitrification better in the longer run. This improved process of denitrification would become more important than higher retention time achieved from the increased depth in some cases.

5.3.2 Increasing Wetland Surface Area

The wetland to watershed area ratio has a significant impact on regulating the retention time of the runoff water in the wetlands and its treatment efficiency [7]. Given its significance, a number of studies have been conducted testing a wide range of wetland to watershed ratios. For instance Woltemade [7] showed that smaller wetland to watershed ratios were unable to reduce nitrogen loads. Similarly, Kovacic et al. [11] found that a higher wetland to watershed ratio was better suited for nitrate removal and suggested a wetland to watershed ratio of in between 1:15 to 1:20 for optimal performance.

The Minnesota Board of Water and Soil Resources [56] developed a state ranking system for potential of wetland restoration with wetland to watershed ratio of less than 1:5 getting the highest score and ratios of 1:20 getting the lowest score. The study also defined a threshold of a minimum wetland surface area of 0.5 acres, below which the cost to benefit ratio of restoring

wetland for treatment purposes was quite poor. Lentz [57] recommended changing the wetland to watershed ratios to account for different climatic conditions. The study concluded that wetter watersheds with high flows or in cold climates should have lower wetland to watershed ratio since wetlands will become saturated with little drainage area in high flow conditions and the microbial activity will be slower in colder climate.

5.3.3 Implementation on Study Site

The watershed to wetland ratios were adjusted in model simulations for both HHM and HHN to examine the effect of relative wetland size on performance. As both HHM and HHN have relatively high watershed:wetland ratios (~ 50:1), these adjustments focused on reducing this ratio. Two different simulations were performed, with watershed:wetland ratios of 20:1 and 5:1 as suggested by Kovacic et al. [11] and Minnesota Board of Water and Soil Resources [56]. The actual wetland area listed in Table 5. 2 is the surface area of each wetland obtained from Stage Storage relationship (i.e., Fig 3. 1), using the maximum free water depth for each wetland (i.e., HHM = 2.07 ft, HHN = 1.94 ft). The watershed area represents the total tile drainage area of the upland cropped fields.

Table 5. 2 Actual and Simulated watershed to wetland ratios with detention time at 50% cdf .

	Site	Wetland Area (ac)	Watershed Area (ac)	Watershed to Wetland Ratio	t_{50} (hrs)
Actual	HHM	0.34	17.40	51:1	5.93
	HHN	0.30	14.64	49:1	3.90
Simulated [1]	HHM	0.87	17.40	20:1	15.42
	HHN	0.73	14.64	20:1	9.91
Simulated [2]	HHM	3.48	17.40	5:1	61.5
	HHN	2.93	14.64	5:1	39.88

The impact of the increased retention time due to decreased watershed to wetland ratios on mean removal efficiency for each pollutant can be seen in Fig 5. 3 below. The calculated retention times (t_{50}) associated with each simulated surface area were first calculated and then used to produce outflow concentration for each pollutant at both study sites using the relaxed tank in series model equation (Eq. 4.2). All four pollutants showed significant increase in removal efficiencies with TP and TSS producing removal > 90% at both study sites with the watershed to wetland ratio of 5. It should be noted that the two nitrogen species showed the largest relative improvement in the removal eficiency with the watershed to wetland ratio of 20. This might be due to the much lower initial level of nitrogen removal under existing conditions.

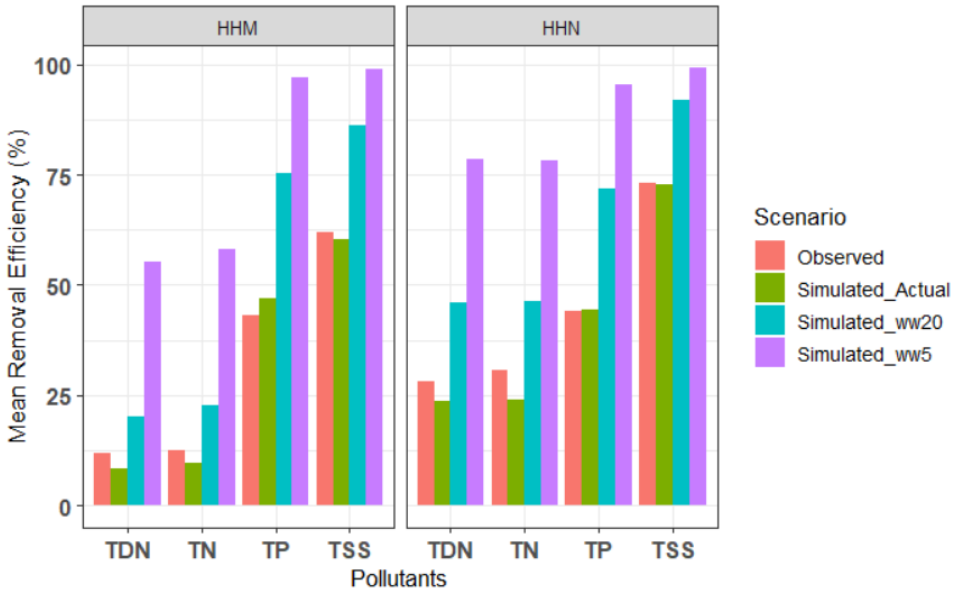

Fig 5. 3 Comparison of observed removal efficiency with the simulated removal efficiencies obtained using the actual wetland to watershed ratio onsite (Simulated Actual), wetland to watershed ratio of 1:20 (Simulated_ww20) and wetland to watershed ratio of 1:5 (Simulated_ww5).

Afterwards, a sensitivity analysis was performed to better understand the degree of impact of decreased watershed to wetland area on the the removal efficiency of the pollutants. As can be seen from Fig 5. 4 below, at both wetlands, the rate of increase in the removal efficiency for the two nitrogen species increases as the watershed to wetland ratio becomes smaller than

approximately 20:1. This indicates a non linear relationship between the the area ratios and the removal capacities of both wetlands. Both Fig 5. 3 and Fig 5. 4 confirms the finding that the change in watershed to wetland ratio to below 20:1 (by increasing the wetland surface area 2.5 times) would be most effective in increasing the nitrogen removal efficiency.

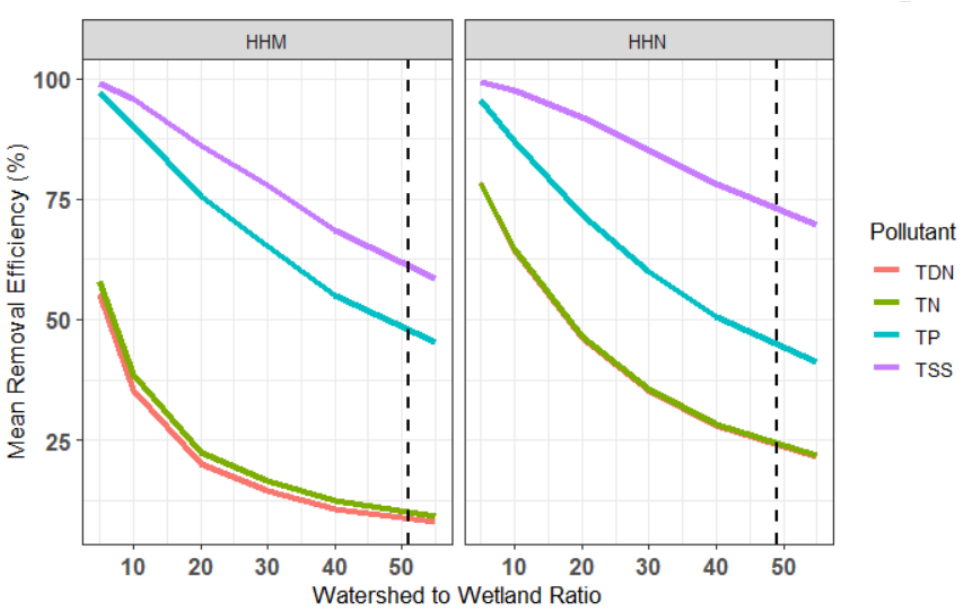

Fig 5. 4 The rate of increase in the mean removal efficiency of the all four pollutants with the decreased watershed to wetland ratio. Dashed lines represent the actual wetland to watershed ratios on site.

5.4 References

1. Tournebize, J., C. Chaumont, and Ü. Mander, *Implications for constructed wetlands to mitigate nitrate and pesticide pollution in agricultural drained watersheds.* Ecological Engineering, 2017. **103**: p. 415-425.
2. Tanner, C.C. and R.H. Kadlec, *Influence of hydrological regime on wetland attenuation of diffuse agricultural nitrate losses.* Ecological engineering, 2013. **56**: p. 79-88.
3. Karpuzcu, M.E. and W.T. Stringfellow, *Kinetics of nitrate removal in wetlands receiving agricultural drainage.* Ecological Engineering, 2012. **42**: p. 295-303.
4. Ardon, M., et al., *The water quality consequences of restoring wetland hydrology to a large agricultural watershed in the southeastern coastal plain.* Ecosystems, 2010. **13**(7): p. 1060-1078.
5. Beutel, M.W., et al., *Nitrate removal in surface-flow constructed wetlands treating dilute agricultural runoff in the lower Yakima Basin, Washington.* Ecological Engineering, 2009. **35**(10): p. 1538-1546.
6. Arheimer, B. and H.B. Wittgren, *Modelling nitrogen removal in potential wetlands at the catchment scale.* Ecological engineering, 2002. **19**(1): p. 63-80.

7. Woltemade, C., *Ability of restored wetlands to reduce nitrogen and phosphorus concentrations in agricultural drainage water.* Journal of Soil and Water Conservation, 2000. **55**(3): p. 303-309.
8. Toet, S., et al., *The effect of hydraulic retention time on the removal of pollutants from sewage treatment plant effluent in a surface-flow wetland system.* Wetlands, 2005. **25**(2): p. 375-391.
9. Tanner, C., *Plants as ecosystem engineers in subsurface-flow treatment wetlands.* Water Science and Technology, 2001. **44**(11-12): p. 9-17.
10. Song, X., P.M. Ehde, and S.E. Weisner, *Effects of water depth and phosphorus availability on nitrogen removal in agricultural wetlands.* Water, 2019. **11**(12): p. 2626.
11. Kovacic, D.A., et al., *Effectiveness of constructed wetlands in reducing nitrogen and phosphorus export from agricultural tile drainage.* Journal of environmental quality, 2000. **29**(4): p. 1262-1274.
12. Kadlec, R.H. and S. Wallace, *Treatment Wetlands*. 2008: CRC Press.
13. Thackston, E.L., F.D. Shields Jr, and P.R. Schroeder, *Residence time distributions of shallow basins.* Journal of Environmental Engineering, 1987. **113**(6): p. 1319-1332.
14. Su, T.-M., et al., *Optimal design for hydraulic efficiency performance of free-water-surface constructed wetlands.* Ecological Engineering, 2009. **35**(8): p. 1200-1207.
15. Liu, L., H. Hu, and J. Qi, *Research on the influencing factors of hydraulic efficiency in ditch wetlands.* Procedia Engineering, 2012. **28**: p. 759-762.
16. Wörman, A. and V. Kronnäs, *Effect of pond shape and vegetation heterogeneity on flow and treatment performance of constructed wetlands.* Journal of Hydrology, 2005. **301**(1-4): p. 123-138.
17. Wahl, M.D., et al., *Quantifying the hydraulic performance of treatment wetlands using reliability functions.* Ecological Engineering, 2012. **47**: p. 120-125.
18. Persson, J., N.L. Somes, and T. Wong, *Hydraulics efficiency of constructed wetlands and ponds.* Water science and technology, 1999. **40**(3): p. 291-300.
19. Shih, S.-S., et al., *A correction coefficient for pollutant removal in free water surface wetlands using first-order modeling.* Ecological engineering, 2013. **61**: p. 200-206.
20. Koskiaho, J., *Flow velocity retardation and sediment retention in two constructed wetland–ponds.* Ecological Engineering, 2003. **19**(5): p. 325-337.
21. Chang, T.-J., et al., *Flow uniformity and hydraulic efficiency improvement of deep-water constructed wetlands.* Ecological Engineering, 2016. **92**: p. 28-36.
22. Zech, W.C., C. Logan, and X. Fang, *State of the practice: Evaluation of sediment basin design, construction, maintenance, and inspection procedures.* Practice Periodical on Structural Design and Construction, 2014. **19**(2): p. 04014006.
23. Ioannidou, V. and J. Pearson, *Seasonal effects of vegetation and flow rate on mixing and pollutant transport in constructed wetlands*. 2015.
24. Suliman, F., et al., *Effect of the inlet–outlet positions on the hydraulic performance of horizontal subsurface-flow wetlands constructed with heterogeneous porous media.* Journal of contaminant hydrology, 2006. **87**(1-2): p. 22-36.
25. Sabokrouhiyeh, N., et al., *A numerical study of the effect of wetland shape and inlet-outlet configuration on wetland performance.* Ecological Engineering, 2017. **105**: p. 170-179.

26. Jenkins, G.A. and M. Greenway, *The hydraulic efficiency of fringing versus banded vegetation in constructed wetlands.* Ecological Engineering, 2005. **25**(1): p. 61-72.
27. Jacobs, A.E. and J.A. Harrison, *Effects of floating vegetation on denitrification, nitrogen retention, and greenhouse gas production in wetland microcosms.* Biogeochemistry, 2014. **119**(1-3): p. 51-66.
28. Hume, N.P., M.S. Fleming, and A.J. Horne, *Denitrification potential and carbon quality of four aquatic plants in wetland microcosms.* Soil Science Society of America Journal, 2002. **66**(5): p. 1706-1712.
29. Liu, W., G. Liu, and Q. Zhang, *Influence of vegetation characteristics on soil denitrification in shoreline wetlands of the Danjiangkou Reservoir in China.* Clean–Soil, Air, Water, 2011. **39**(2): p. 109-115.
30. Miller, R.C. and J.B. Zedler, *Responses of native and invasive wetland plants to hydroperiod and water depth.* Plant ecology, 2003. **167**(1): p. 57-69.
31. Raulings, E.J., et al., *The importance of water regimes operating at small spatial scales for the diversity and structure of wetland vegetation.* Freshwater Biology, 2010. **55**(3): p. 701-715.
32. Weisner, S.E. and G. Thiere, *Effects of vegetation state on biodiversity and nitrogen retention in created wetlands: a test of the biodiversity–ecosystem functioning hypothesis.* Freshwater Biology, 2010. **55**(2): p. 387-396.
33. Weisner, S., et al., *Influence of macrophytes on nitrate.* Ambio, 1994. **23**(6): p. 363-366.
34. Bodin, H., et al., *Tracer behaviour and analysis of hydraulics in experimental free water surface wetlands.* Ecological Engineering, 2012. **49**: p. 201-211.
35. Berthold, M., et al., *Potential export of soluble reactive phosphorus from a coastal wetland in a cold-temperate lagoon system: buffer capacities of macrophytes and impact on phytoplankton.* Science of the Total Environment, 2018. **616**: p. 46-54.
36. Kao, J.T., J.E. Titus, and W.-X. Zhu, *Differential nitrogen and phosphorus retention by five wetland plant species.* Wetlands, 2003. **23**(4): p. 979-987.
37. White, J.R. and K. Reddy, *Nitrification and denitrification rates of Everglades wetland soils along a phosphorus-impacted gradient.* Journal of Environmental Quality, 2003. **32**(6): p. 2436-2443.
38. White, J. and K. Reddy, *Influence of nitrate and phosphorus loading on denitrifying enzyme activity in Everglades wetland soils.* Soil Science Society of America Journal, 1999. **63**(6): p. 1945-1954.
39. Veraart, A.J., *Denitrification in ditches, streams and shallow lakes*. 2012.
40. Kim, S.Y., et al., *Combined effects of carbon, nitrogen and phosphorus on CH4 production and denitrification in wetland sediments.* Geoderma, 2015. **259**: p. 354-361.
41. Grebliunas, B.D. and W.L. Perry, *The role of C: N: P stoichiometry in affecting denitrification in sediments from agricultural surface and tile-water wetlands.* SpringerPlus, 2016. **5**(1): p. 359.
42. Hernandez, M.E. and W.J. Mitsch, *Denitrification in created riverine wetlands: Influence of hydrology and season.* Ecological Engineering, 2007. **30**(1): p. 78-88.
43. Burgoon, P., *Denitrification in free water surface wetlands receiving carbon supplements.* Water science and technology, 2001. **44**(11-12): p. 163-169.

44. Royer, T.V. and M.B. David, *Export of dissolved organic carbon from agricultural streams in Illinois, USA.* Aquatic Sciences, 2005. **67**(4): p. 465-471.
45. Li, H., et al., *Stimulation of optimized influent C: N ratios on nitrogen removal in surface flow constructed wetlands: Performance and microbial mechanisms.* Science of The Total Environment, 2019. **694**: p. 133575.
46. Zhu, H., et al., *Removal of nitrogen and COD in horizontal subsurface flow constructed wetlands under different influent C/N ratios.* Ecological Engineering, 2014. **63**: p. 58-63.
47. Zhao, Y.J., et al., *Performance of pilot-scale vertical-flow constructed wetlands in responding to variation in influent C/N ratios of simulated urban sewage.* Bioresource Technology, 2010. **101**(6): p. 1693-1700.
48. Fan, J., et al., *Nitrogen removal in intermittently aerated vertical flow constructed wetlands: impact of influent COD/N ratios.* Bioresource technology, 2013. **143**: p. 461-466.
49. Saeed, T. and G. Sun, *A review on nitrogen and organics removal mechanisms in subsurface flow constructed wetlands: dependency on environmental parameters, operating conditions and supporting media.* Journal of environmental management, 2012. **112**: p. 429-448.
50. Greenan, C.M., et al., *Comparing carbon substrates for denitrification of subsurface drainage water.* Journal of environmental quality, 2006. **35**(3): p. 824-829.
51. Fernández-Nava, Y., et al., *Denitrification of high nitrate concentration wastewater using alternative carbon sources.* Journal of Hazardous Materials, 2010. **173**(1-3): p. 682-688.
52. Fernández-Nava, Y., et al., *Denitrification of wastewater containing high nitrate and calcium concentrations.* Bioresource Technology, 2008. **99**(17): p. 7976-7981.
53. Davidsson, T.E. and M. Ståhl, *The influence of organic carbon on nitrogen transformations in five wetland soils.* Soil Science Society of America Journal, 2000. **64**(3): p. 1129-1136.
54. Holland, J.F., et al., *Effects of wetland depth and flow rate on residence time distribution characteristics.* Ecological Engineering, 2004. **23**(3): p. 189-203.
55. Liu, J.J., et al., *Variations of effective volume and removal rate under different water levels of constructed wetland.* Ecological Engineering, 2016. **95**: p. 652-664.
56. Resources, M.B.o.W.a.S., *Wetlands Restoration Strategy: A Framework for Prioritizing Efforts in Minnesota. Supplement to the Minnesota Wetlands Conservation Plan 1997*. 2009.
57. Lentz, A., *Physical criteria for wetland targeting on a watershed scale*. 2012.

Chapter 6

Conclusion and Future Study

The modeling of constructed stormwater treatment wetlands receiving high-nutrient runoff from agricultural watersheds with tile outlet terraced systems poses several challenges that are not addressed well by traditional models for treatment wetlands. The major issues encountered, and the solutions developed in this work for addressing these issues are described below:

- **Rainfall-runoff modeling:** Small watersheds and wetland systems such as those studied here present unique challenges that required the development of customized models to accurately represent observational data. Runoff from these terraced watersheds cannot be well-modelled by a standard curve number approach due to varying vegetation and soil conditions. However, a custom model that accounts for antecedent precipitation and variations in vegetative cover during the year was able to reproduce flow patterns observed at these sites. Specifically, the Antecedent Precipitation Index (API) and Atmospherically Resistant Vegetation Index were incorporated into the Curve Number prediction equation (chapter 2).
- **Hydrographs modification:** The high-sloping terracing fields, saturated soil conditions, and tile drain systems combine to result in flashy hydrographs with very high receding limb to peaking limb ratios. The structure of the default SCS Unit hydrograph method was modified with a Peak Rate Factor of 100 (Default: 484) to simulate the high flow rates entering into the wetland (chapter 2).
- **Dynamic water budget development:** The dynamic water level in the wetlands, which varied from a maximum height of around 2 ft to a minimum of 0 ft during the study

period, required the development of a full-scale water budget model. The response of the the water level to high flow influent water varies dramatically with respect to the preceding conditions in the wetland (chapter 3). These situations were simulated in the wetland water budget model, which also incorporated evapotranspiration, seepage, and effluent flows during storm events.

- **Detention time calculations:** Seasonal variability presents an additional challenge to modeling wetland retention time and performance. The large number of potential factors affecting water flow and pollutant removal can make it difficult to develop large enough datasets for conventional fitting approaches. A stochastic model that used a Monte Carlo simulation was developed to examine the likely distribution of retention times under different rainfall and seasonal conditions (chapter 3).
- **Water treatment modeling:** The intermittent nature of the constructed wetlands behaves as something between a plug flow and completely mixed system and was thus modeled using a relaxed tank in series model. The model was used to provide information about contaminant removal rates and wetland mixing. With the level of data available however, it was not possible to fully disentangle the relative contributions of reactivity and mixing. A Bayesian analysis was therefore used to once again provide a most probable range of constituent removals for these wetlands (chapter 4).
- **Low nitrogen removal:** The presence of high influent flow rate produced unusually low retention times in the wetlands for some storm events. The low retention time caused low removal efficiencies for the two nitrogen pollutant species as denitrification, responsible for the major removal of these pollutants, occurs at a much slower rate than sedimentation which is the major removal mechanism for particulate solids and

phosphorus. The effect of these low removal rates can be quantified by the low reaction rate (k) values modeled for nitrogen removal (chapter 4).

The custom models developed for this study were able to incorporate the effects of the first five conditions listed above. However, the models consistently reported a low nitrogen removal efficiency even under sensitivity analysis. This may be a true representation of the wetland performance, but it may also reflect the limits of the tank in series model applied to this type of dynamic wetland system. In Chapter 5, hypothetical scenarios were created to illustrate the potential improvements in removal efficiencies that can be obtained from these systems if special design considerations were implemented (chapter 5). The major lessons from this work are presented as recommendations in the following sections.

6.1 Recommendations for enhancing efficiency of existing systems:

The study wetlands produced low removal ranges for the nitrogen species compared to those reported in the literature for similar sized wetlands. While this low removal could be influenced by multiple factors, the high influent flow rate likely plays a major role. The two primary reason for this high flow rate are the tile outlet terraced systems that exist on our site and the presence of saturated soil conditions during high intensity storm events. Modifications to the tile drain systems could help mitigate these issues to some extent. In particular, the flashy behavior of runoff hydrographs (Fig 2. 8 and Fig 2. 9) can be slowed down by modifying the configuration of the risers controlling the outflow from the terraces. Increasing the vertical distance between the discharge holes of the risers would ensure the gradual discharge of the runoff water as it continues to get ponded up in the terraces following a storm event. This

modification will help in delaying the peak flow discharge, especially during the high flow storm events. It would, however, result in slower drainage from the fields.

The other design modification option would be to install a sedimentation basin prior to the wetlands. The sedimentation basin would not only help in increasing the detention times inside the wetlands by decreasing the hydraulic loading rate but will also contribute directly in water quality improvement. In a study done by Beutel [1], the presence of a deep sedimentation basin decreased the hydraulic loading rate in wetlands from 125 cm/d to 12 cm/d. If implemented on our study site, this will significantly decrease the high flow rate of the storm runoff coming from the upland watersheds and will help in ensuring the optimal removal efficiency from the downstream wetlands.

Additionally, sedimentation basins have been found to function as algal ponds. These basins have the tendency to convert the incoming dissolved nitrogen into particulate nitrogen, significant portion of which settles inside the sedimentation basin [2]. The rest of the converted particulate nitrogen can then be dealt with more easily as both of our study wetlands are efficient particulate removing systems (i.e., particulate TP and TSS have much higher removal efficiency than nitrogen, which is mostly dissolved).

Having some macrophytes present will also help in improving the removal efficiency of the nitrogen species. As documented earlier in section 5.2.1, denitrification accounts for the majority of the removal pathways for wetlands receiving nitrogen. The lack of carbon in the wetland environment hinders the process of denitrification (see section 5.2.3). The appropriate vegetation presence ensures sufficient organic carbon for the denitrifying bacteria. Additionally, the N accumulation by wetland plants have been found to efficiently remove nitrate [3, 4]. However, they have been found to act as a secondary removal pathway to the denitrification

process in most cases [5, 6] and have a potential of releasing the nitrogen back to water during plant decay[7]. This can be overcome by regular harvesting practices, but plants in agricultural watersheds are usually not harvested due to their potential of acting as an important organic source [6, 8]. Additionally, if not restricted, the growth of plants can cover the whole of wetland volume, leading to the channelizing of flowing water and creating low velocity zones as a consequence [9].

Therefore, optimally enhancing the development of emergent or submerged vegetation species on our study sites will be a challenging task, but the deployment of floating mats provides an efficient alternative. Floating mats, unlike rooted emergent or submergent vegetation species, grow on the surface of the water, supported on a floating raft structure [10]. Floating mats are particularly suited for stormwater wetlands as they adjust with the seasonally changing water levels [11]. Additionally, denitrification has been found to be the main process for nitrogen removal for floating vegetation mats. The mats themselves serve as a physical barrier to oxygen intrusion, resulting in low dissolved oxygen levels within the pore waters. Biofilms present in the mat structure also increase the organic carbon supply to microbial biomass [12].To successfully improve nitrate removal, a minimum floating mat surface area coverage of 50m^2, or between 10% to 50% of the wetland surface, has been recommended [13].

6.2 Recommendations for design of new systems:

With respect to future implementation of wetlands at other field sites, it may be possible to improve nutrient removal (particularly nitrogen) through changes to wetland design. In general, more retention time will increase treatment performance. Creating larger wetlands will increase volume and retention time, but there are limitations to this approach. The deeper Cain wetland showed poor removal for dissolved nitrogen relative to the two shallower sites at the

Harvest Hills watershed, so increasing area, rather than depth, would likely be more effective at improving nitrogen removal. As seen in Fig 5. 4, decreasing the watershed to wetland ratio on the Harvest Hills sites increased the removal efficiency, with a higher rate of increase below a 20:1 areal ratio. Although similar sized watershed to wetland areal ratios have been found to improve removal performance, special consideration should be placed on the watershed dynamics. In the case of high flow rate producing watersheds with saturated soil conditions, like a tile outlet terraced system on uncropped agricultural fields, stormwater constructed wetlands might have increased surface area requirements. However, this would require a larger footprint. For instance, there would be some periods, such as those in May-June 2015 on our study sites, where there would be so much runoff volume being generated that it would be very difficult to supply enough additional volume to significantly increase retention times.

For more frequently occurring moderate storm events, however, improvement in wetland design could help maximize the amount of treatment achieved within the same space. Designing more-channelized flow paths through careful inlet and outlet placement [14], placing baffles in the wetland (section 5.1.2) and better vegetation planting, such as the use of floating vegetation mats (section 6.1) or designing a hybrid depth wetland model to promote submerged and emergent vegetation growth (section 5.2.1) could contribute to improving the removal efficiency within a similar overall volume. This approach would likely add to the upfront design and construction costs in some cases but could produce long-term benefit.

The actual effect of the baffles/islands on retention time can only be represented correctly by doing a tracer study and observing the timing of the tracer concentration at the outlet. Usage of a two dimensional depth- averaged finite element numerical hydrodynamic models like (RMA-2), can be used to plot the 2d velocity profiles inside the wetland [15]. This will help in

placing the baffles and islands at the correct positions by detecting the low velocity zones in the cases where the outer boundary of the wetlands cannot be changed.

In addition of the inlet and outlet boundary conditions which would be inflow flow rate and water levels at the outlet, the input to the RMA2 model requires:

- A mesh describing the bathymetry of the wetland.
- Manning's coefficients and eddy viscosities for each material type defined in the floor meshes. The Manning's coefficient will vary across the mesh cells depending upon the vegetation density at various parts of the wetland.

In light of the literature review performed and the response of our study wetlands as the result of the hypothetical implementation of the increased aspect ratio, surface area and reaction rate constant, a step by step design process would be the best approach for these treatment wetlands. Ideally all of these factors should be addressed during the design phase of the wetlands. However, most of the initial efforts should be placed upon achieving the desired retention time by modifying the hydraulic efficiency and the increase in wetland land area should be taken as a last step due to economic considerations. The optimal design procedure can be given as follows:

- Using the proposed aspect ratio of the wetland, determine the hydraulic efficiency. To provide a more accurate estimate, the measurement of several other parameters would be required including the wetland active area, plant density, and wetland floor bathymetry among others (see chapter 5).
- In case of unsatisfactory potential hydraulic efficiency as compared to the pre-defined threshold, a decision would be made whether to redesign the wetland using a new aspect ratio or to modify the inlet and outlet configurations.

- If the hydraulic efficiency is still not above the threshold, the designer can then decide to add obstructions (for instance baffles) to improve the aspect ratio of the wetlands internally. Consideration should be given to wetlands with fringing/riparian vegetation and the design equations should be used accordingly.
- If the hydraulic efficiency is still not above the threshold or if the achieved threshold does not provide with the required detention time, increase in wetland size, improving denitrification through vegetation modification or other wetland modifications including the installation of a sedimentation basin should be taken into the consideration.

6.3 Application of models for future research:

The models developed for terraced runoff and wetland performance at these sites also have potential to improve wetland design and site selection. More-specific estimates of runoff volumes could provide better initial calculations for wetland size requirements that could help in selecting sites for implementation and in locating wetland placement on those sites.

While a key part of the overall wetland modelling process, the runoff model (chapter 2) developed for small, terraced fields can also be used as a stand-alone model to help design drainage systems for these sites. The proposed runoff model accounts for the varying land use coverage and the leftover soil moisture. Additionally, the ease of using a CN method to quantify the runoff generation on site provides a simpler modeling route to help small scaled quantification of agricultural runoff. Caution should be used in the application of the proposed model on sites with different physical characteristics due to the change in geographical location or watershed design. The necessity of representing the specific site conditions has led to the over calibration of these models which may not be applicable to other sites as it is. However, using

the model development and parameter selection techniques presented here, a site-specific custom CN model can be generated.

The wetland water budget model (chapter 3) can be used to track the dynamic water level changes in the wetland. The specific model schematic presented alongside the Python scripts (in supplemental material) can be used to track the changes in wetland water levels throughout the year. Improvements in the model results can be made by collecting extensive site-specific data. The measurements will include but are not limited to water temperature, wetland floor bathymetry and wind velocity.

The Monte Carlo methodology was used to generate the retention time cumulative distribution curves (chapter 3). For the analysis presented here, the median retention times were used to model wetland treatment analysis. Similarly, further insights about the wetland behavior could be found by replicating the modeling process for different retention time values. As the slow moving runoff dominates the upper 50% of the retention time curve, modeling with the 70^{th} or 90^{th} percentile retention time values would enable simulation of the wetland behavior during small storm events and might present new insights. Nutrient removal models (chapter 4) can also be used to test the sensitivity of wetland treatment performance to key design parameters and determine ideal ranges for each parameter that can better inform future wetland design. The ability to model variations in storm intensity and influent nutrient concentration are key core characteristics of this approach. As presented in this study, in the absence of a tracer study, the relaxed tank in series model provides an efficient modelling alternative. However, the reaction rate (k) and mixing parameter (P) should be modeled for each site separately as the extrapolation of the modeled parameters presents various challenges. The use of pre-calibrated parameter

values from a similar wetland to simulate the potential treatment performance of a prospective wetland should only be done after addressing the following questions as laid out in [16]:

- Do the inlet and outlet concentration ranges used in the calibration dataset match the ranges expected in the potential wetland design?
- Will the potential wetland expected to experience similar retention time and hydraulic loading rates as the calibration site?
- Is the configuration of the two wetlands similar? This will include the aspect ratio, size and other physical makeup of the wetlands.
- Are the climatic conditions similar? This will include precipitation, evapotranspiration, water temperature and other variables.
- Do the ecology of the two wetlands match? At minimum, this will include the vegetation type, species and density.

However, if used correctly, scenario modeling can help to establish expected ranges of wetland performance and identify the contribution wetlands can make to controlling nutrient runoff in northeastern Kansas watersheds.

6.4 References

1. Beutel, M.W., et al., *Nitrate removal in surface-flow constructed wetlands treating dilute agricultural runoff in the lower Yakima Basin, Washington.* Ecological Engineering, 2009. **35**(10): p. 1538-1546.
2. Kadlec, R.H., et al., *Water quality performance of treatment wetlands in the Imperial Valley, California.* Ecological Engineering, 2010. **36**(8): p. 1093-1107.
3. Gottschall, N., et al., *The role of plants in the removal of nutrients at a constructed wetland treating agricultural (dairy) wastewater, Ontario, Canada.* Ecological engineering, 2007. **29**(2): p. 154-163.
4. Jacobs, A.E. and J.A. Harrison, *Effects of floating vegetation on denitrification, nitrogen retention, and greenhouse gas production in wetland microcosms.* Biogeochemistry, 2014. **119**(1-3): p. 51-66.

5. Bachand, P.A. and A.J. Horne, *Denitrification in constructed free-water surface wetlands: II. Effects of vegetation and temperature.* Ecological engineering, 1999. **14**(1-2): p. 17-32.
6. Vymazal, J., *The use of constructed wetlands for nitrogen removal from agricultural drainage: A review.* Scientia agriculturae bohemica, 2017. **48**(2): p. 82-91.
7. Longhi, D., M. Bartoli, and P. Viaroli, *Decomposition of four macrophytes in wetland sediments: Organic matter and nutrient decay and associated benthic processes.* Aquatic Botany, 2008. **89**(3): p. 303-310.
8. Vymazal, J., *Emergent plants used in free water surface constructed wetlands: a review.* Ecological engineering, 2013. **61**: p. 582-592.
9. Jansson, M., et al., *Wetlands and lakes as nitrogen traps.* Ambio, 1994: p. 320-325.
10. Headley, T., C.C. Tanner, and A.R. Council, *Application of floating wetlands for enhanced for stormwater treatment: a review*. 2008: Auckland Regional Council Auckland, New Zealand.
11. Lane, S., et al., *Recommendations of the Expert Panel to Define Removal Rates for Floating Treatment Wetlands in Existing Wet Ponds.* 2016.
12. Borne, K.E., C.C. Tanner, and E.A. Fassman-Beck, *Stormwater nitrogen removal performance of a floating treatment wetland.* Water science and technology, 2013. **68**(7): p. 1657-1664.
13. Borne, K.E., et al., *Implementation and maintenance of floating treatment wetlands for urban stormwater management.* Journal of Environmental Engineering, 2015. **141**(11): p. 04015030.
14. Su, T.-M., et al., *Optimal design for hydraulic efficiency performance of free-water-surface constructed wetlands.* Ecological Engineering, 2009. **35**(8): p. 1200-1207.
15. Koskiaho, J., *Flow velocity retardation and sediment retention in two constructed wetland–ponds.* Ecological Engineering, 2003. **19**(5): p. 325-337.
16. Kadlec, R.H. and S. Wallace, *Treatment wetlands*. 2008: CRC press.